A MATTER OF PERSPECTIVE:
root adaptive responses to endoparasitic cyst nematodes

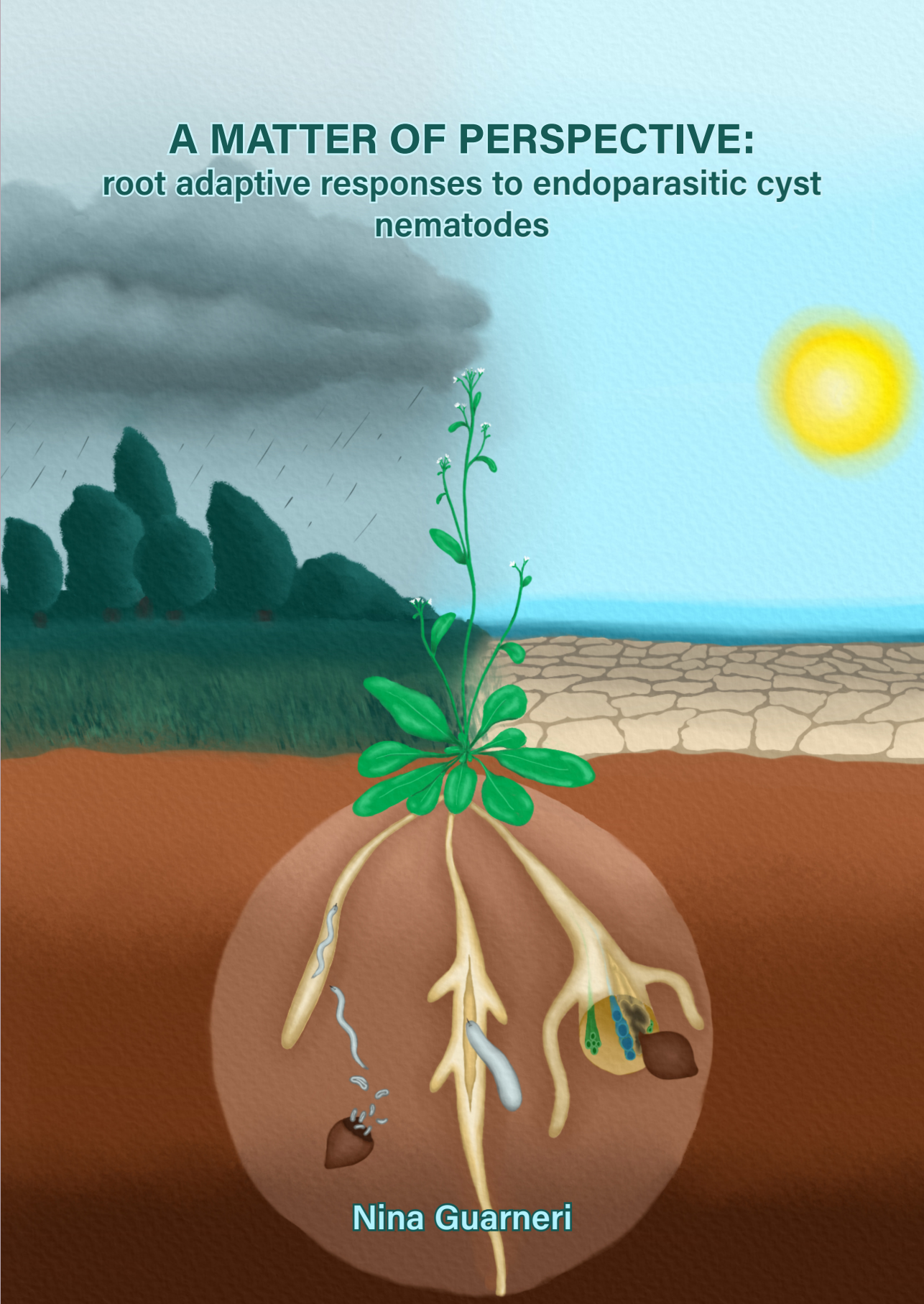

Nina Guarneri

Propositions

1. Root architecture plasticity influences the soil abundance of plant-parasitic nematodes.
   (this thesis)

2. Plant phenotypic plasticity is a driving force of adaptive evolution.
   (this thesis)

3. Cognitive dissonance plays a significant role in paper rejections during peer review.

4. PhD programs should include training for work in the industry.

5. Creativity is based on our ability to forget.

6. Societal impact of a finding is dependent on the timing of its dissemination.

Propositions belonging to the thesis, entitled

A matter of perspective: root adaptive responses to endoparasitic cyst nematodes

Nina Guarneri
Wageningen, 20 March 2024

A matter of perspective: root adaptive responses to endoparasitic cyst nematodes

Nina Guarneri

Thesis committee

Promotor

Prof. Dr G. Smant
Professor of Nematology
Wageningen University & Research

Co-promotors
Dr A. Goverse
Associate professor at the Laboratory of Nematology
Wageningen University & Research

Dr J. L. Lozano Torres
Assistant professor at the Laboratory of Nematology
Wageningen University & Research

Other members
Prof. Dr C. S. Testerink, Wageningen University & Research
Prof. Dr J. H. B. Sprakel, Wageningen University & Research
Dr G. W. van Esse, Wageningen University & Research
Prof. Dr T. Kyndt, Ghent University, Belgium

This research was conducted under the auspices of the Graduate School
Experimental Plant Sciences

A matter of perspective: root adaptive responses to endoparasitic cyst nematodes

Nina Guarneri

Thesis
submitted in fulfilment of the requirements for the degree of doctor
at Wageningen University
by the authority of the Rector Magnificus,
Prof. Dr C. Kroeze,
in the presence of the
Thesis Committee by the Academic Board
to be defended in public
on Wednesday 20 March 2024
at 4 p.m. in the Omnia Auditorium.

Nina Guarneri

A matter of perspective: root adaptive responses to endoparasitic cyst nematodes, 160 pages.

PhD thesis, Wageningen University, Wageningen, the Netherlands (2024)
With references, with summary in English

ISBN: 978-94-6447-980-5
DOI: 10.18174/642074

Table of Contents

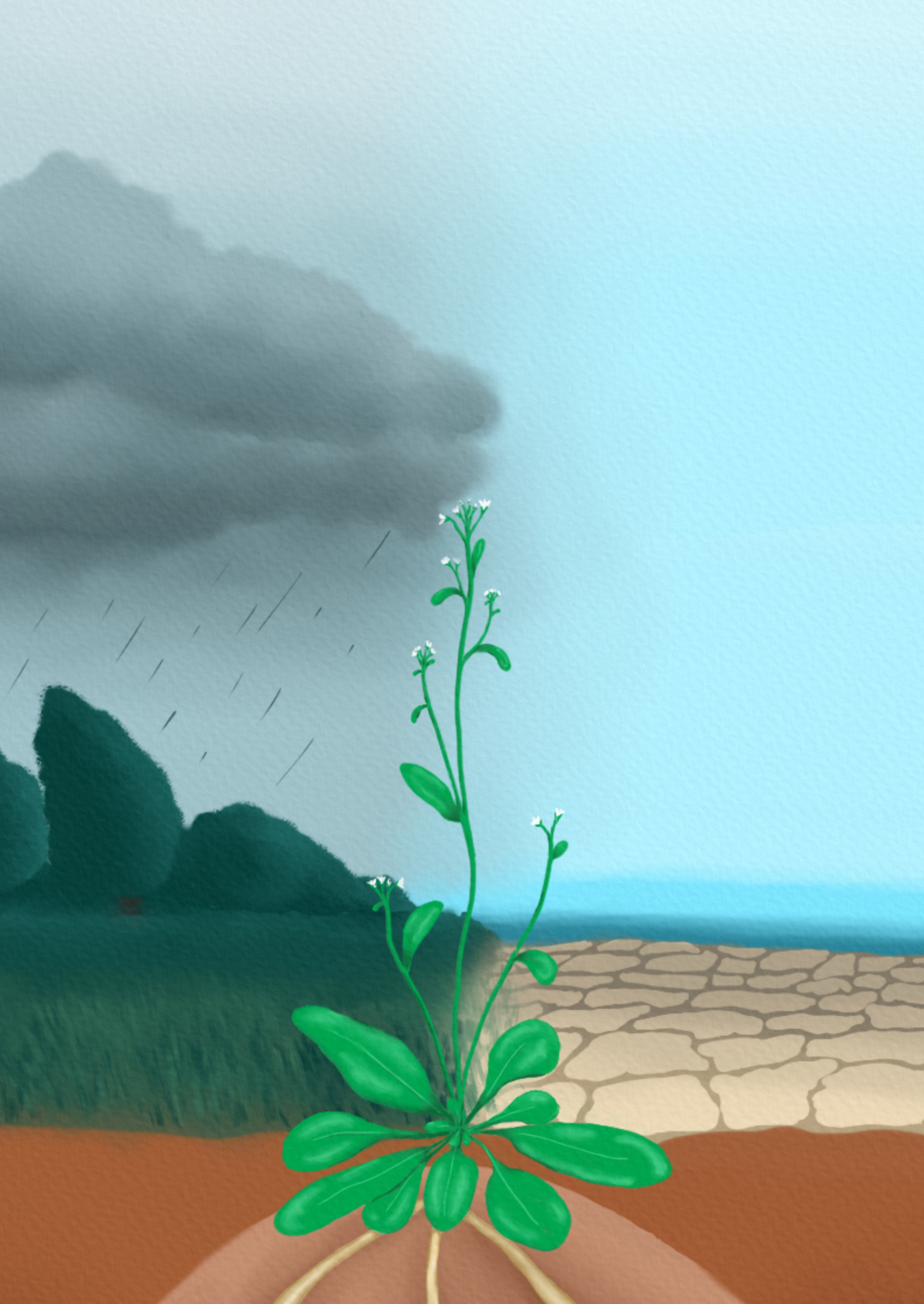

Chapter 1

General introduction

1

"If all the matter in the universe except the nematodes were swept away, our world would still be dimly recognizable, and if, as disembodied spirits, we could then investigate it, we should find its mountains, hills, vales, rivers, lakes, and oceans represented by a film of nematodes" – Nathan Cobb.

Small but huge: the impact of microscopic worms on Earth

Nematodes are the most abundant animals on Earth. They are found in most ecosystems, at all latitudes and altitudes, in fresh or marine water, and soil. It was estimated that only the nematodes in the soil make up four-fifths of the animals on Earth, occupying all trophic levels of the soil food web (van den Hoogen *et al.*, 2019). While there are approximately 30,000 known nematode species, only around 4,300 of them are plant parasites (Ali *et al.*, 2017). Among these plant-parasitic nematodes, a relatively small percentage, roughly 6%, inflict severe damage to agricultural crops. This damage results in up to 12.3% of global yield losses (Abad *et al.*, 2008; Jones *et al.*, 2013). Yet, these agricultural losses are only the tip of the iceberg, as experts believe that a significant portion of yield losses mistakenly attributed to abiotic stress is actually due to plant-parasitic nematodes (Nicol *et al.*, 2011; Jones *et al.*, 2013). Aboveground symptoms of nematode infection, such as yellowing leaves, stunted plants, and wilting, are nonspecific, leading to misdiagnosis as water and nutrient deficiencies. In contrast, the specific signs of nematode infection, such as the formation of galls, the presence of cysts, root swelling, and root lesions, remain concealed belowground (Nicol *et al.*, 2011).

The damage of nematodes to agriculture and society is the result not only of a decreased food production but also of expensive and often harmful control measures. In fact, the most effective measure against nematodes is the application of nematicides, chemical broad-spectrum pesticides with high volatility and soil penetration capacity. However, various nematicides have been banned in many countries due to their toxicity to humans and the environment (Desaeger *et al.*, 2020). A newly discovered class of nematicides called selectivins has shown high selectivity for nematodes, suggesting it may not harm humans or wildlife (Burns *et al.*, 2023). Nevertheless, the safety and efficacy of selectivins still require many years of testing. Environmentally friendly approaches currently used for nematode control include crop rotation, flooding, biological control, and natural pesticides. However, their efficacy is limited when dealing with widespread nematode populations on a large scale (Nicol *et al.*, 2011). The most effective and sustainable nematode control method at present is the use of resistant crop varieties. Plant resistance is conferred by resistance(R)-genes, which encode proteins that recognize nematodes and trigger a resistance response to impede parasitism (Davies and Elling, 2015). Yet, only a few

R-genes against nematodes have been identified in wild relatives of crops. Moreover, the incorporation of such a limited number of R-genes into commercial crop varieties has resulted in the genetic selection of new virulent nematode populations that evade host recognition, undermining the durability of crop resistance (Davies and Elling, 2015). Thus, it is urgent to make serious efforts to develop alternative strategies that minimize nematode damage to agriculture.

Consequences of climate change on plant-parasitic nematodes and their hosts

Climate change is affecting the distribution and severity of plant diseases (Raza and Bebber, 2022). Since the 18th century, our atmosphere has experienced a 50% increase in carbon dioxide, which has caused a 1°C rise in the average global temperature and may lead to a 2.4-2.6°C increase by the end of the 21st century (www.climate.nasa.gov; Dutta and Phani, 2023). As a result of global warming, extreme weather events, such as heat waves, heavy rainfalls and droughts, are becoming more frequent (www.epa.gov/climate-indicators). Altered precipitations, elevated temperatures and carbon dioxide levels have been observed to increase the abundance of many plant-parasitic nematode species (Dutta and Phani, 2023). For instance, abundant rainfall increased the prevalence of *Heterodera* and *Pratylenchus* spp. in Northern Ireland (Fleming *et al.*, 2016), whereas elevated temperatures augmented the incidence of *Longidorus caespiticola*, *Rotylenchus reniform* and *Bursaphelenchus xylophilus* in multiple countries (Dutta and Phani, 2023). Furthermore, global warming has resulted in a shift in the geographical distribution of nematodes towards the northern hemisphere (Bebber *et al.*, 2013). Besides, higher temperatures can suppress plant immunity, leading to more severe disease symptoms or to a loss of resistance (Cheng *et al.*, 2019). For example, temperatures above 28°C were found to inactivate the *Mi-1* R-gene in tomato and thereby break plant resistance to the root-knot nematode *Meloidogyne incognita* (Williamson and Kumar, 2006).

Therefore, an understanding of how plants can withstand or adapt to new combinations of biotic and abiotic stresses caused by climate change is indispensable. Genetic and epigenetic factors are known to regulate plant acclimation and adaptive responses to the environment (Zandalinas *et al.*, 2021). These responses can mediate plant resilience and tolerance to variations and increasing levels of environmental stresses, respectively (Brooker *et al.*, 2022). However, further research into stress sensing, signaling pathways and developmental responses is required to identify strategies to breed for crops that are resilient and tolerant to multifactorial stresses.

Plant developmental plasticity: a plant response to environmental shifts

Plants, as sessile organisms, have evolved to respond rapidly to environmental changes. For instance, plants adjust their leaf orientation to redirect towards light in shade conditions, while below ground, they alter their root distribution based on factors like soil moisture, nutrient availability, temperature, and salinity (Koevoets *et al.*, 2016). Plant responses to environmental cues are not limited to abiotic factors but also include biotic interactions. Plant colonization by beneficial rhizobacteria, for example, is associated with the formation of lateral roots, leading to improved shoot growth (Verbon and Liberman, 2016). In turn, changes in root architecture influence the chemical properties of the rhizosphere, shaping the microbial communities associated with plant roots (Verbon and Liberman, 2016). Thus, plant developmental plasticity is a crucial strategy for plants to establish favorable conditions for growth and survival.

While above-ground plasticity mechanisms have been extensively studied and utilized to maximize yields, exploring below-ground root plasticity has gained attention only in recent years. Non-destructive phenotyping systems have facilitated the observation of root development without disturbing plants in their growth substrate (Koevoets *et al.*, 2016). Additionally, researchers have elucidated various molecular pathways regulating plant plasticity responses to nutrient starvation, temperature, salt, and drought stress (Koevoets *et al.*, 2016). However, the molecular underpinnings of plant plasticity responses to biotic stress by soil-borne pathogens remain mostly unknown.

Biotic stress by sedentary endoparasitic nematodes

The two most damaging classes of plant-parasitic nematodes are the root-knot nematodes (*Meloidogyne spp.*) and the cyst nematodes (*Heterodera spp.* and *Globodera spp.*). Although they belong to different phylogenetic clades, root-knot and cyst nematodes have independently evolved similar feeding behaviors (Holterman *et al.*, 2009). In the soil, nematode eggs hatch into infective second-stage juveniles (J2s) that move toward the host following chemical cues released by the roots (Abad and Williamson, 2010). J2s possess a needle-like oral stylet connected to three salivary glands and a pumping muscle. The function of the stylet is to perforate plant cells during host invasion and to secrete molecules called effectors that aid parasitism by altering the structure and function of host cells (Abad and Williamson, 2010; Zhang *et al.*, 2022). During penetration, J2s secrete effectors to degrade plant cell walls and facilitate migration through the root tissue. Additionally, once they have reached the plant vasculature, J2s release effectors that suppress plant defenses and transform

plant cells into permanent feeding sites. These feeding sites establish specialized connections with the plant vasculature to ensure nutrient and water uptake for the feeding J2s. Next, J2s lose their motility and undergo three molts to reach full maturity and reproduce eventually (Fig. 1). This feeding behavior defines root-knot and cyst nematodes as obligate biotrophic sedentary endoparasitic nematodes (Abad and Williamson, 2010).

What mainly distinguishes root-knot from cyst nematodes is their migratory behavior and the type of permanent feeding site they induce. Root-knot nematodes penetrate the root elongation zone, the region above the root apical meristem where plant cells elongate before differentiating into mature cells (Abad and Williamson, 2010). Subsequently, J2s migrate in between cells first towards the meristem and then, making a U-turn, towards the maturation zone of the root tip. Intercellular migration allows root-knot nematodes to cause minimal damage to plant cells and thus partially avoid triggering plant defense responses. The permanent feeding sites induced by root-knot nematodes are called giant cells and are made of extremely expanded cells, surrounded by a proliferating tissue that forms a gall (Abad and Williamson, 2010). The female nematodes feed intermittently on each giant cell by moving their head from one cell to another (Smant *et al.*, 2018) and finally produce egg masses. Although most root-knot nematodes reproduce asexually, a few species require egg fertilization by males (Castagnone-Sereno, 2006).

In contrast, cyst nematodes can penetrate plant roots at various locations (Grymaszewska and Golinowski, 1991) but are seldom found at the root tip. They break the root tissue by stylet thrusts and migrate intracellularly, leaving a path of cell death behind (Wyss and Zunke, 1986; Grundler *et al.*, 1994). Cyst nematodes induce feeding sites called syncytia by transforming a single cell (the initial syncytial cell), which later fuses to hundreds of neighboring cells through partial cell-wall degradation. The syncytium expands radially due to hypertrophy of the partially fused cells, known as syncytial elements. While immobile nematode females keep eggs within their bodies, males regain motility and fertilize the females (Golinowski *et al.*, 1996; Abad and Williamson, 2010).

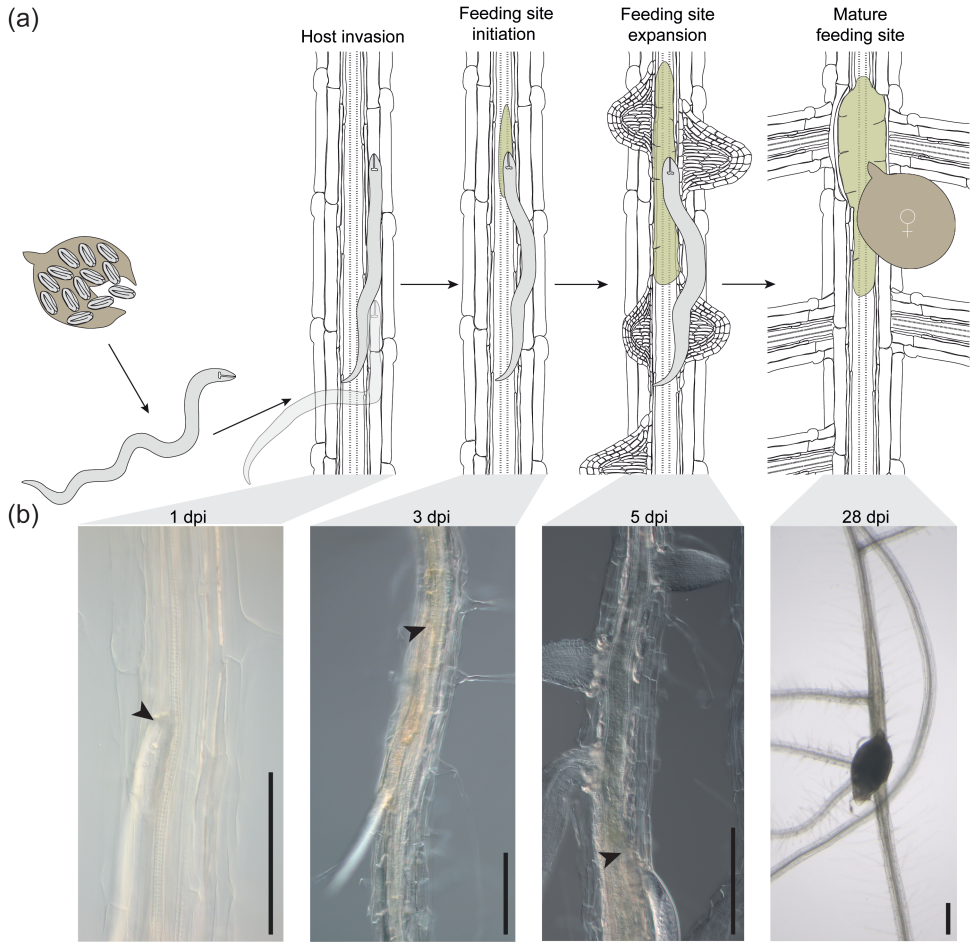

Fig. 1 Life cycle of the endoparasitic cyst nematode *Heterodera schachtii* in Arabidopsis. (a) Schematic representation of the life cycle of *H. schachtii*. Infective juveniles hatch from the dead body of a female and invade host roots. After migrating through the host tissues, juveniles select a cell near the plant vasculature and initiate a feeding site. Over time, the feeding site expands, and secondary roots are formed in near proximity. Nematodes feed on plant roots for about four weeks, until they develop into adult females. (b) Microscopy pictures of nematode infection sites at 1, 3, 5 and 28 days post inoculation (dpi). Black arrowheads indicate the nematode head. Scale bar is 200 µm.

Mechanical wounding by nematode infection induces root architecture plasticity

When grown vertically *in vitro* and without stress, the model plant Arabidopsis forms two types of roots: a primary root and multiple lateral roots. After primary root emergence from the seed coat, oscillating maxima of the hormone auxin at the primary

root tip prime cells to form lateral roots. While the primary root grows, lateral roots emerge acropetally (i.e., the closer to the primary root tip, the younger the root) and in a regularly spaced pattern (Wan *et al.*, 2023). However, infections by endoparasitic nematodes alter the root system architecture. The primary root shortens, and secondary roots emerge at nematode infection sites (Lee *et al.*, 2011; Villordon and Clark, 2018; Zhou *et al.*, 2019; Levin *et al.*, 2020; Willig *et al.*, 2022). These secondary roots differ from acropetal lateral roots, as they are formed *de novo* in the mature root region and often emerge in clusters, resulting in an irregular bushy root system.

Interestingly, mechanical wounding of the primary root also induces *de novo* formation of secondary roots with an irregular pattern (Sheng *et al.*, 2017). In this context, such roots are defined as adventitious lateral roots, since they share regulatory molecular mechanisms with adventitious roots that form from leaf explants (Wan *et al.*, 2023). In leaf explants, wounding triggers a transient accumulation of the plant hormone jasmonate (JA), which, upon perception by the receptor COI1, induces the expression of the transcription factor ERF109 (Zhang *et al.*, 2019). In turn, ERF109 regulates local auxin biosynthesis, causing auxin accumulation (Zhang *et al.*, 2019). Auxin accumulation at the wound site activates the transcription factor WOX11 and its downstream target LBD16 (Hu and Xu, 2016; Sheng *et al.*, 2017). Finally, the transcription factor LBD16 regulates the asymmetric division of root founder cells, leading to the formation of a root primordium. Thus, the ERF109/WOX11/LBD16 pathway regulates adventitious root formation in leaf explants (Hu and Xu, 2016; Sheng *et al.*, 2017; Zhang *et al.*, 2019). Similarly, adventitious lateral root formation from primary roots is dependent on auxin-responsive WOX11 and LBD16 (Sheng *et al.*, 2017). Whether the same molecular mechanisms also regulate *de novo* secondary root formation in response to nematode infection remains unknown.

Another form of root plasticity, typically observed in response to root-knot nematode infection, is the regeneration of the root apical meristem. Nematode migration exerts mechanical pressure on meristematic cells, inhibiting primary root growth (Zhou *et al.*, 2019). However, plant damage perception triggers a regeneration response that heals the root apical meristem and resumes growth (Zhou *et al.*, 2019). Specifically, root-knot nematode host invasion induces JA and JA-dependent ERF109 signaling, which activates ERF115 and thereby regulates regeneration. Repression of the transcription downstream of ERF115 decreases plant growth recovery after nematode invasion and thus results in shorter primary roots compared to when ERF115-mediated transcription is enabled (Zhou *et al.*, 2019). This suggests that plants can activate multiple compensatory mechanisms to mitigate the impact of endoparasitic nematodes on growth.

Furthermore, *de novo* secondary root formation induced by nematode infection may

act as a compensatory mechanism for enhanced water and nutrient absorption despite primary root damage. In fact, the ability of some cultivars to form secondary roots was observed to correlate with better maintenance of shoot growth upon nematode infection (Trudgill and Cotes, 1983; Miltner *et al.*, 1991; Villordon and Clark, 2018). However, whether *de novo* secondary root formation is induced by mechanical damage during nematode infection still needs to be investigated.

Do nematodes hijack root plasticity?

Root plasticity implies the formation of new root organs or regeneration of a meristem in response to environmental changes. Similarly, nematode feeding sites are root-associated (pseudo-)organs (Kyndt *et al.*, 2013). Both processes involve cell division, cellular expansion, and tissue organization. Additionally, root plasticity and nematode feeding site development often occur in close proximity (Golinowski *et al.*, 1996; Zhou *et al.*, 2019; Levin *et al.*, 2020; Olmo *et al.*, 2020). This suggests that the molecular mechanisms regulating root plasticity could partially overlap with permanent feeding site development and contribute to nematode root parasitism. Furthermore, root plasticity likely enhances the host's nutritional status during infection, which may indirectly increase the availability of water and nutrients for the nematode (Levin *et al.*, 2020). Consequently, root plasticity could facilitate faster nematode life cycle progression and higher nematode female fecundity (i.e., the number of eggs produced by a female), leading to increased nematode populations in the field. As this is undesirable for agricultural purposes, understanding the implications of root plasticity on endoparasitic nematodes is of high importance. Previous studies have shown that activation of the regeneration marker ERF115 promotes root-knot nematode gall development (Zhou *et al.*, 2019), but it remains unknown whether root plasticity mechanisms can benefit cyst nematodes.

Scope of this thesis

This thesis aims to investigate the contribution of root plasticity responses to cyst nematode infections and how this impacts plant growth and development. Using the model plant Arabidopsis and the beet cyst nematode *Heterodera schachtii* in a combination of cell biology techniques, nematode *in vitro* assays, and greenhouse experiments, the following three main research questions were addressed:

1. What are the molecular mechanisms regulating *de novo* secondary root formation at cyst nematode infection sites?

2. Does *de novo* secondary root formation benefit plants by mitigating the negative

impact of cyst nematodes on growth?

3. Does *de novo* secondary root formation benefit cyst nematode parasitism by promoting nematode feeding?

In Chapter 2, we hypothesize that *de novo* secondary root formation is a plant response to the mechanical damage caused by intracellular nematode host invasion. Using Arabidopsis fluorescent reporters and loss-of-function mutants, we test whether host invasion by *H. schachtii* induces damage signaling via the JA-dependent ERF109 pathway. Furthermore, we investigate whether this leads to local biosynthesis of auxin and thereby triggers *de novo* secondary root formation at nematode infection sites.

In Chapter 3, we ask whether the secondary roots induced by *H. schachtii* host invasion are adventitious lateral roots and whether they are beneficial to plant growth and development. Thus, we verify if *de novo* secondary root formation at nematode infection sites is dependent on WOX11. Moreover, we investigate if WOX11-dependent root plasticity mitigates the impact of *H. schachtii* infections on plant root and shoot growth, thereby modulating plant tolerance to cyst nematodes.

In Chapter 4, we investigate whether activation of the adventitious lateral root pathway benefits syncytium expansion and female fecundity. Our findings prompt us to further dive into the role of WOX11 in cell-wall plasticity mechanisms and ROS homeostasis that could possibly regulate the radial expansion of *H. schachtii* syncytia and thereby their nutritional status.

In Chapter 5, we propose a shift in perspective based on recent findings suggesting that the formation of adventitious lateral roots is, at least partly, a response of the plant to tolerate cyst nematode infection. By examining relevant literature, we illustrate how considering both a pathogen-centered and a plant-centered perspective can re-shape our current understanding of biotic interactions and generate novel research questions on this topic (Fig. 2).

Finally, in Chapter 6, we combine the main findings of this thesis into a working model and discuss them in the context of evolution and plant adaptation to the environment. From here, a picture emerges where plants likely have conserved mechanisms regulating developmental plasticity in response to multiple abiotic and biotic stresses including nematodes. In our opinion, further research into plant developmental plasticity and its role in biotic interactions is crucial for the development of climate-proof crop varieties that are resilient and tolerant to multifactorial stresses.

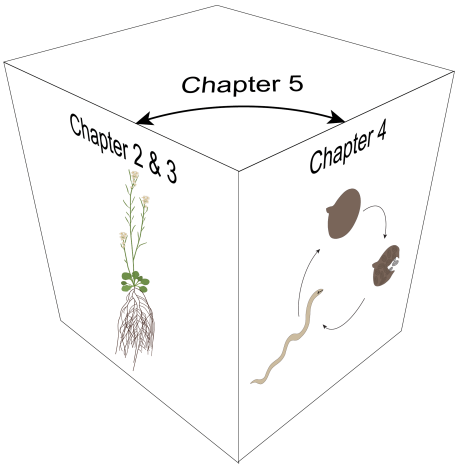

Fig. 2 Thesis outline. Chapters 2 and 3 focus on plant root architecture plasticity in response to cyst nematode infection and its contribution to plant tolerance. Chapter 4 looks at the impact of root plasticity on nematode fitness. Chapter 5 demonstrates how shifting from a plant-centered to a pathogen-centered perspective, and vice versa, can improve our understanding of plant interactions with biotrophic pathogens and help generate novel research questions. Image was partially made using Biorender.

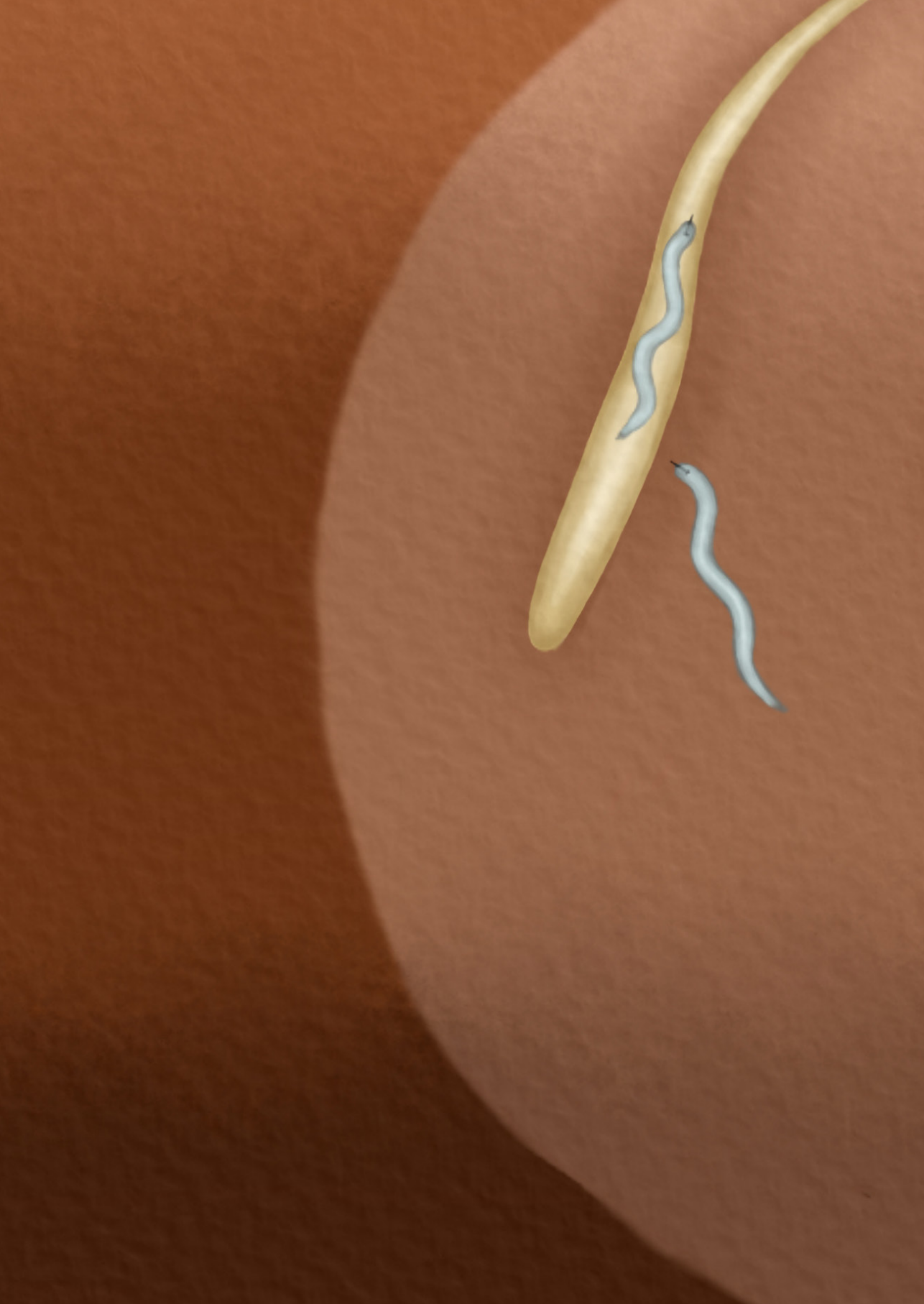

Chapter 2

Root architecture plasticity in response to endoparasitic cyst nematodes is mediated by damage signaling

Nina Guarneri[1,‖], Jaap-Jan Willig[1,‖], Mark G. Sterken[1], Wenkun Zhou[2,3], M. Shamim Hasan[4], Letia Sharon[4], Florian M. W. Grundler[4], Viola Willemsen[2], Aska Goverse[1], Geert Smant[1,‡], and Jose L. Lozano-Torres[1,‡]

[1]Laboratory of Nematology, Wageningen University & Research, 6708 PB Wageningen, the Netherlands

[2]Laboratory of Molecular Biology, Cluster of Plant Developmental Biology, Wageningen University & Research, 6708 PB Wageningen, the Netherlands

[3]State Key Laboratory of Plant Physiology and Biochemistry, College of Biological Sciences, China Agricultural University, Beijing, 100193 China

[4]Institute of Crop Science and Resource Conservation (INRES), Molecular Phytomedicine, University of Bonn, INRES, 53115 Bonn, Germany

‖ - these authors contributed equally

‡ - these authors contributed equally

Published in *New Phytologist* (2023) 237:807–822

Abstract

Plant root architecture plasticity in response to biotic stresses has not been thoroughly investigated. Infection by the endoparasitic cyst nematodes induces root architectural changes that involve the formation of secondary roots at infection sites. However, the molecular mechanisms regulating secondary root formation in response to cyst nematode infection remain largely unknown. We first assessed whether secondary roots form in a nematode-density dependent manner by challenging wild-type Arabidopsis plants with increasing numbers of cyst nematodes (*Heterodera schachtii*). Next, by using jasmonate-related reporter lines and knock-out mutants, we tested if tissue damage by nematodes triggers jasmonate-dependent secondary root formation. Finally, we verified whether damage-induced secondary root formation depends on local auxin biosynthesis at nematode infection sites. Intracellular host invasion by *H. schachtii* triggers a transient local increase in jasmonates, which activates the expression of ERF109 in a COI1-dependent manner. Knock-out mutations in COI1 and ERF109 disrupt the nematode-density dependent increase of secondary roots observed in wild-type plants. Furthermore, ERF109 regulates secondary root formation upon *H. schachtii* infection via local auxin biosynthesis.Host invasion by *H. schachtii* triggers secondary root formation via the damage-induced jasmonate-dependent ERF109 pathway. This points at a novel mechanism underlying plant root plasticity in response to biotic stress.

Introduction

Plants utilize root plasticity as a key strategy to survive in a changing soil environment. Remodeling of root systems allows plants to cope with nutrient deficiencies, drought, salinity, and other abiotic stresses (Koevoets *et al.*, 2016). However, little is known about root architecture plasticity in response to soil-borne biotic stresses. Infections by cyst nematodes are known to induce elaborate root architectural changes in host plants. Secondary roots form locally at cyst nematode infection sites (Grymaszewska and Golinowski, 1991; Goverse *et al.*, 2000; Lee *et al.*, 2011). Furthermore, the ability to form secondary roots in response to nematode infection can result in better maintenance of shoot growth in some potato and soybean cultivars (Trudgill and Cotes, 1983; Miltner *et al.*, 1991). Nevertheless, the molecular mechanisms regulating secondary root formation in response to belowground herbivory are not well understood.

Cyst nematodes are microscopic root endoparasites that cause large agricultural losses worldwide. These nematodes can persist in the soil in a dormant state for many years (Jones *et al.*, 2013). Exudates from host roots trigger hatching of

dormant second-stage juveniles (J2s) and guide their migration to the root surface. Here, the J2s penetrate the root epidermis of the differentiation or mature root zone by piercing plant cell walls with their needle-like oral stylet and by secreting plant cell-wall degrading enzymes (Bohlmann and Sobczak, 2014). Subsequently, juveniles migrate intracellularly within the cortex, leaving behind a trail of destruction (Wyss and Zunke, 1986; Grundler *et al.*, 1994). Plant cell-wall fragments released during nematode migration can act as damage-associated molecular patterns triggering defense signaling in the host (Shah *et al.*, 2017). Nematode migration also activates biosynthesis and signaling of the defense hormone jasmonate (JA) (Kammerhofer *et al.*, 2015). Upon successful arrival at the vascular cylinder, cyst nematodes utilize stylet-secreted effectors to manipulate plant developmental pathways to transform host cells into permanent feeding sites (Gheysen and Mitchum, 2011). Together with permanent feeding site development, multiple *de novo* formed secondary roots emerge in clusters at nematode infection sites (Grymaszewska and Golinowski, 1991; Goverse *et al.*, 2000; Lee *et al.*, 2011).

Nematode feeding sites are characterized by the local accumulation of the plant hormone auxin (Karczmarek *et al.*, 2004; Grunewald *et al.*, 2009). Auxin transport and auxin-insensitive Arabidopsis mutants infected by cyst nematodes show smaller females and smaller feeding sites, respectively (Goverse *et al.*, 2000; Grunewald *et al.*, 2009). Additionally, auxin is an important regulator of secondary root formation. Oscillations of auxin maxima at the root tip determine the formation of lateral roots in a regularly spaced pattern along the primary root (Fukaki and Tasaka, 2009). However, these oscillations are not required for the *de novo* formation of secondary roots. Ectopic induction of local auxin biosynthesis in pericycle cells via an inducible promoter is sufficient to trigger *de novo* secondary root formation (Dubrovsky *et al.*, 2008). Auxin accumulation in multiple neighboring pericycle cells can lead to the formation of secondary root clusters (Dubrovsky *et al.*, 2008). The spatial co-occurrence of nematode feeding sites and secondary root clusters often corresponds to overlapping regions of auxin accumulation (Karczmarek *et al.*, 2004; Absmanner *et al.*, 2013). This suggests that secondary roots could be induced as the sole consequence of the auxin that accumulates during nematode feeding site development (Goverse *et al.*, 2000). Alternatively, damage caused by nematode infection might also lead to local auxin accumulation and secondary root formation.

Tissue damage triggers auxin accumulation and *de novo* root formation via the JA-dependent ERF109 transcription factor in leaf explants (Liu *et al.*, 2014; Chen *et al.*, 2016; Hu and Xu, 2016; Zhang *et al.*, 2019). Herein, JA accumulates at the site of wounding within a few hours of leaf detachment and triggers expression of the transcription factor ERF109 via the JA receptor COI1. ERF109 binds to the promoter

of the auxin biosynthesis gene *ASA1*, which induces root formation in a process referred to as *de novo* root organogenesis. Direct interaction of JAZ proteins inhibits *ERF109* expression in a negative feedback loop to avoid wound hypersensitivity (Zhang *et al.*, 2019). Sterile mechanical injury in primary roots of Arabidopsis can trigger auxin accumulation at the wounding site and subsequent secondary root formation (Sheng *et al.*, 2017). However, whether this occurs via the same damage signaling pathway as *de novo* root organogenesis from leaf explants is unknown. Furthermore, mechanical injury is an artificial condition and therefore it remains unclear whether the JA-dependent ERF109 pathway is involved in the regulation of secondary root formation also upon naturally occurring damage by herbivory or pathogen penetration.

Previously, we showed that components of the JA-dependent ERF109 pathway are induced by root-knot nematode (*Meloidogyne* spp.) infection (Zhou *et al.*, 2019). Differently from cyst nematodes, root-knot nematodes penetrate roots at the elongation zone and migrate towards the root apical meristem by moving in between cells. Although this type of migration creates minimal tissue damage, root-knot nematode invasion of the root apical meristem induces expression of the *ERF109* transcription factor. This eventually promotes tissue regeneration and reduces the inhibitory effect of nematode infection on primary root growth (Zhou *et al.*, 2019). Thus, wound signaling can mediate primary root growth compensation in response to damage by stealthily migrating root-knot nematodes. However, further research is needed to understand whether JA-dependent wound signaling regulates root architectural changes to compensate for tissue destruction by the more damaging cyst nematodes in the differentiation and mature root zones.

In this study, we hypothesized that local tissue damage by cyst nematode host invasion causes secondary root formation at infection sites via the JA-dependent ERF109 pathway. By challenging Arabidopsis seedlings with increasing numbers of J2s of the beet cyst nematode *Heterodera schachtii*, we found that secondary root formation is induced at infection sites in a nematode-density dependent manner. With time course confocal microscopy of JA biosensors and ERF109 reporter lines in Arabidopsis, we provide evidence that secondary root formation is preceded by the transient and local JA-dependent expression of *ERF109*. Moreover, the nematode-density dependent increase in secondary roots is abolished in *coi1-2* and *erf109* knock-out mutants. By selectively applying the auxin biosynthesis chemical inhibitor L-kynurenine (L-kyn) to shoots and roots, we further found that the ERF109-mediated formation of secondary roots is dependent on local auxin biosynthesis. We therefore conclude that tissue damage by host invading cyst nematodes induces secondary root formation by altering local auxin biosynthesis via the JA-dependent

ERF109 pathway. Altogether, our results show that damage signaling via the JA-dependent ERF109 pathway regulates root architectural plasticity in response to cyst nematode infection.

Materials and methods

Plant material and growth conditions

The Arabidopsis (*Arabidopsis thaliana*) lines Col-0, *pAOS::YFP$_N$* (Poncini *et al.*, 2017), *DR5::GUS/Col-0,* and *DR5::GUS/erf109* (Cai *et al.*, 2014), *p35S::JAS-VENUS/p35S::H2B-RFP* (Larrieu *et al.*, 2015) and *pERF109::GFP/Col-0* (Zhou *et al.*, 2019) were used. The *erf109* mutant was chosen because of the extensive characterization in previous research (Cai *et al.*, 2014; Kong *et al.*, 2018; Zhang *et al.*, 2019; Ye *et al.*, 2020). The weak allele *coi1-2* mutant (Xu *et al.*, 2002) was used since it allows for propagation of homozygous plants and therefore does not need pre-selection with MeJA, which could interfere with the ERF109 pathway. *pERF109::GFP/coi1-2* was obtained through crossing followed by selection of homozygous plants on selective ½ MS medium containing 15 µg ml^{-1} hygromycin B (Melford Laboratories Ltd.) and 20 µg ml^{-1} MeJA (Sigma-Aldrich). Arabidopsis plants were vertically grown in sterile conditions on modified Knop medium (Sijmons *et al.*, 1991) in a growth chamber with a 16 h: 8 h, light: dark photoperiod at 21°C.

Nematode sterilization

Heterodera schachtii (Woensdrecht population from IRS, the Netherlands) cysts were extracted from sand of *Brassica oleracea* infected plants as previously described (Baum *et al.*, 2000) and incubated for seven days in a solution containing 1.5 mg ml^{-1} gentamycin sulfate, 0.05 mg ml^{-1} nystatin and 3mM $ZnCl_2$. Hatched second-stage juveniles (J2s) were purified by centrifugation on a 35% sucrose gradient and surface sterilized for 15 minutes in a solution containing 0.16 mM $HgCl_2$, 0.49 mM NaN_3, and 0.002% Triton X-100. After washing three times with sterile tap water, *H. schachtii* J2s were re-suspended in a sterile 0.7% Gelrite (Duchefa Biochemie) solution. A similar concentration of Gelrite solution was used as mock treatment.

Inoculation density-response curve

Individual Arabidopsis seeds were sown in square Petri dishes. Nine-day-old seedlings were inoculated with 0 (mock), 50, 100, 200, 350, or 500 *H. schachtii* J2s. Specifically, two 5 µl drops of solution (with J2s or mock) were pipetted at opposite sides of each seedling while keeping the Petri dishes vertical. This allowed for a homo-

geneous smear of J2s along the whole length of the root. At 7 days post inoculation (dpi), scans were made of whole seedlings using an Epson Perfection V800 photo scanner. The root architecture (total root length, primary root length, total secondary root length) was measured using the WinRHIZO package for Arabidopsis (Regent Instrument Inc.). For the *coi1-2* mutant, primary root length was measured manually because of the convoluted root system. The number of root tips was counted manually based on the scans. Furthermore, nematodes within the roots were stained with acid fuchsin and counted as previously described (Warmerdam *et al.*, 2018). For comparisons between genotypes, the background effect of the mutation on the root architecture was corrected by normalizing each measured component in infected seedlings to the average respective component in mock-inoculated roots. Additionally, the presence of clusters and the number of secondary roots per cluster were scored using a binocular.

Histology and microscopy

Four-day-old Arabidopsis seedlings were inoculated with either 15 *H. schachtii* J2s or a mock solution. The choice of using younger seedlings like previously done by Zhou *et al.* (2019) was made to reduce the damage inflicted to the seedling during sample preparation for microscopy. Root architecture was inspected using an Olympus SZX10 binocular with a 1.5x objective and 2.5x magnification. Pictures were taken with an AxioCam MRc5 camera (Zeiss). For confocal and brightfield microscopy, single-nematode infection sites were selected for observation. For histochemical staining of β-glucuronidase (GUS) activity, seedlings were incubated in a GUS staining solution as previously described (Zhou *et al.*, 2019) for four hours. Stained seedlings were mounted in a chloral hydrate clearing solution (12 M chloral hydrate, 25% glycerol) and inspected with an Axio Imager.M2 light microscope (Zeiss) via a 20x objective. Differential interference contrast (DIC) images were taken with an AxioCam MRc5 camera (Zeiss). GUS saturation was quantified as previously described (Beziat *et al.*, 2017) using Fiji software (Schindelin *et al.*, 2012). For confocal laser scanning microscopy, seedlings were mounted either in water or in 10 µg ml^{-1} propidium iodide and imaged using a Zeiss LSM 710 system via 10x and 40x objectives. The following wavelengths were used: 600–640 nm for PI, 500-540 nm for GFP, 520-560 nm for YFP, and 590-680 nm for RFP. For *pAOS::YFP*$_N$ and *JAS9-VENUS* reporters, the fluorescent signal was imaged at the focal plane displaying the xylem vessels, where the nematode head is found. For the *pERF109::GFP* reporter, Z-stacks of six 13 µm-slices were made of the entire root depth. Images were taken using the ZEN 2009 software (Zeiss) and processed using Fiji software. To make the fluorescence more visible, the brightness was enhanced for all the representative pictures in the same way using Adobe Photoshop 2021. Fluorescence intensity was

quantified using the Fiji software. Specifically, the region of interest was selected using a set threshold and then the integrated density was measured. Z-Stacks were projected using the maximum intensity method.

Auxin biosynthesis inhibition

For split-plate assays, we used the method described in Matosevich *et al.* (2020). For the L-kyn split plate assay the following four treatment combinations were prepared: MM (modified Knop medium and 0.02% DMSO), KK (modified Knop medium, 10 µM L-kynurenine (Sigma-Aldrich) and 0.02% DMSO), MK (L-kyn only in the root), and KM (L-kyn only in the shoot). The Yucasin split plate assay is described in Fig. S1. Four-day-old Arabidopsis seedlings were inoculated with 15 *H. schachtii* J2s. Sixteen hours post inoculation (hpi), when J2s are still migrating through the root, seedlings were transferred to the treatment plates, so that the shoot and the hypocotyl were in contact with the medium in the upper half of the plate and the nematode-infected root was on the medium in the lower half of the plate. For microscopy, seedlings were collected at 3 dpi and GUS staining was performed. For root architecture inspection, scans were made of whole seedlings at 7 dpi using an Epson Perfection V800 photo scanner. The total number of secondary roots per plant was counted based on the scans. Additionally, the presence of clusters and the number of secondary roots per cluster were scored using an Olympus SZX10 binocular.

Reverse transcription-quantitative real-time PCR

For reverse transcription-quantitative real-time PCR (RT-qPCR) analysis, several hundred root segments (~0.2 cm) harboring nematode infection sites or similar root segments of mock-inoculated 12-day old seedlings of Arabidopsis were collected at 12 hpi. Attention was paid not to include root tips and secondary root primordia. Subsequently, RNA extraction and qPCR were performed as previously described (Chopra *et al.*, 2021; Hasan *et al.*, 2022). *ERF109* was amplified using the primers CTTATGATCGAGCCGCGATT and TCCTCCGTTCCATTGCTCTG (Cai *et al.*, 2014; Zhou *et al.*, 2019). Three independent biological replicates of the experiment were performed, with three technical replicates per each biological replicate. Relative expression of *ERF109* was calculated based on the endogenous control *18S rRNA* (Pfaffl, 2001). The average *ERF109* expression in the mock-inoculated wild-type roots of the first biological replicate was used as a reference to normalize the average expression in the other samples (Hasan *et al.*, 2022).

Statistical analyses

Statistical analyses were performed using the R software version 3.6.3 (Windows,

x64). Correlation between variables was calculated using Spearman Rank-Order Correlation coefficient. Significance of the differences between samples was calculated as indicated in the figure legends. The confidence interval of the inoculum density-response curves was calculated by loess regression (as per default in geom_smooth) in R.

Results

H. schachtii infection induces local formation of secondary roots in a nematode density-dependent manner

To test if tissue damage by invading nematodes in roots triggers the formation of secondary roots, we analyzed root branching upon penetration by increasing numbers of nematodes. We inoculated seedlings with 0, 50, 100, 200, 350, or 500 J2s of *H. schachtii* and counted both the number of nematodes that penetrated the roots and the total number of secondary roots at 7 dpi (Fig. 1). Here, the total number of secondary roots in infected seedlings was normalized to the average respective number in uninfected roots. We found that the number of nematodes that penetrated the roots increased by inoculum density for up to 350 J2s per plant, whereafter it remained the same (Fig. 1a). Furthermore, we observed that the number of penetrated nematodes correlated positively with the total number of secondary roots per plant (Fig. 1b). Next, we investigated if the clustering of secondary roots around nematode infections sites also correlates with the inoculum density (Fig. 1c,d). For this, we challenged Arabidopsis with four inoculum densities (0, 50, 100, and 350) to establish an incremental increase in the number of nematode infection sites per plant. Infection sites were identified by the local discoloration of root tissue due to cell necrosis along the migratory tract of the nematode (Grundler *et al.*, 1994). Roots were counted as clusters when more than one secondary root emerged in proximity of an infection site. Also, we counted the number of secondary roots per cluster. We found that uninfected seedlings showed a typical pattern of lateral roots regularly distributed along the primary root (Fig. 1c). However, in infected seedlings clusters of secondary roots emerged close to nematode infection sites in an inoculum density-dependent manner (Fig. 1c,d). Interestingly, also the number of secondary roots per cluster significantly increased at inoculum density 350 compared to 50 (Fig. 1c,e). Moreover, higher inoculation densities caused more extensive discoloration at the infection sites indicating higher levels of tissue damage. Altogether, these observations showed that infection by *H. schachtii* triggers local density-dependent formation of secondary roots.

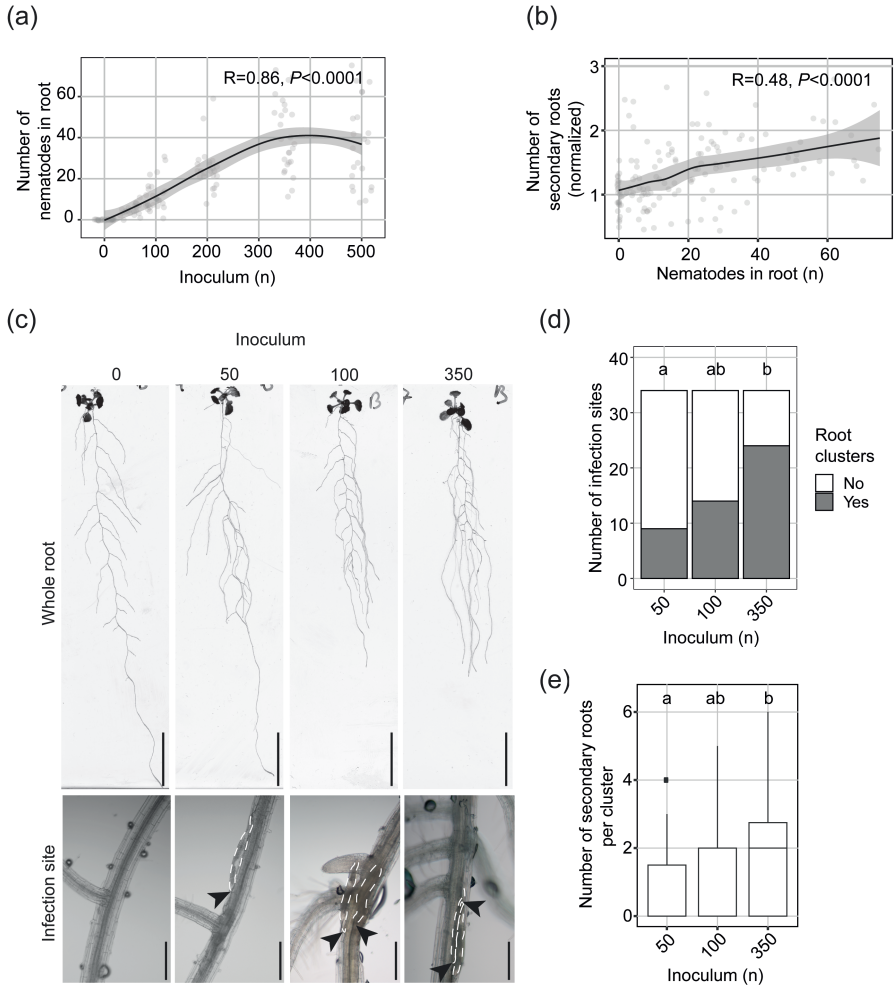

Fig. 1 Secondary roots form locally at *Heterodera schachtii* infection sites in a nematode density-dependent manner. Nine-day-old Arabidopsis Col-0 seedlings were inoculated with increasing numbers of *H. schachtii* second-stage juveniles (J2s), ranging from 0 (mock) to 500 J2s per seedling. At 7 days post inoculation (dpi), scans were made of the root systems and the total number of secondary roots per plant was counted. Fuchsin staining was performed to count the number of J2s that had penetrated the roots. Additionally, the presence of clusters and the number of secondary roots per cluster was scored. (a) Number of nematodes that successfully penetrated the roots per inoculum. (b) Number of secondary roots formed per number of nematodes inside the roots. The total number of secondary roots in infected seedlings was normalized to the average respective component in uninfected roots and correlated with the number of nematodes inside the roots. Data from three independent biological repeats of the experiment was combined. Correlation (R) between two variables was calculated using Spearman's Rank-Order Correlation coefficient (n=30, P<0.0001). Grey area indicates the 95% confidence interval. (c) Representative pictures of whole roots and infection sites in Col-0 seedlings inoculated with 0 (mock), 50, 100, and 350

J2s. Scale bars in whole root and infection site pictures are 2 cm and 200 µm, respectively. Black arrowheads indicate the nematodes head; white dotted lines outline the nematodes body. (d) The proportions of secondary root clusters close to infection sites in Arabidopsis seedlings inoculated with 50, 100, and 350 J2s. Statistical significance was calculated by a Pairwise Z-test (n=34, $P<0.05$). (e) Number of secondary roots within each root cluster in Arabidopsis seedlings inoculated with 50, 100, and 350 J2s. Statistical significance was calculated by pairwise Wilcoxon test followed by false discovery rate correction for multiple comparisons (n=34, $P<0.001$). For boxplots, the horizontal line represents the median, the whiskers indicate the maximum/minimum range and the black dots represent the outliers. Different letters indicate statistically different groups.

H. schachtii host invasion induces JA biosynthesis and signaling

Artificially induced tissue damage can trigger the formation of roots via JA-dependent signaling pathways. For instance, wounding induces JA-dependent *de novo* root organogenesis in leaf explants (Zhang *et al.*, 2019). Infective juveniles of *H. schachtii* invade the host by destructive thrusts of the oral stylet and release of plant cell-wall degrading enzymes causing extensive cell damage during host invasion (Grundler *et al.*, 1994; Tytgat *et al.*, 2002; Vanholme *et al.*, 2007). We hypothesized that secondary root formation in proximity of *H. schachtii* infection sites might be regulated by JA, in response to tissue damage associated with nematode host invasion. To test our hypothesis, we investigated whether JA biosynthesis and signaling were activated during *H. schachtii* infection using the JA biosynthesis reporter line *pAOS::YFP*$_N$ (Poncini *et al.*, 2017) and the JA signaling biosensor *JAS9-VENUS* (*p35S::JAS9-VENUS/p35S::H2B-RFP*) (Larrieu *et al.*, 2015) (Fig. 2). We chose three timepoints that reflect the early parasitic stages of intracellular host invasion (12 hpi), permanent feeding site initiation (24 hpi), and permanent feeding site expansion (168 hpi) (Tytgat *et al.*, 2002; Hewezi *et al.*, 2014; Kammerhofer *et al.*, 2015; Marhavy *et al.*, 2019). Importantly, to avoid interference of signals due to the presence of multiple nematodes at one infection site, we selected single-nematode infection sites for our observations. We found that infection with *H. schachtii* significantly induces transient expression of *pAOS::YFP*$_N$, with the highest level of expression at 12 hpi (Fig. 2a-d). Likewise, *JAS9-VENUS* showed a strong JA signaling activity (i.e., low VENUS/RFP ratio) in infected roots at 12 hpi, which decreased over time to the level of uninfected root tissue at 168 hpi (Fig. 2e-h). These observations demonstrated that both JA biosynthesis and JA signaling are strongly induced during and shortly after *H. schachtii* host invasion close to the nematode infection site. We therefore concluded that tissue damage caused by *H. schachtii* during intracellular host invasion triggers local JA biosynthesis and signaling in Arabidopsis.

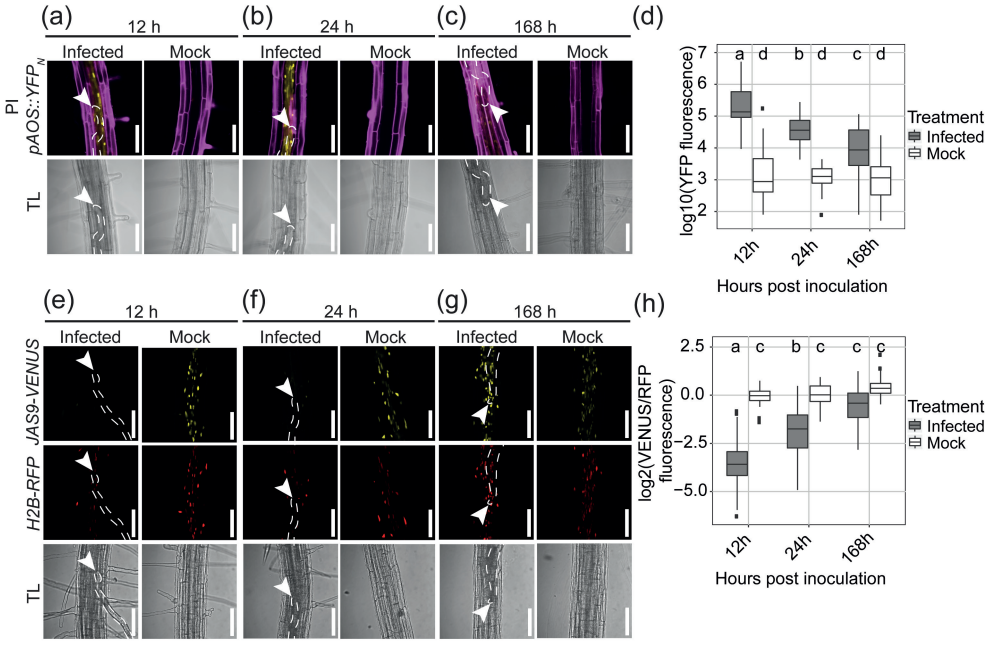

Fig. 2 Transient induction of jasmonate (JA) biosynthesis and signaling at *Heterodera schachtii* infection sites. Four-day-old Arabidopsis seedlings were either inoculated with 15 *H. schachtii* second-stage juveniles (J2s) or mock-inoculated. At 12, 24, and 168 hours post inoculation (hpi) seedlings were mounted in 10 µg ml^{-1} propidium iodide (PI) and then imaged using a fluorescent confocal microscope. Single-nematode infection sites were selected for observation. (a-c) Representative pictures of infected and non-infected roots expressing the JA biosynthesis marker *pAOS::YFP$_N$*. To make the fluorescence more visible, the brightness was enhanced for all the representative pictures in the same way. (d) Quantification of YFP intensity in the *pAOS::YFP$_N$* line. Values represent the log$_{10}$ of the YFP integrated density. (e-g) Representative pictures of infected and non-infected roots expressing the JA biosensor *p35S::JAS9-VENUS/p35S::H2B-RFP*. To make the fluorescence more visible, the brightness was enhanced for all the representative pictures in the same way. (h) Quantification of the JA signaling repressor motif *JAS9*. Values represent the log$_2$ of the fluorescence ratio between *JAS9-VENUS* and *H2B-RFP* raw integrated densities. Data from three independent biological repeats of the experiment was combined. Significance of differences between fluorescent intensities in nematode-infected and non-infected seedlings over the different timepoints was calculated by ANOVA followed by Tukey's HSD test for multiple comparisons (n=30, *P*<0.0001). For boxplots, the horizontal line represents the median, the whiskers indicate the maximum/minimum range and the black dots represent the outliers. Different letters indicate statistically different groups. White arrowheads indicate the nematode head; white dotted lines outline the nematode body. TL=transmission light. Scale bar is 100 µm.

COI1-mediated JA signaling regulates ERF109 expression upon H. schachtii infection

Root tip resection or wounding in leaf explants induce *ERF109* expression in a

COI1-dependent manner (Zhang *et al.*, 2019; Zhou *et al.*, 2019). To determine if *H. schachtii*-induced JA signaling also triggers *ERF109* expression, we monitored *pERF109::GFP* expression within single-nematode infection sites in the *coi1-2* mutant and wild-type Arabidopsis Col-0 plants during the early stages of infection by *H. schachtii* (Fig. 3). Similar to what we observed for JA biosynthesis and signaling, *ERF109* expression was induced at early timepoints (12 and 24 hpi) of *H. schachtii* infection around the migratory track of the nematodes in wild-type Col-0 (Fig. 3a-c). Moreover, in the *coi1-2* mutant, *pERF109::GFP* fluorescence was significantly reduced compared to wild-type Arabidopsis (Fig. 3d). Nevertheless, we observed a slight increase in fluorescence in *coi1-2* mutant over time, which reached the fluorescence levels detected in Col-0 at 168 hpi. The fluorescence detected in wild-type Col-0 and *coi1-2* mutant at 168 hpi might be caused by tissue autofluorescence from the cell walls of the permanent feeding sites (Hoth *et al.*, 2005). Since *pERF109::GFP* has a nuclear-cytoplasmic localization (Zhou *et al.*, 2019) due to GFP diffusion into the nucleus (Hanson and Kohler, 2001), autofluorescence from cell walls in syncytia cannot be easily distinguished from the cytoplasmic part of the *pERF109::GFP* signal. However, after quantifying only nuclear-localized *pERF109::GFP*, the initially observed fluorescence in the nematode-infected wild-type Col-0 and *coi1-2* mutant plants at 168 hpi was not detected anymore, pointing at autofluorescence as the most plausible cause (Fig. S2). To independently verify a COI1-dependent regulation of *ERF109* expression, we also performed a RT-qPCR on ERF109 transcripts in root segments containing nematode infection sites collected from *coi1-2* and wild-type Col-0 at 12 hpi. Consistent with the observed regulation of *pERF109::GFP* fluorescence, we found significantly fewer transcripts of *ERF109* in *coi1-2* compared to wild-type Col-0 (Fig. 3e). We therefore concluded that *H. schachtii* induces *ERF109* expression during host invasion in a JA-dependent manner.

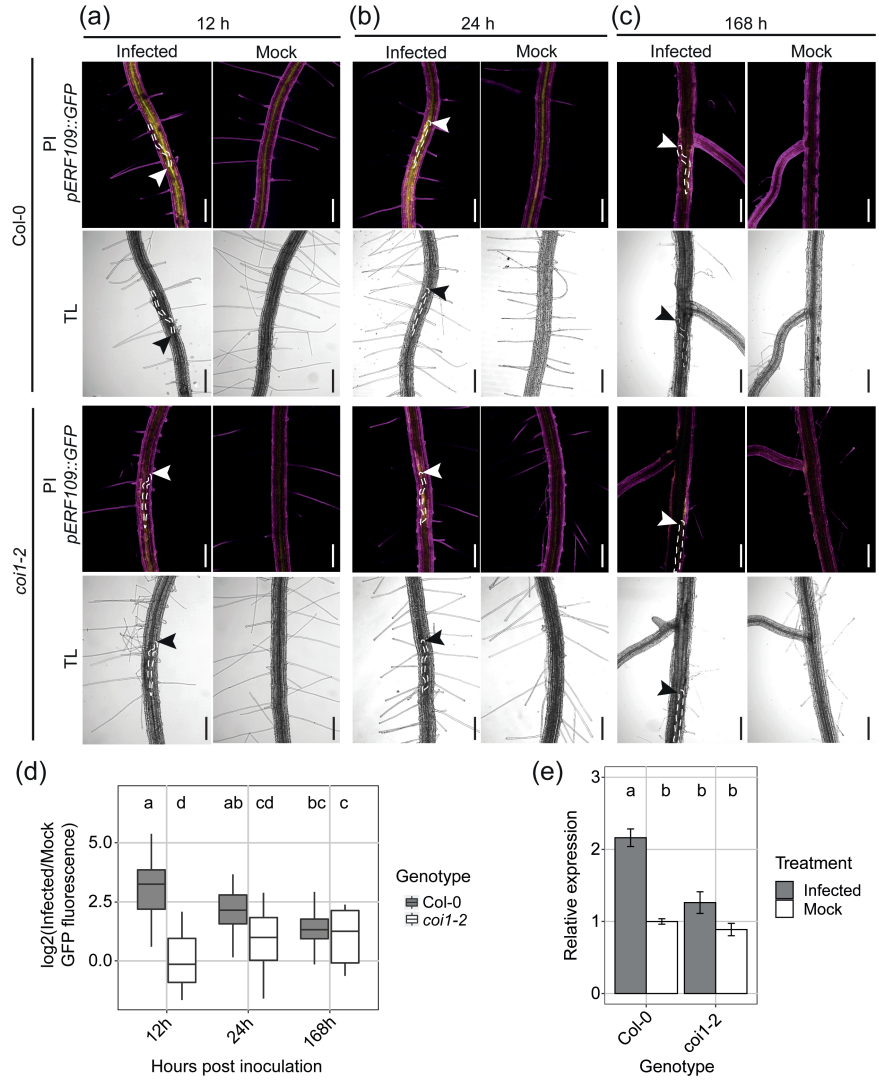

Fig. 3 *ERF109* expression upon *Heterodera schachtii* host invasion is dependent on COI1-mediated jasmonate (JA) signaling. (a-d) Four-day-old Arabidopsis seedlings were either inoculated with 15 *H. schachtii* second-stage juveniles (J2s) or mock-inoculated. At 12, 24, and 168 hours post inoculation (hpi) seedlings were mounted in 10 µg ml^{-1} propidium iodide (PI) and then imaged using a fluorescent confocal microscope. Single-nematode infection sites were selected for observation. (a-c) Representative pictures of infected and mock-inoculated seedlings expressing the *pERF109::GFP* construct in either wild-type Col-0 or mutant *coi1-2* background at 12 hpi (a), 24 hpi (b), and 168 hpi (c). To make the fluorescence more visible, the brightness was enhanced for all the representative pictures in the same way. (d) Quantification of *pERF109::GFP* fluorescent intensity induced by infection of Col-0 and *coi1-2* roots. Values represent $\log_2$ of the fluorescence ratio between the GFP integrated density of infected and non-infected roots. Data from two independent biological repeats of the experiment was combined. Significance of dif-

ferences between fluorescent intensities in Col-0 and *coi1-2* roots over the different timepoints was calculated by ANOVA followed by Tukey's HSD test for multiple comparisons (n=20, $P<0.05$). For boxplots, the horizontal line represents the median and the whiskers indicate the maximum/minimum range. Different letters indicate statistically different groups. White and black arrowheads indicate the nematode head; white dotted lines outline the nematode body. TL=transmission light. Scale bar is 200 µm. e) 12-day-old Col-0 and *coi1-2* Arabidopsis plants were inoculated with *H. schachtii.* At 12 hpi, RNA was extracted from root segments of ~ 0.2 cm harboring nematode infection sites or similar root segments of mock-inoculated seedlings. Data represents three independent biological replicates with three technical replicates per biological replicate. Relative expression of *ERF109* was first calculated based on the endogenous control *18s rRNA* and then normalized to the mock-inoculated wild-type samples in the first biological replicate. Significance of differences between *ERF109* relative expression in Col-0 and *coi1-2* infected roots was calculated by ANOVA followed by Tukey's HSD test for multiple comparisons (n=3 biological replicates, $P<0.01$). Different letters indicate statistically different groups. Error bars represent standard error of the mean.

COI1 and ERF109 regulate secondary root formation upon H. schachtii infection

Next, we asked if the activation of JA-dependent expression of *ERF109* is required for the formation of secondary roots during *H. schachtii* infections. If this holds true, the nematode density-dependent increase in secondary roots observed for wild-type Col-0 should be altered in both *coi1-2* and *erf109* mutants. To test this, we performed the same density-response experiment as shown in Figure 1a and b. At 7 dpi, the number of nematodes that had successfully penetrated the roots did not differ significantly between wild-type Col-0 and the *erf109* mutant (Fig. 4). In contrast, the number of nematodes was significantly higher in roots of the *coi1-2* mutant compared to wild-type Arabidopsis plants, indicating a role of COI1 in plant susceptibility to penetration by *H. schachtii* (Fig. 4b). However, it must be noted that the uninfected *coi1-2* mutant had a much larger root system compared to wild-type Arabidopsis Col-0 (Fig. S3), which also may influence the number of nematode penetrations. Nevertheless, while nematode infections in wild-type Arabidopsis induced the formation of secondary roots, no such increase was observed for *erf109* and *coi1-2* mutants (Fig. 4c). In conclusion, both COI1 and ERF109 regulate the density-dependent induction of secondary root formation by *H. schachtii*. This induction of secondary root formation is independent from plant susceptibility to nematode penetration.

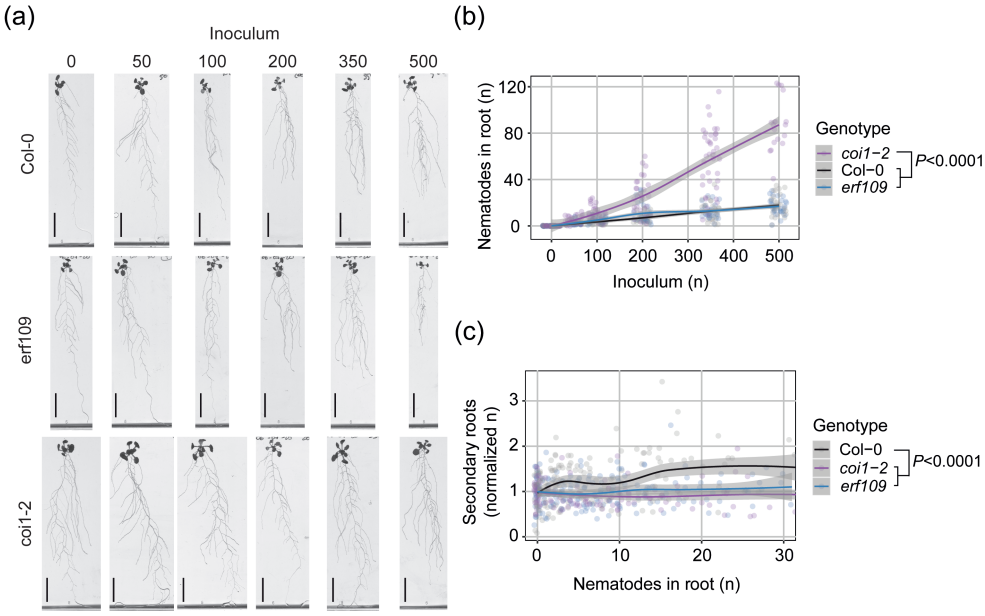

Fig. 4 ERF109 and COI1 regulate the nematode density-dependent secondary root formation that is triggered by *Heterodera schachtii* infections. Nine-day-old wild-type Col-0, *erf109,* and *coi1-2* seedlings were inoculated with increasing numbers of *H. schachtii* second-stage juveniles (J2s), ranging from 0 (mock) to 500 J2s per seedling. At 7 days post inoculation, scans were made of the root systems and the number of secondary roots per plant was counted. Fuchsin staining was performed to count the number of J2s that had penetrated the roots. (a) Representative pictures of wild-type Col-0, *erf109,* and *coi1-2* infected seedlings at 7 dpi. (b) Number of nematodes that successfully penetrated the roots per inoculum. (c) Secondary roots formed per number of nematodes inside the roots. The total number of secondary roots in infected seedlings was normalized to the average respective component in mock-treated roots. Data of three independent biological repeats of the experiment was combined. Significance of differences between genotypes was calculated by ANOVA followed by Tukey's HSD test for multiple comparisons (n=30, P<0.0001). Grey area indicates the 95% confidence interval. Scale bar is 2 cm.

ERF109-mediated induction of secondary root formation compensates for primary root growth inhibition by H. schachtii

The induction of secondary root formation by cyst nematodes might compensate for a possible inhibition of root growth by nematode invasion. To test this hypothesis, we investigated whether the total length of the entire root system, the primary root length, and the total length of the secondary roots were altered in the infected *erf109* mutant compared to wild-type Col-0 (Fig. 5). To eliminate the background effect of the mutation on the root architecture, we normalized each measured component in infected seedlings to the average respective component in uninfected roots. We found that the total length of the root system of wild-type Col-0 at increasing num-

bers of nematodes remains similar to that of uninfected plants (i.e., close to 1 in Fig. 5a). In contrast, the total length of the entire root system in the *erf109* mutant decreased by nematode density as compared to uninfected plants. As the total length of the root system is the sum of the lengths of the primary roots and the secondary roots, we also analyzed these components separately. The primary root length of both wild-type Col-0 and the *erf109* mutant declined by nematode density (Fig. 5b). This decline was slightly but significantly exacerbated by the *erf109* mutation. However, we found a more striking difference in the total length of the secondary roots between wild-type Col-0 and the *erf109* mutant (Fig. 5c). In wild-type Col-0, we observed a significant increase in the total length of the secondary roots by nematode density, sufficient to compensate for the loss in primary root length. However, we observed no significant increase in the total length of the secondary roots by nematode density in the *erf109* mutant, which explains why the total length of the root system by nematode density remained stable for wild-type Col-0, but not for the *erf109* mutant. Based on our data, we conclude that ERF109-mediated formation of secondary roots compensates for primary root growth inhibition by *H. schachtii*.

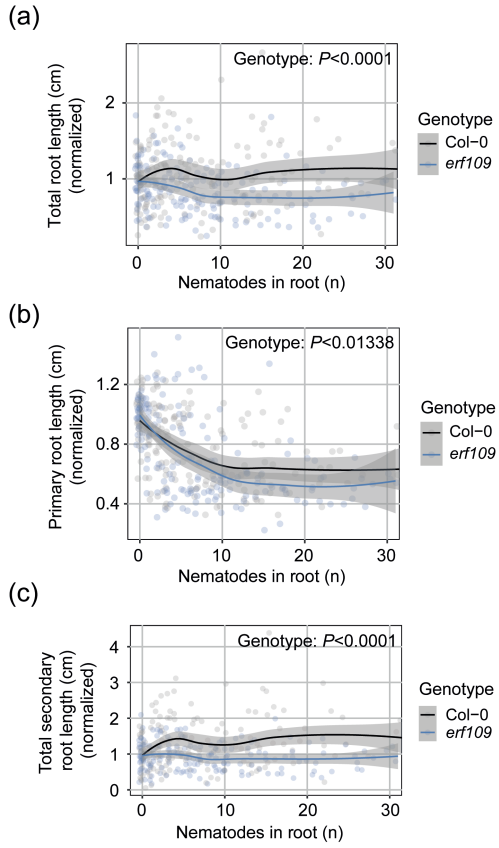

Fig. 5 ERF109-mediated secondary root formation allows for maintenance of total root length despite primary root growth inhibition by *Heterodera schachtii*. Nine-day-old Col-0 and *erf109* Arabidopsis seedlings were inoculated with increasing *H. schachtii* densities ranging from 0 (mock) to 500 second-stage juveniles (J2s) per seedling. At 7 days post inoculation, scans were made of the root systems and the root length was measured using WinRHIZO. Total, primary, and secondary root length was normalized to the average respective component in mock-treated roots. Fuchsin staining was performed for counting the number of J2s that penetrated the roots. (a) Total root length per number of nematodes in the roots. (b) Primary root length per number of nematodes in the roots. (c) Total secondary root length per number of nematodes in the roots. Data from three independent biological repeats of the experiment was combined. Significance of differences between genotypes was calculated by ANOVA (n=30). Grey area indicates the 95% confidence interval.

ERF109 regulates local auxin biosynthesis at the nematode infection site

ERF109 mediates JA-induced secondary root formation by directly binding to the promoter of auxin biosynthesis genes *ASA1* and *YUC2* (Cai *et al.*, 2014). We hypothesized that ERF109 regulates secondary root formation by inducing local auxin

biosynthesis at the nematode infection site. Thus, we used a split plate assay containing growth media with and without L-kyn to chemically inhibit auxin biosynthesis in the shoots and/or the roots of infected wild-type and *erf109* plants (Fig. 6). The local accumulation of auxin was monitored using the *DR5::GUS* reporter (Fig. 6a). When seedlings were grown on regular medium or when auxin biosynthesis was inhibited by L-kyn only in the shoots, *DR5::GUS* was expressed at nematode infection sites in wild-type Col-0 seedlings. However, when auxin biosynthesis was inhibited in both shoots and roots or only in the roots by treatment with L-kyn, no *DR5::GUS* expression was observed (Fig. 6b,c). This suggested that auxin accumulation at nematode infection sites was dependent on local auxin biosynthesis in the roots. Importantly, we observed that the auxin accumulation at nematode infection sites via root-localized auxin biosynthesis was disrupted in the *erf109* mutant. Indeed, *DR5::GUS* expression was significantly lower at the nematode infection sites in *erf109* seedlings compared to wild-type Col-0 when auxin biosynthesis was permitted in the root (Fig. 6b,c). To determine if the differences in *DR5::GUS* between the two Arabidopsis genotypes were only local at the nematode infection site or systemic throughout the root system, we also looked at *DR5::GUS* expression in root tips (Fig. 6d, S4). In contrast to nematode infection sites, when auxin biosynthesis was inhibited only in the shoots, we observed no difference between *erf109* and wild-type Col-0 in *DR5::GUS* expression in the root tip (Fig. 6d, S4). Since L-kyn has been shown to also inhibit ethylene-induced auxin biosynthesis (He *et al.*, 2011) we also performed the experiment using the auxin biosynthesis inhibitor Yucasin (Yuc). Due to the higher concentration of DMSO used to dissolve Yuc, an overall lower frequency of *DR5:GUS* staining was observed. Nevertheless, the Yuc split plate assay showed the same trend as the L-kyn experiment (Fig. S1). From these results, we concluded that ERF109 regulates local auxin biosynthesis at infection sites of *H. schachtii*.

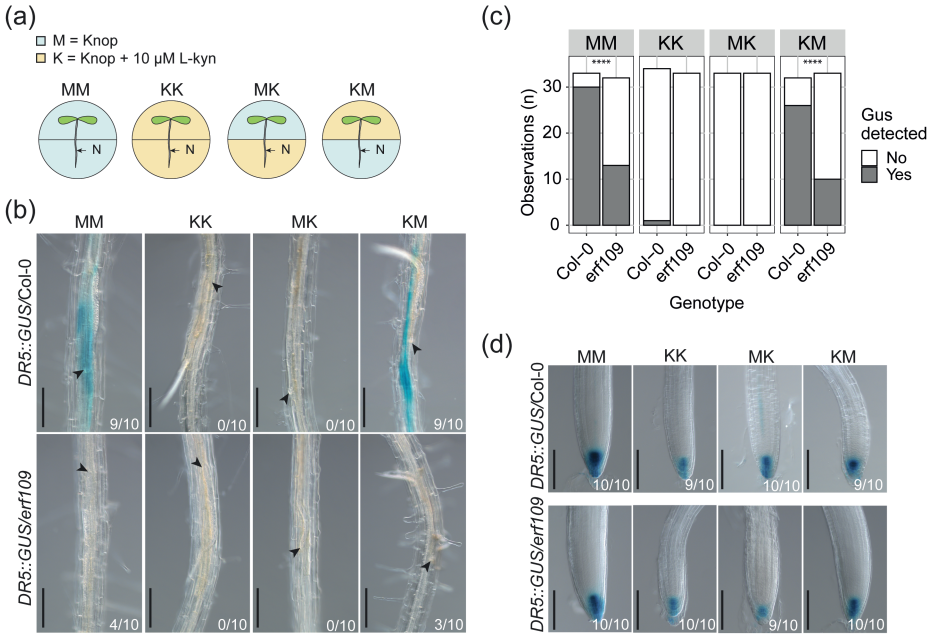

Fig. 6 ERF109 regulates local auxin biosynthesis at *Heterodera schachtii* infection sites. Four-day-old Arabidopsis Col-0 and *erf109* seedlings expressing the auxin *DR5::GUS* reporter were infected with 15 *H. schachtii* second-stage juveniles (J2s). At 16 hours post inoculation, seedlings were transferred to treatment plates. Four treatment combinations were prepared: MM (modified Knop medium and 0.02% DMSO), KK (modified Knop medium, 10µM L-kyn and 0.02% DMSO), MK (L-kyn only in the root), KM (L-kyn only in the shoot). At 3 days post inoculation GUS staining assay was performed for 4 hours and seedlings were imaged. Single-nematode infection sites were selected for observation. (a) Experimental design with Arabidopsis seedlings transferred to split plates with modified Knop medium either with or without L-kyn. N = nematode. (b) *DR5::GUS* expression at nematode infection sites in wild-type Col-0 and *erf109* roots in the four different treatment combinations with or without L-kyn applied to shoots and/or roots. (c) Number of observations with (Yes) or without (No) GUS staining at the nematode infection sites in roots of wild-type Col-0 and *erf109* plants. Statistical significance was calculated by a Pairwise Z-test (n=33, ****, $P<0.0001$). (d) *DR5::GUS* expression in the root tips of Col-0 and *erf109* roots. Black arrowheads indicate the nematode head. Frequencies at the bottom right corner indicate how many times GUS staining was observed in one of the three independent biological repeats of the experiment. Scale bar is 200 µm.

ERF109-induced secondary root formation upon H. schachtii infection is dependent on local auxin biosynthesis

We found that ERF109 regulates local auxin biosynthesis at *H. schachtii* infection sites. This raised the question if the ERF109-mediated secondary root formation upon *H. schachtii* infection is dependent on this local biosynthesis of auxin. To test this, we inoculated four-day-old wild-type Col-0 and *erf109* seedlings with either 15

H. schachtii J2s or a mock solution. At 16 hpi, seedlings were transferred to the four previously described split-plates containing medium with and without 10 µM L-kyn (Fig. 6a). At 7 dpi, the total number of secondary roots was scored. As expected, the different treatment combinations with and without L-kyn in the shoots and/or roots led to a different number of lateral roots in the uninfected roots (Fig. S5). Therefore, to calculate the number of additional secondary roots induced by nematode infection, the number of secondary roots in infected roots was normalized to the average respective component in uninfected roots. Additionally, we scored how often a cluster of roots occurs in proximity of an infection site and the number of secondary roots per cluster (Fig. 7). When auxin biosynthesis was inhibited in both shoots and roots or only in the roots no additional secondary roots formed in infected Col-0 wild-type seedlings (Fig. 7a,b). Consistently, no clusters of secondary roots were found at nematode infection sites (Fig. 7c-e). However, inhibition of auxin biosynthesis in the shoots alone led to a significant reduction in the total number of secondary roots in infected seedlings (Fig. 7a, b) as well as in the number of clusters and the number of secondary roots per cluster compared to when auxin biosynthesis was permitted in both shoots and roots (Fig. 7c-e; treatment MM versus KM). Thus, secondary root formation upon *H. schachtii* infection is dependent on local auxin biosynthesis, although polar auxin transport from the shoots might still play a role. Furthermore, the mutation in *erf109* strongly affected secondary root formation when auxin biosynthesis was permitted in the roots. Indeed, a significant decrease in the number of additional secondary roots, the number of clusters of secondary roots, and the number of secondary roots per cluster was observed for *erf109* when compared to wild-type Col-0 (Fig. 7). Altogether, we concluded that ERF109-dependent secondary root formation upon *H. schachtii* infection relies at least partially on local auxin biosynthesis.

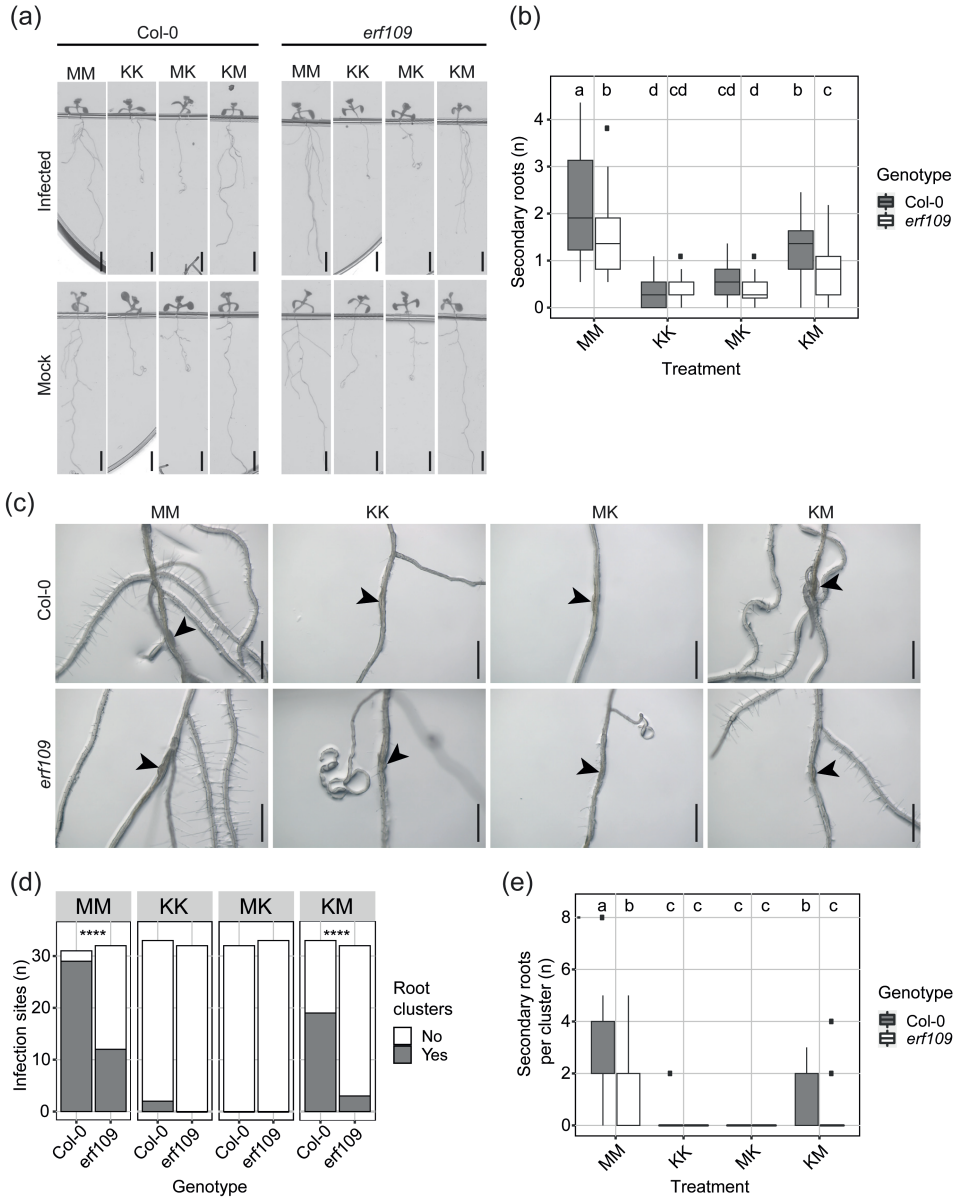

Fig. 7. ERF109-dependent local auxin biosynthesis regulates secondary root formation upon *Heterodera schachtii* infection. Four-day-old Arabidopsis Col-0 and *erf109* seedlings were either infected with 15 *H. schachtii* second-stage juveniles (J2s) or mock-inoculated. At 16 hours post inoculation, seedlings were transferred to treatment plates. Four treatment combinations were prepared: MM (modified Knop medium and 0.02% DMSO), KK (modified Knop medium, 10µM L-kyn and 0.02% DMSO), MK (L-kyn only in the root), KM (L-kyn only in the shoot). At 7 days post inoculation, scans were made of the root systems and

the total number of secondary roots per plant was counted. Additionally, the presence of clusters and the number of secondary roots per cluster was scored. (a) Representative pictures of wild-type Col-0 and *erf109* mutant seedlings. (b) Number of secondary roots in infected versus non-infected roots of wild-type Col-0 and *erf109* seedlings. Data of two independent biological repeats of the experiment was combined. Significance of differences in secondary roots between the different treatment combinations was calculated by ANOVA followed by Tukey's HSD test for multiple comparisons (n=43-45, $P<0.05$). (c) Representative images of nematode infection sites in wild-type Col-0 and *erf109* mutant. (d) Number of secondary root clusters that are associated with *H. schachtii* infection sites. Data of two independent biological repeats of the experiment was combined. Statistical significance was calculated by a Pairwise Z-test n=31-33, ****, $P<0.0001$). (e) Number of secondary roots per cluster. Data of two independent biological repeats of the experiment was combined. Significance of differences between secondary roots within a cluster was calculated by Aligned Rank Transform for non-parametric factorial ANOVA followed by Tukey's HSD test for multiple comparisons (n=31-33, $P<0.0001$). For boxplots, the horizontal line represents the median, the whiskers indicate the maximum/minimum range and the black dots represent the outliers. Difference in letters indicates statistically different groups. Black arrowheads indicate the infection site. Scale bar is 0.5 cm.

Discussion

Root architecture plasticity in response to stress by soil-borne pathogens and pests is a largely unexplored field of research. Root parasitism by cyst nematodes is often associated with formation of secondary roots in proximity of infection sites (Grymaszewska and Golinowski, 1991; Goverse *et al.*, 2000; Lee *et al.*, 2011). However, the molecular mechanisms regulating secondary root formation in response to cyst nematode infection have thus far remained unclear. Here, we provide evidence for a model wherein formation of secondary roots near *H. schachtii* infection sites is triggered by tissue damage caused by nematode invasion. This response is regulated by the JA-dependent ERF109-activated local biosynthesis of auxin.

Our data demonstrates that secondary root formation is most likely initiated by tissue damage brought about by cyst nematode infections. The number of secondary roots induced by *H. schachtii* correlated positively with the number of nematodes that penetrated the roots. This increase in the number of secondary roots may be simply due to an increase in the number of infection sites. However, we also observed more nematodes within infection sites at higher inoculation densities, which correlated well with the number of secondary roots per infection site. This may mean that infection sites containing multiple nematodes developed a higher number of secondary roots per cluster compared to single-nematode associated infection sites. Moreover, we saw more extensive root tissue damage (i.e., root discoloring) at infection sites harboring multiple nematodes. We therefore consider tissue damage by infective juveniles inside roots as the likely cause of enhanced local secondary root formation.

Tissue damage in Arabidopsis leaf explants triggers *de novo* root organogenesis in a JA-dependent manner (Zhang *et al.*, 2019). We found that intracellular host invasion by *H. schachtii* transiently induces JA biosynthesis and signaling, and that the JA receptor mutant *coi1-2* is defective in secondary root formation upon *H. schachtii* infection. Our results are in line with whole transcriptome analyses of root segments of Arabidopsis harboring migrating juveniles of *H. schachtii* at 10 hpi, which also showed that JA biosynthesis and signaling genes are upregulated during host invasion (Kammerhofer *et al.*, 2015; Mendy *et al.*, 2017). In contrast, recent reports indicate that host invasion by *H. schachtii* does not activate the JA signaling biosensor *JAZ10::NLS-3xVENUS* in Arabidopsis roots (Marhavy *et al.*, 2019). The discrepancy between our observations with the *JAS9-VENUS* biosensor and the observations with the *JAZ10::NLS-3xVENUS* biosensor might be due to differences in sensitivity of both sensor constructs. As compared to *JAZ10::NLS-3xVENUS,* the *JAS9-VENUS* biosensor is particularly sensitive to biologically active JA (JA-isoleucine) enabling the visualization of local JA signaling in response to stress in Arabidopsis roots at a high spatiotemporal resolution (Larrieu *et al.*, 2015). Furthermore, *JAS9-VENUS* has been used to monitor the dynamics of JA signaling in response to single-cell ablation and intercellular migration of the less-damaging root-knot nematodes in Arabidopsis roots (Zhou *et al.*, 2019). Therefore, based on the activity of the *JAS9-VENUS* biosensor in our experiments, we conclude that the tissue damage associated with host invasion triggers a JA signal in cells close to the infection site of *H. schachtii*. Moreover, the transient nature of the JA signal suggests that the damage trigger decreases after nematode host invasion, or that JA signaling is actively suppressed by *H. schachtii* when infective juveniles become sedentary.

JA signaling during *H. schachtii* migration also results in activation of plant defense responses (Kammerhofer *et al.*, 2015). We observed that the *coi1-2* mutant is more susceptible to penetration by *H. schachtii*, which is in line with previous findings showing a negative effect of exogenous JA on *H. schachtii* penetration rate (Kammerhofer *et al.*, 2015). However, after nematode penetration, COI1 does not affect the rate at which J2s induce a permanent feeding site (Marhavy *et al.*, 2019). Altogether, these findings suggest that JA signaling both negatively regulates host penetration rate by *H. schachtii* and mediates secondary root formation at *H. schachtii* infection sites.

The damage-induced formation of secondary roots by *H. schachtii* appears to be regulated by the JA-dependent expression of *ERF109*. We found that the expression of *ERF109*, which showed the same transient induction pattern as the JA biosynthesis reporter *AOS* and *JAS9-VENUS* biosensor, was abrogated in *coi1-2* mutant. Moreover, the *erf109* mutant was as defective as the *coi1-2* mutant in the densi-

ty-dependent secondary root formation upon *H. schachtii* infection. Consistently with our data, *ERF109* expression showed a COI1-dependent transient expression upon wounding in leaf explants (Zhang *et al.*, 2019). Furthermore, the *erf109* mutation also disrupted the induction of secondary root formation by exogenous application of JA (Cai *et al.*, 2014). Altogether, our findings show that tissue damage by invading nematodes triggers a JA signal, which induces the ERF109-dependent formation of secondary roots.

Next, our data provides evidence that damage-induced activation of *ERF109* regulates formation of secondary roots via local auxin biosynthesis. The local accumulation of auxin at nematode infection sites (i.e., expression of the auxin reporter *DR5::GUS*) was strongly reduced in the *erf109* mutant compared to wild-type plants. However, when auxin biosynthesis was blocked in whole seedlings or only in roots, the local accumulation of auxin at nematode infection sites was completely abolished in both the *erf109* mutant and wild-type Arabidopsis. Taken together, this demonstrates that auxin accumulation at nematode infection sites is at least partially dependent on ERF109-regulated local auxin biosynthesis. Importantly, the patterns observed for local accumulation of auxin at nematode infection sites matched the patterns of secondary root formation in absence or presence of the auxin biosynthesis inhibitor. The inhibition of auxin biosynthesis in the roots, but not in the shoots, abolished the formation of secondary roots upon nematode infection. Previously, ERF109 was shown to regulate secondary root formation by binding the promoter of auxin biosynthesis genes upon exogenous application of JA (Cai *et al.*, 2014). Here, our data shows that tissue damage by nematodes activates JA signaling and subsequently induces ERF109, which on its turn regulates secondary root formation via local biosynthesis of auxin.

After blocking auxin biosynthesis in the shoots, we observed auxin accumulation and formation of secondary roots at nematode infection sites, which indicates that polar auxin transport from the shoots is not required for secondary root formation at nematode infection sites. Nevertheless, we noted a quantitative effect of the inhibition of auxin biosynthesis in shoots, leading to the formation of fewer secondary root clusters and fewer secondary roots per cluster as compared to untreated plants. This implies that polar auxin transport from the shoots may still play a complementary role in secondary root formation at nematode infection sites, albeit below the detection levels of the *DR5::GUS* reporter. Polar auxin transport from the shoots and further redistribution in root tissue results from the coordinated activities of auxin influx and efflux carrier proteins (Petrasek and Friml, 2009). Lee *et al.* (2011) showed that *H. schachtii* induces the formation of secondary roots in double *aux1lax3* and quadruple *aux1lax1lax2lax3* influx carrier mutants, which are otherwise unable to form sec-

ondary roots. This suggests that the accumulation of auxin and subsequent formation of secondary roots may be regulated independently of the activity of these influx carriers. There is ample evidence that auxin efflux carriers (i.e., PIN proteins) are important for the susceptibility of Arabidopsis to infections of *H. schachtii* (Grunewald *et al.*, 2009). However, if and how they might contribute to the accumulation of auxin underlying the damage-induced formation of secondary roots needs further investigation.

Here, we demonstrate that ERF109-mediated local adaptations in root architecture compensate for primary root growth inhibition in response to nematode infection. In wild-type Arabidopsis, increasing densities of J2s led to a decline in the length of infected primary roots. However, this reduction in length of infected primary roots did not result into a smaller root system, because of an increase in the total length of secondary roots. Our data shows that these adaptations in root architecture depend on the transient and local activation of *ERF109* by JA at nematode infection sites. Consistently, the JA signaling mutant *coi1-2* showed a similar impairment as *erf109* in compensating primary root length inhibition by an increase in total secondary root length (Fig. S6). Nevertheless, since COI1 also affects plant susceptibility to nematode penetration more complex defense versus growth trade-offs may influence root growth in the *coi1-2* mutant. Importantly, loss of function mutations in *ERF109* do not alter the susceptibility of Arabidopsis to *H. schachtii* penetration, but instead affect root architecture plasticity in response to nematode infection. Further research is needed to understand whether ERF109-mediated compensatory adaptations in root architecture could mediate tolerance of Arabidopsis to infections by *H. schachtii*.

It was previously shown that meristem damage caused by *M. incognita* root tip penetration triggers regeneration via JA- and ERF109-mediated damage signaling (Zhou *et al.*, 2019). Here, we show that *H. schachtii* penetration of the mature root zone causes damage-induced secondary root formation, which compensates for primary root growth inhibition. Therefore, we consider root tip regeneration and secondary root formation as two different outcomes of the same compensatory mechanism in response to tissue damage in different root zones.

Furthermore, we show the first case of a naturally occurring and biotic stress that triggers damage signaling-mediated secondary root formation. Primary roots can form two types of secondary roots (Sheng *et al.*, 2017). One type, referred to as lateral root, forms during the physiological post-embryogenic development of plants and is regulated by ARF7 and ARF19 auxin response factors. The other type is induced by sterile mechanical injury of the mature root zone, soil penetration, or osmotic stress, and is dependent on the transcription factor WOX11. Sterile mechanical injury causes a different type of root tissue damage compared to a biotic stress

such as cyst nematodes (Marhavy *et al.*, 2019). Sterile mechanical injury damages many root cells at one time. Instead, cyst nematode host invasion causes the rupture of multiple single cells one after the other over the course of many hours (Wyss and Zunke, 1986). Thus, our results provide biological relevance for a mechanism so far only observed upon artificial conditions.

As a natural trigger for damage signaling, *H. schachtii* can be used to further elucidate the pathway leading to secondary root formation. ERF109 was previously found to be responsive to reactive oxygen species (ROS) (Kong *et al.*, 2018). It would be interesting to test whether ROS mediate ERF109-dependent secondary root formation upon *H. schachtii* infection. Furthermore, follow-up research could investigate if damage receptors activated during *H. schachtii* migration (Shah *et al.,* 2017) act upstream of ERF109. The root-knot nematode *M. javanica* triggers expression of LBD16, a downstream target of both WOX11, and ARF7 and ARF19 (Cabrera *et al.*, 2014; Olmo *et al.*, 2017). Moreover, *M. javanica* infection of primary roots induces secondary root formation independently from ARF7 and ARF19 (Olmo *et al.*, 2017). This suggests that nematode-induced secondary root formation could be regulated by WOX11. However, whether WOX11-mediated secondary root formation acts downstream of the ERF109-damage signaling pathway remains unknown.

In summary, we showed that *H. schachtii* triggers the formation of secondary roots via JA- and ERF109-mediated damage signaling (Fig. 8). Furthermore, ERF109-mediated secondary root formation compensates for primary root growth inhibition associated with *H. schachtii* infection. Thus, damage signaling-induced formation of secondary roots points at a novel mechanism underlying plant root architecture plasticity to biotic stress. Further research is needed to investigate whether damage-induced root architecture plasticity can contribute to plant tolerance to belowground herbivory.

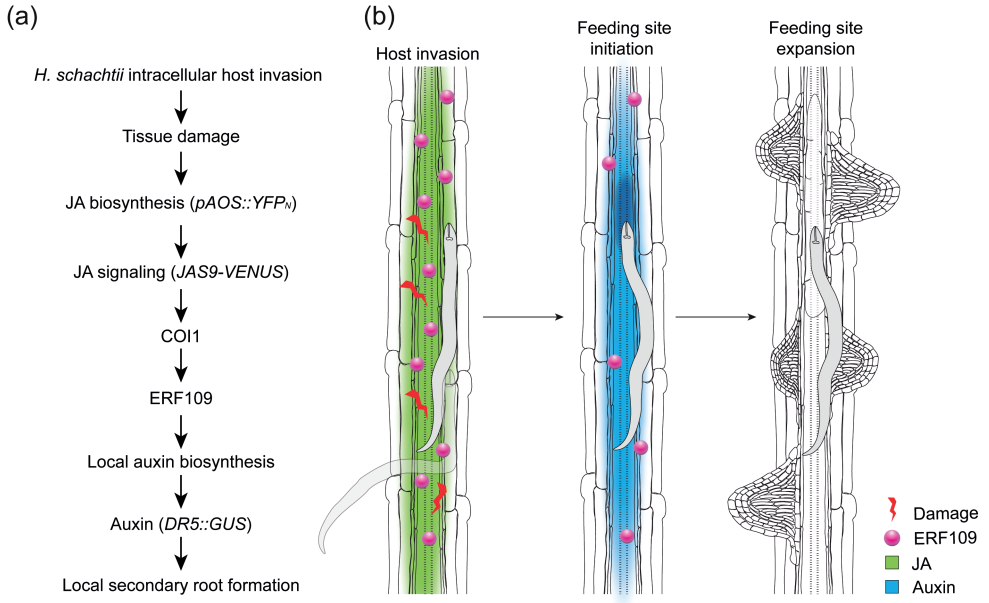

Fig. 8 Model of the pathway regulating *Heterodera schachtii*-induced secondary root formation. (a) Intracellular invasion of host roots by *H. schachtii* causes tissue damage, which triggers jasmonate (JA) biosynthesis (*pAOS::YFP*$_N$). JA signaling (*JAS9-VENUS*) via COI1 induces expression of *ERF109*, which leads to auxin accumulation (*DR5::GUS*) via local auxin biosynthesis. ERF109-mediated local auxin biosynthesis finally results in the formation of secondary roots at *H. schachtii* infection sites. (b) Graphical model illustrating the pathway investigated in this paper.

Acknowledgments

We thank Hang Liu for the help provided with data collection as part of his MSc Thesis at Wageningen University. This work was supported by the Graduate School Experimental Plant Sciences (EPS). WZ was funded by EMBO long-term fellowship (ALTF 784-2014) and the National Natural Science Foundation of China (32070874). JJW was funded by Dutch Top Sector Horticulture & Starting Materials (TU18152). MGS was supported by NWO domain Applied and Engineering Sciences VENI grant (17282). JLLT was supported by NWO domain Applied and Engineering Sciences VENI (14250) and VIDI (18389) grants. No conflict of interest declared.

Author contributions

JLLT, GS, NG, JJW, AG, WZ, and VW conceived the project. NG, JJW, MSH and LS designed the experiments and performed data collection. WZ and VW provided most

of the Arabidopsis mutants and granted access to the confocal microscope. WZ performed the crossing to obtain the *pERF109::GFP/coi1-2* Arabidopsis line, while homozygous plants were selected by both WZ and NG. Data was analyzed and interpreted by NG, JJW, MSH and MGS. NG, JLLT, GS, and JJW wrote the article with inputs from AG, MGS, VW, WZ, MSH, LS and FMWG.

Data availability

The data that supports the findings of this study are available in the supplementary material of this article.

Supporting information

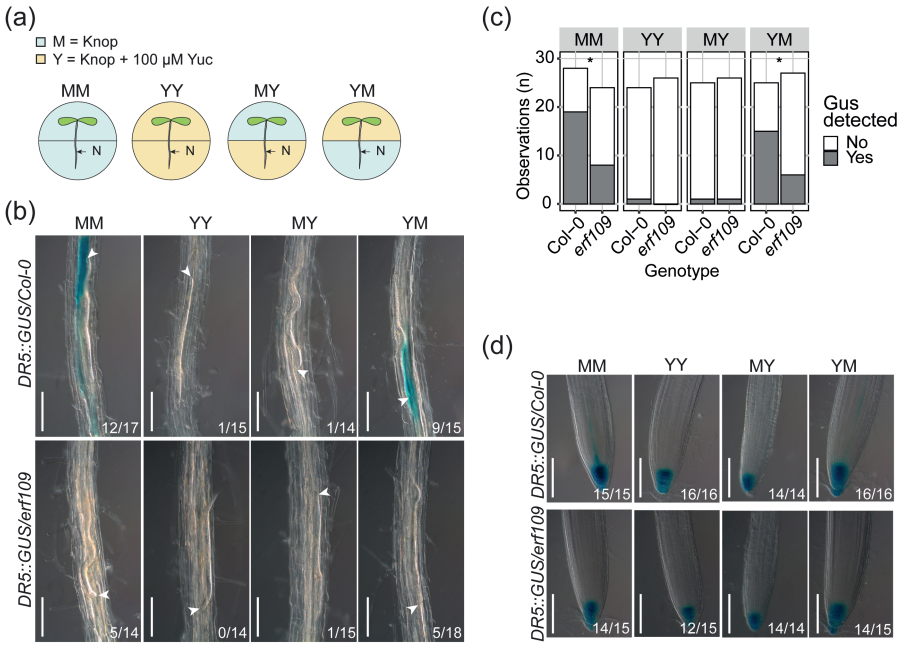

Fig. S1 Yuc split plate assay showing that ERF109 regulates local auxin biosynthesis at the nematode infection site. Four-day-old Arabidopsis Col-0 and erf109 seedlings expressing the auxin DR5::GUS reporter were infected with 15 Heterodera schachtii second-stage juveniles (J2s). At 16 hours post inoculation, seedlings were transferred to treatment plates. Four treatment combinations were prepared: MM (modified Knop medium and 0.2% DMSO), YY (modified Knop medium, 100µM Yuc and 0.2% DMSO), MK (Yuc only in the root), YM (Yuc only in the shoot). At 3 days post inoculation GUS staining assay was performed for 4 hours and seedlings were imaged. Single-nematode infection sites were selected for observation. (a) Experimental design with Arabidopsis seedlings transferred to split plates with modified Knop medium either with or without Yuc. N = nematode. (b) *DR5::GUS* expression at nematode infection sites in wild-type Col-0 and erf109 roots in the four different treatment combinations with or without Yuc

applied to shoots and/or roots. (c) Number of observations with (Yes) or without (No) GUS staining at the nematode infection sites in roots of wild-type Col-0 and erf109 plants. Statistical significance was calculated by a Pairwise Z-test (n=33, *, P<0.05). (d) *DR5::GUS* expression in the root tips of Col-0 and erf109 roots. White arrowheads indicate the nematode head. Frequencies at the bottom right corner indicate how many times GUS staining was observed in one of the three independent biological repeats of the experiment. Scale bar is 200 µm.

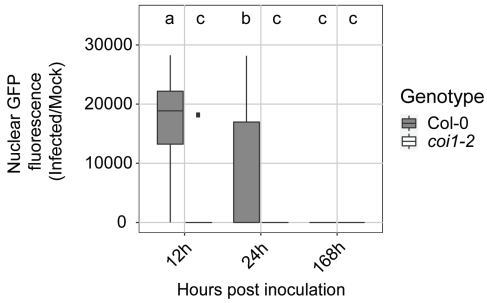

Fig. S2 Induction of *pERF109::GFP* nuclear fluorescence by *Heterodera schachtii* host invasion is disrupted in the *coi1-2* Arabidopsis mutant. Four-day-old Arabidopsis seedlings were either inoculated with 15 *H. schachtii* second-stage juveniles (J2s) or mock inoculated. At 12, 24, and 168 hpi seedlings were mounted in 10 µg ml^{-1} propidium iodide and then imaged. Nuclei were selected and the integrated density was measured using Fiji software. Ratio of the nuclear GFP fluorescence between infected and non-infected seedlings of wild-type Col-0 and *coi1-2* mutant. Significance of differences between fluorescent intensity in Col-0 and *coi1-2* roots over the different timepoints was calculated by Aligned Rank Transform for non-parametric factorial ANOVA followed by Tukey's HSD test for multiple comparisons (n=30, *P*<0.001). For boxplots, the horizontal line represents the median, the whiskers indicate the maximum/minimum range and the black dots represent the outliers. Difference in letters indicates statistically different groups.

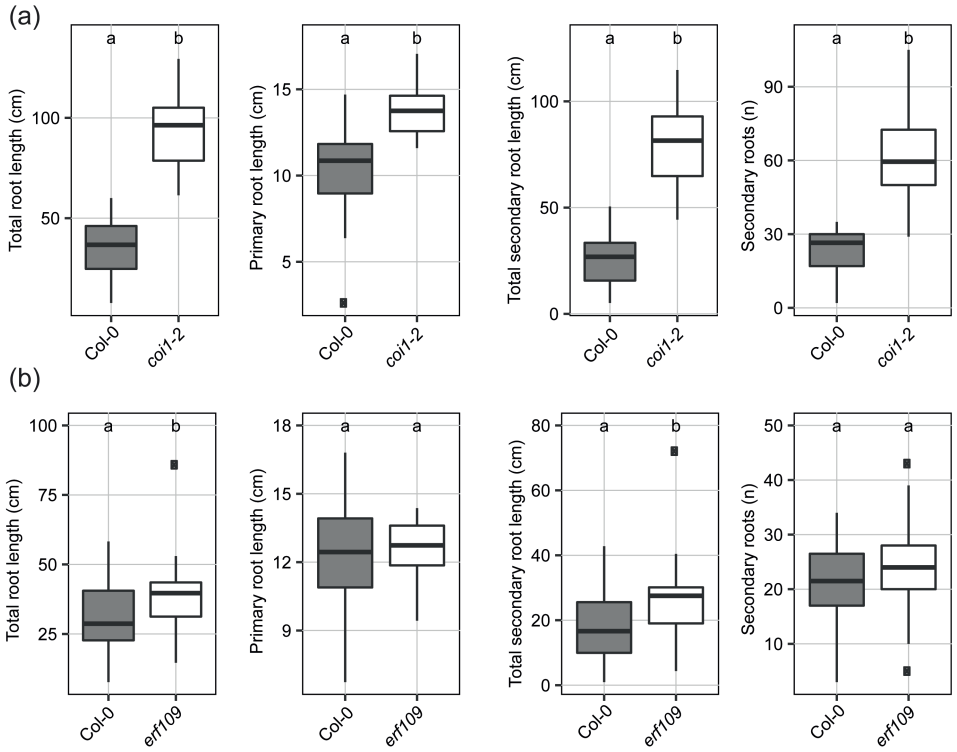

Fig. S3 The root architecture of uninfected *coi1-2* and *erf109* Arabidopsis plants differs from wild-type Col-0 plants. Scans of the roots of 16-day-old plants were made and the total root length was measured using WinRHIZO. For the experiment including *coi1-2* (a) the primary root was measured manually using ImageJ because of the complex root system of the mutant. For the experiment including *erf109* (b) the primary root length was automatically measured by WinRHIZO. Total secondary root length was calculated by subtracting the primary root length from the total root length. Data from three independent biological repeats of the experiment was combined. Significance of differences between genotypes was calculated by Student's T test (n=30, $P<0.05$). For boxplots, the horizontal line represents the median, the whiskers indicate the maximum/minimum range and the black dots represent the outliers. Different letters indicate statistically different groups.

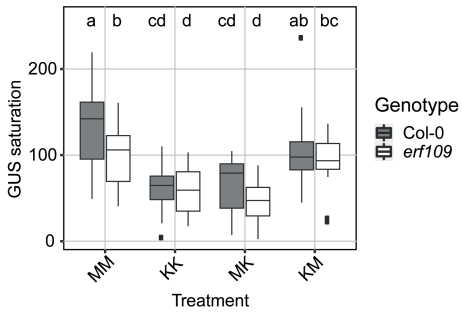

Fig. S4 *DR5::GUS* expression at the root tip does not differ between infected wild-type Col-0 and *erf109* seedlings when auxin biosynthesis is inhibited only in the shoot. Four-day-old wild-type Arabidopsis Col-0 and *erf109* mutant seedlings expressing the auxin *DR5::GUS* reporter were infected with 15 *Heterodera schachtii* second-stage juveniles (J2s). At 16 hours post inoculation, seedlings were transferred to treatment plates in a split-plate design. Four treatment combinations were prepared in split-plate assay: MM (modified Knop medium and 0.02% DMSO), KK (modified Knop medium, 10µM L-kyn and 0.02% DMSO), MK (L-kyn only in the root), KM (L-kyn only in the shoot). At 3 days post inoculation GUS staining was performed for 4 hours and seedlings were imaged. GUS saturation was measured as mean grey value using Fiji software. Data of two independent biological replicates was combined. Significance was calculated by ANOVA followed by Tukey's HSD test (n=20, P<0.05). For boxplots, the horizontal line represents the median, the whiskers indicate the maximum/minimum range and the black dots represent the outliers. Difference in letters indicates statistically different groups.

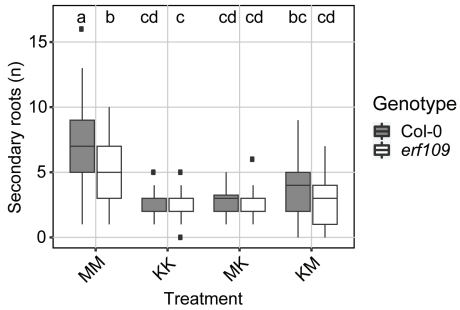

Fig. S5 The number of lateral roots in non-infected wild-type Col-0 and *erf109* mutant seedlings is affected by L-kyn treatment. Four-day-old Arabidopsis wild-type Col-0 and *erf109* seedlings were either infected with 15 *Heterodera schachtii* second-stage juveniles (J2s) or mock inoculated. At 16 hours post inoculation, seedlings were transferred to treatment plates in a split-plate design. Four treatment combinations were prepared: MM (modified Knop medium and 0.02% DMSO), KK (modified Knop medium, 10µM L-kyn and 0.02% DMSO), MK (L-kyn only in the root), KM (L-kyn only in the shoot). At 7 days post inoculation, scans were made of the root systems and the total number of secondary roots per plant was counted. Data of two independent biological repeats of the experiment was combined. Significance of differences in secondary roots between the different treatment combinations was calculated by ANOVA followed by Tukey's HSD test for multiple comparisons (n=43-45, P<0.001). For boxplots, the horizontal

line represents the median, the whiskers indicate the maximum/minimum range and the black dots represent the outliers. Difference in letters indicates statistically different groups.

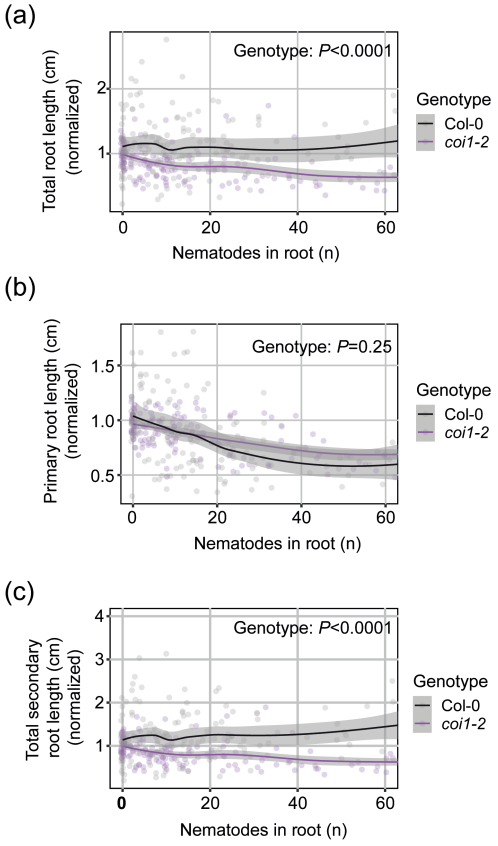

Fig. S6 COI1-mediated secondary root formation allows for maintenance of total root length despite primary root growth inhibition by *Heterodera schachtii.* Nine-day-old Col-0 and *coi1-2* Arabidopsis seedlings were inoculated with increasing *H. schachtii* densities ranging from 0 (mock) to 500 second-stage juveniles (J2s) per seedling. At 7 days post inoculation, scans were made of the root systems and the root length was measured using WinRHIZO. Total, primary, and secondary root length was normalized to the average respective component in mock-treated roots. Fuchsin staining was performed for counting the number of J2s that penetrated the roots. (a) Total root length per number of nematodes in the roots. (b) Primary root length per number of nematodes in the roots. (c) Total secondary root length per number of nematodes in the roots. Data from three independent biological repeats of the experiment was combined. Significance of differences between genotypes was calculated by ANOVA (n=30). Grey area indicates the 95% confidence interval.

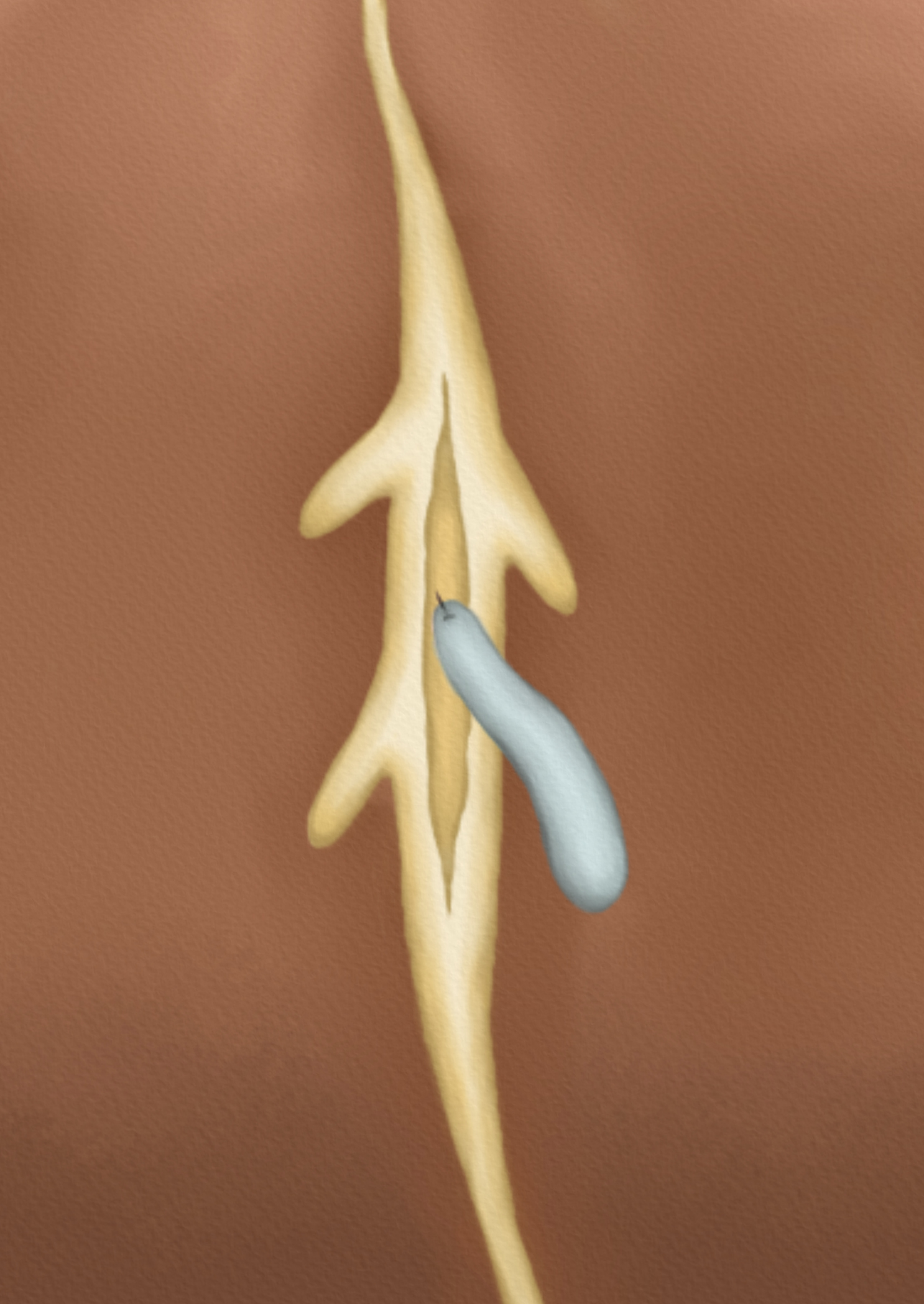

Chapter 3

WOX11-mediated adventitious lateral root formation modulates tolerance of Arabidopsis to cyst nematode infections

Jaap-Jan Willig[1‖], Nina Guarneri[1‖], Thomas van Loon[1], Sri Wahyuni [1], Ivan E. Astudillo-Estévez[1#], Lin Xu[2], Viola Willemsen[3], Aska Goverse[1], Mark G. Sterken[1], José L. Lozano-Torres[1], Jaap Bakker[1], Geert Smant[1]

[1]Laboratory of Nematology, Wageningen University & Research, 6708 PB Wageningen, the Netherlands

[2]National Key Laboratory of Plant Molecular Genetics, CAS Center for Excellence in Molecular Plant Sciences, Institute of Plant Physiology and Ecology, Chinese Academy of Sciences, Shanghai 200032, China

[3]Cluster of Plant Developmental Biology, Cell and Developmental Biology, Wageningen University & Research, 6708 PB Wageningen, the Netherlands

[#] - Present address: Instituto de Microbiología, Universidad San Francisco de Quito, Quito, Ecuador

[‖] - These authors have contributed equally.

Manuscript submitted; pre-print published on bioRxiv (2023)

Abstract

The transcription factor *WUSCHEL-RELATED HOMEOBOX11* (WOX11) in Arabidopsis initiates the formation of adventitious lateral roots upon mechanical injury in primary roots. Root-invading nematodes also induce *de novo* root organogenesis leading to excessive root branching, but it is not known if this symptom of disease involves mediation by WOX11 and if it benefits the plant. Here, we show with targeted transcriptional repression and reporter gene analyses in Arabidopsis that the beet cyst nematode *Heterodera schachtii* activates WOX11-adventitious lateral rooting from primary roots close to infection sites. The activation of WOX11 in nematode-infected roots occurs downstream of jasmonic acid-dependent damage signaling via *ETHYLENE RESPONSIVE FACTOR109*, linking adventitious lateral root formation to nematode damage to host tissues. By measuring different root system components, we found that WOX11-mediated formation of adventitious lateral roots compensates for nematode-induced inhibition of primary root growth. Our observations further demonstrate that WOX11-mediated rooting reduces the impact of nematode infections on aboveground plant development and growth. Altogether, we conclude that the transcriptional regulation by WOX11 modulates root system plasticity under biotic stress, which is one of the key mechanisms underlying tolerance of Arabidopsis to cyst nematode infections.

Introduction

Soil-borne infections by cyst nematodes affect above- and below-ground plant development and growth, sometimes resulting in large yield losses in agriculture (Jones *et al.*, 2013). Biotic stress induced by cyst nematodes in roots of host plants occurs at different stages of their infection cycle. Firstly, the infective second stage juveniles (J2s) invade host roots and migrate intracellularly through the epidermis and cortex, causing extensive damage to root tissue. Secondly, after becoming sedentary, cyst nematodes take up large amounts of plant assimilates during feeding from modified plant cells, which therefore develop strong metabolic sink activity (Gheysen and Mitchum, 2011; Jones *et al.*, 2013; Bebber *et al.*, 2014). As a response to nematode infections, plants remodel their root system by forming additional secondary roots (Goverse *et al.*, 2000; Olmo *et al.*, 2020; Willig *et al.*, 2022; Guarneri *et al.*, 2023). The *de novo* formation of secondary roots in response to endoparasitism by nematodes might be a mechanism to compensate for primary root growth inhibition caused by nematode infection (Guarneri *et al.*, 2023). However, whether such a form of root system plasticity contributes to overall plant tolerance to cyst nematode infections remains to be investigated.

Depending on where and how secondary roots are formed, they are either classified as lateral roots or adventitious lateral roots (Sheng *et al.*, 2017). During post-embryonic development in Arabidopsis, periodic oscillations of auxin maxima at the root tip prime cells to form lateral roots that emerge in a regular acropetal pattern from the growing primary root (Fukaki and Tasaka, 2009; van den Berg *et al.*, 2016). The emergence of lateral roots is controlled by AUXIN RESPONSE FACTOR (ARF)7 and ARF19, which directly regulate *LATERAL ORGAN BOUNDARIES DOMAIN* (*LBD)16* and other *LBD* genes (Okushima *et al.*, 2007). In contrast, adventitious lateral roots do not follow an acropetal pattern as they emerge in between and opposite of existing lateral roots. Moreover, adventitious lateral roots emerge in response to tissue damage, and their formation is regulated by a separate pathway mediated by the transcription factor WUSCHEL-RELATED HOMEOBOX (WOX)11 (Liu *et al.*, 2014; Hu and Xu, 2016; Sheng *et al.*, 2017). After cutting the primary root, local accumulation of auxin activates *WOX11* transcriptional activity through auxin response elements in its promotor region (Liu *et al.*, 2014). Subsequently, WOX11 induces the expression of *LBD16* but also the expression of other *WOX* genes (Hu and Xu, 2016; Sheng *et al.*, 2017). Ultimately, this leads to the *de novo* formation of secondary roots close to the injury site (Cai *et al.*, 2014; Liu *et al.*, 2014; Hu and Xu, 2016; Sheng *et al.*, 2017). Cyst nematode infection in primary roots of Arabidopsis triggers the formation of secondary roots which does not follow an acropetal patterning (Guarneri *et al.*, 2023). Instead, secondary roots often form clusters at nematode infection sites. As to whether the formation of these secondary roots depends on the WOX11-mediated pathway and whether they should thus be classified as adventitious lateral roots is still a knowledge gap.

We have recently demonstrated that the formation of secondary roots near nematode infection sites involves damage-induced jasmonic acid (JA) signaling (Guarneri *et al.*, 2023). Tissue damage caused by intracellular migration of infective juveniles of *H. schachtii* induces the biosynthesis of JA, which activates the transcription factor *ETHYLENE RESPONSIVE FACTOR* (ERF)109 via the JA receptor *CORONATINE INSENSITIVE* (COI)1. ERF109, in turn, can trigger local biosynthesis of auxin by directly binding to the promoters of auxin biosynthesis genes *ASA1* and *YUC2* (Cai *et al.*, 2014). Indeed, our data showed that COI1/ERF109-mediated formation of secondary roots from nematode-infected primary roots depends on local biosynthesis and accumulation of auxin (Guarneri *et al.*, 2023). WOX11-mediated formation of adventitious lateral roots upon root injury also involves local accumulation of auxin (Liu *et al.*, 2014). However, it remains to be demonstrated if WOX11 becomes activated by COI1- and ERF109-mediated damage signaling in nematode-infected roots.

Several recent reports in the literature point at a role for WOX11-mediated root

plasticity in modulating plant responses to abiotic stresses. For instance, *WOX11*, designated as *PagWOX11/ WOX12a*, in poplar mediates changes in root system architecture in response to drought and salt stress (Wang *et al.*, 2020; Wang, LQ *et al.*, 2021). Overexpression and dominant repression of this gene in poplar plants alters the number of adventitious roots formed under high saline conditions (Liu *et al.*, 2022). Likewise, the loss-of-function mutant *wox11* in rice exhibits reduced root system development in response to drought as compared to wild-type plants (Cheng *et al.*, 2016). Based on these findings, WOX11-mediated root plasticity is thought to enhance plant tolerance to abiotic stress. However, whether WOX11-mediated root plasticity is also involved in mitigating the impact of biotic stresses on the root system is not known.

In this study, we first addressed whether cyst nematode-induced secondary roots qualify as damage-induced adventitious lateral roots. Hereto, we monitored *de novo* secondary root formation in Arabidopsis seedlings of the double mutant *arf7/arf19* and the WOX11 transcriptional repressor mutant *35S::WOX11-SRDX* in the *arf7/ arf19* background (Hiratsu *et al.*, 2003) infected with *H. schachtii.* Next, we asked whether the regulation of *WOX11* in nematode-infected Arabidopsis roots occurs downstream of JA-dependent damage signaling through COI1 and ERF109. To answer this question we performed a time course experiment measuring *pWOX11::GFP* expression with confocal microscopy in wild-type, *coi1-2*, and *erf109* infected mutant seedlings. Third, we assessed if WOX11-mediated root system plasticity compensates for the inhibition of primary root growth upon cyst nematode infection. For this, we measured different components of root system architecture of nematode-infected WOX11 transcriptional repressor mutant and wild-type Arabidopsis plants. Last, we tested if WOX11-mediated root system plasticity contributes to the overall tolerance of Arabidopsis to cyst nematode infections. To this end, we compared the aboveground plant growth and development of cyst nematode-infected *35S::WOX11-SRDX* mutants and wild-type Arabidopsis for a period of three weeks after inoculation. Based on our data, we propose a model wherein the formation of WOX11-mediated adventitious lateral roots enhances tolerance of Arabidopsis to biotic stress by cyst nematode infections.

Materials and Method

Plant material and culturing

The Arabidopsis (*Arabidopsis thaliana*) lines wild-type Col-0 (N60.000), *35S::WOX11-SRDX/arf7-1/19-1*, *arf7-1/19-1*, *LBD16pro::LBD16-GUS* and *35S::WOX11-SRDX/ LBD16pro::LBD16-GUS* (Sheng *et al.*, 2017), *pWOX11::GFP*, *pWOX11::GFP/coi1-*

2, *pWOX11::GFP/erf109*, *coi1-2* and *erf109* were used. For in vitro experiments, seeds were vapor sterilized for 3-4 hours using a mixture of hydrochloric acid (25%) and sodium hypochlorite (50 g L^{-1}). Finally, sterile seeds were stratified for 4 days at 4 °C, after which they were sown on square Petri dishes (120x120 mm) containing modified Knop medium (Sijmons *et al.*, 1991) in a growth chamber with a 16-h-light/8-h-dark photoperiod at 21°C. For in vivo pot experiments, seeds were stratified for 4 days and sown on silver sand in 200 ml pots. Seedlings were grown at 19 °C and 16-h-light/8-h-dark conditions with LED light (150 lumen), as previously described in Willig *et al.* (2023b).

Hatching and sterilization of Heterodera schachtii

H. schachtii cysts (Woensdrecht population from IRS, the Netherlands) were separated from sand of infected *Brassica oleracea* plants as previously described (Baum *et al.*, 2000). Cysts were transferred into a clean Erlenmeyer containing water with 0.02% sodium azide. This mixture was gently stirred for 20 min. Later, sodium azide was removed by washing with tap water. Cysts were then incubated for 4-7 days in a solution containing 1.5 mg ml^{-1} gentamycin sulfate, 0.05 mg ml^{-1} nystatin and 3 mM $ZnCl_2$. Hatched J2s were purified by centrifugation on a 35% sucrose gradient, transferred to a 2 ml Eppendorf tube and surface sterilized for 15 minutes in a solution containing 0.16 mM $HgCl_2$, 0.49 mM NaN_3, and 0.002% Triton X-100. After washing the J2s three times with sterile tap water, *H. schachtii* J2s were re-suspended in a sterile 0.7% Gelrite (Duchefa Biochemie, Haarlem, the Netherland) solution. A similar concentration of Gelrite solution was used as mock treatment.

For *in vivo* pot experiments, J2s were hatched and collected in a similar way as described above. Non-sterile J2s were purified by centrifugation on a 35% sucrose gradient and washed three times with tap water. Nematodes were resuspended in tap water for specific inoculation densities.

Quantifying root system architecture of nematode-infected Arabidopsis

Seven-day-old *35S::WOX11-SRDX/arf7-1/19-1* and *arf7-1/19-1* Arabidopsis seedlings were inoculated with either 90 *H. schachtii* J2s or a mock solution. Root architecture was inspected at 7 dpi using an Olympus SZX10 binocular with a 1.5x objective and 2.5x magnification. Scans were made of whole seedlings using an Epson Perfection V800 photo scanner. Pictures of nematode infections were taken with a AxioCam MRc5 camera (Zeiss) and the ZEN 3.2 blue edition software (Zeiss).

Nine-day-old *35S::WOX11-SRDX* and wild-type Col-0 seedlings, grown on 120x120 mm square Petri dishes were inoculated with 0 (mock), 0.5, 1.0, 2.5, 5.0, and 7.5 *H. schachtii* J2s per ml of modified Knop medium as previously described (Guarneri

et al., 2023). Inoculations were done with two 5 µl drops that were pipetted at opposite sides of each seedling while keeping the petri dishes vertical. At 7 dpi, scans were made of whole seedlings using an Epson Perfection V800 photo scanner. The architecture (i.e., total root length, primary root length, total secondary root length) was measured using the WinRHIZO package for Arabidopsis (WinRHIZO pro2015, Regent Instrument Inc., Quebec, Canada). The number of root tips was counted manually based on the scans.

Acid fuchsine staining of nematodes

Nematodes within the roots were stained with acid fuchsin and counted as previously described (Warmerdam *et al.*, 2018). For comparisons between genotypes, the background effect of the mutation on the root architecture was corrected by normalizing each measured root architecture component in infected seedlings to the median respective component in mock-inoculated roots.

Histology and brightfield microscopy

Four-day-old Arabidopsis seedlings were inoculated with 20 *H. schachtii* J2s or a mock solution. For histochemical staining of β-glucuronidase (GUS) activity, seedlings were incubated in a GUS staining solution (1 mg ml^{-1} X-GlcA in 100 mM phosphate buffer pH 7.2, 2 mM potassium ferricyanide, 2 mM potassium ferrocyanide, and 0.2 % Triton X-100) at 37 °C (Zhou *et al.*, 2019) for 3 hours. Stained seedlings were mounted in a chloral hydrate clearing solution (12 M chloral hydrate, 25% glycerol) and inspected with an Axio Imager nM2 light microscope (Zeiss) via a 20x objective. Differential interference contrast (DIC) images were taken with an AxioCam MRc5 camera (Zeiss) and the ZEN 3.2 blue edition software (Zeiss).

Confocal laser microscopy of single H. schachtii infection sites

Four-day-old Arabidopsis seedlings were inoculated with roughly five sterile *H. schachtii* J2s in 10 µL 0.7% Gelrite. Single nematode infection sites were selected for observation at 2, 3, 4, and 7 dpi. Infection sites were inspected using a Zeiss LSM 710 confocal laser scanning microscope and a 40x objective. After a single infection site was located, a Z-stack of ten 13 µm-slices was made. Z-stacks were taken using the ZEN 2009 software (Zeiss). The imaging settings in ZEN 2009 were as follows: Laser 488 at 50%, Pinhole 41.4 µm, eGFP 645 nm, tPMT 217 nm. Z-stacks were processed with ImageJ Version 1.53 to quantify the fluorescence integrated density.

The post-processing in ImageJ of one individual image was as follows: Firstly, an auto-scaled compressed-hyper-Z-stack was created of the 10 layers made with the confocal microscope by using the Z-compression function at max intensity (Fig. S4).

Secondly, a duplicate of the original Z-stack was created, and a Gaussian filter with a sigma value of 2.0 was applied to this duplicate. This duplicate was subtracted from the original image by using the image calculator function. Thirdly, the image threshold limits were set to a specific range ranging from 0 to 100 depending on the quality of the image. The same threshold limits were applied on all images that were taken on the same day. Lastly, the particles were analysed using Analyse Particles at size 0-Infinity and circularity 0.00-1.00.

High throughput analysis of the green canopy area of nematode-infected Arabidopsis plants

Plants were imaged and analyzed as previously described (Willig *et al.,* 2023b). Prior to sowing, pots, were filled with silver sand, covered with black coversheets, and were watered with Hyponex (1.7 mM NH_4^+, 4.1 mM K^+, 2 mM Ca_2^+, 1.2 mM Mg_2^+, 4.3 mM NO_3^-, 3.3 mM SO_4^{2-}, 1.3 mM $H_2PO_4^-$, 3.4 µM Mn, 4.7 µM Zn, 14 µM B, 6.9 µM Cu, 0.5 µmM Mo, 21 µmM Fe, pH 5.8) for five minutes. Seven days after sowing, seedlings were watered again for five minutes. Nine-day-old seedlings were inoculated with increasing densities of *H. schachtii* (0 to 10 juveniles per g dry sand). For our experiments we did not use a blocking design as it would greatly increase the chance for error when manually inoculating plants. Every hour, pictures were taken of the plants (15 pictures per day) for a period of 21 days. At the end of the experiment, colour corrections were done using Adobe Photoshop (Version: 22.5.6 20220204.r.749 810e0a0 x64). The surface area of the rosette was determined using a custom-written ImageJ macro (ImageJ 1.51f; Java 1.8.0_321 [32-bit]) and Java was used to make GIFs.

Plant growth analysis and tolerance modelling using a high-throughput phenotyping platform

To analyse the growth data of the plants obtained from the high-throughput platform, we followed the same approach and used the same functions as in our previously published analytical pipeline (Willig *et al.,* 2023b); available via Gitlab: https://git.wur.nl/published_papers/willig_2023_camera-setup).

In short, the measurement used was the median daily leaf area (cm^2), calculated from the 15 daily measurements. We used $\log_2$-transformed data, where the rate of growth was determined per day per plant by (equation 1)

$$R_{x,t} = \log_2(A_{x,t-1} - A_{x,t})$$

where $R_{x,t}$ is the transformed growth rate of plant *x* at day *t* from day *t-1* to day *t* based on the median Green canopy area *Ax,t*.

The tolerance limit was modelled using a previously described method based on fitting growth models (Willig *et al.,* 2023b). Here we fitted a logistic growth model using the *growthrates* package on the median daily leaf area A_t (cm^2) (equation 2),

$$A_t = \frac{K \times A_0}{A_0 + (K - A_0) \times e^{(-r \times t)}}$$

where K is the maximum green canopy area (cm^2), A_0 is the initial canopy area (cm^2), and r is the intrinsic growth rate (d^{-1}), which were determined as a function of time t (d) ($p < 0.1$).

Based on the relation between K and density we could identify the tolerance limit (equation 3)

$$K = K_B + \frac{K_\sigma}{P_\sigma} \times e^{-\left(\frac{P_i - P_M}{P_\sigma}\right)^2}$$

where P_i is the initial nematode density in nematodes per gram soil, K_B is the basal canopy size, K_σ is the normalized maximum canopy area that can be achieved over the P_i range, P_σ is the deviation around the nematode density allowing maximum growth, P_M is the nematode density at which maximum growth is achieved. We modelled the parameter values using *nls* and extracted confidence intervals using the *nlstools* package (Baty *et al.*, 2015). The tolerance limit, $2*P_M$, could such be determined as in Willig *et al.* (2023b).

Statistical analyses

Statistical analyses were performed using the R software version 3.6.3 (Windows, x64). The R packages used are *tidyverse* (https://CRAN.R-project.org/package=tidyverse), *ARTool* (https://CRAN.R-project.org/package=ARTool) and *multcompView* (https://CRAN.R-project.org/package=multcompView). Correlation between variables was calculated using Spearman Rank-Order Correlation coefficient. For binary data, significance of the differences between proportions was calculated by a Pairwise Z-test. For normally distributed data, significance of the differences among means was calculated by ANOVA followed by Tukey's HSD test for multiple comparisons. A non-parametric pairwise Wilcoxon test followed by false discovery rate correction for multiple comparisons was used for data with other distributions and one grouping factor. For the high-throughput platform data we used the Wilcoxon test as implemented in the *ggpubr* package (https://cran.r-project.org/web/packages/ggpubr/index.html). The confidence interval of the inoculum density-response curves was calculated by loess regression (as per default in *geom_smooth*) in R.

Results

Cyst nematodes induce the formation of adventitious lateral roots

Our earlier work showed that *H. schachtii* induces the *de novo* formation of secondary roots between or across fully developed lateral roots near nematode infection sites (Guarneri *et al.*, 2023). Here, we hypothesized that these secondary roots are adventitious lateral roots, the formation of which depends on WOX11-mediated transcriptional regulation (Fig. 1a). To test this hypothesis, we inoculated *H. schachtii* on the lateral root-deficient *arf7-1/19-1* double mutant, which is unable to form acropetal lateral roots, and the transcription repressor mutant *35S::WOX11-SRDX/arf7-1/19-1* (Hiratsu *et al.*, 2003), which is unable to form neither acropetal nor adventitious lateral roots (Fig. 1b-d). Importantly, we observed no difference in the number of nematodes per plant between *arf7-1/19-1* and *35S::WOX11-SRDX/arf7-1/19-1* (Fig. 1c), indicating that both Arabidopsis lines were exposed to similar levels of biotic stress. However, the number of *35S::WOX11-SRDX/arf7-1/19-1* plants that showed secondary root formation upon inoculation with *H. schachtii* was significantly smaller than for the *arf7-1/19-1* mutant line (Fig. 1b, d and Fig. S1). From this, we concluded that the induction of secondary roots by *H. schachtii* is mediated by WOX11 and that these secondary roots therefore qualify as adventitious lateral roots.

WOX11-mediated formation of adventitious lateral roots from primary roots of Arabidopsis involves the downstream transcriptional activation of *LBD16* (Fig. 1a) (Sheng *et al.*, 2017). To test if WOX11 activates *LBD16* in nematode-infected Arabidopsis roots, we monitored the expression of *LBD16* fused to *GUS* in wild-type (*LBD16pro::LBD16-GUS*) and *35S::WOX11-SRDX* (*35S::WOX11-SRDX/LBD16pro::LBD16-GUS*) seedlings inoculated with *H. schachtii* (Fig. 1e and f). We found that *LBD16* was highly expressed in nematode infection sites in the wild-type, but not in the *35S::WOX11-SRDX* background. This demonstrates that *H. schachtii* activates *LBD16* expression in a WOX11-dependent manner. Based on these observations, we concluded that cyst nematode infections activate the WOX11/LBD16-mediated pathway to form adventitious lateral roots from primary roots.

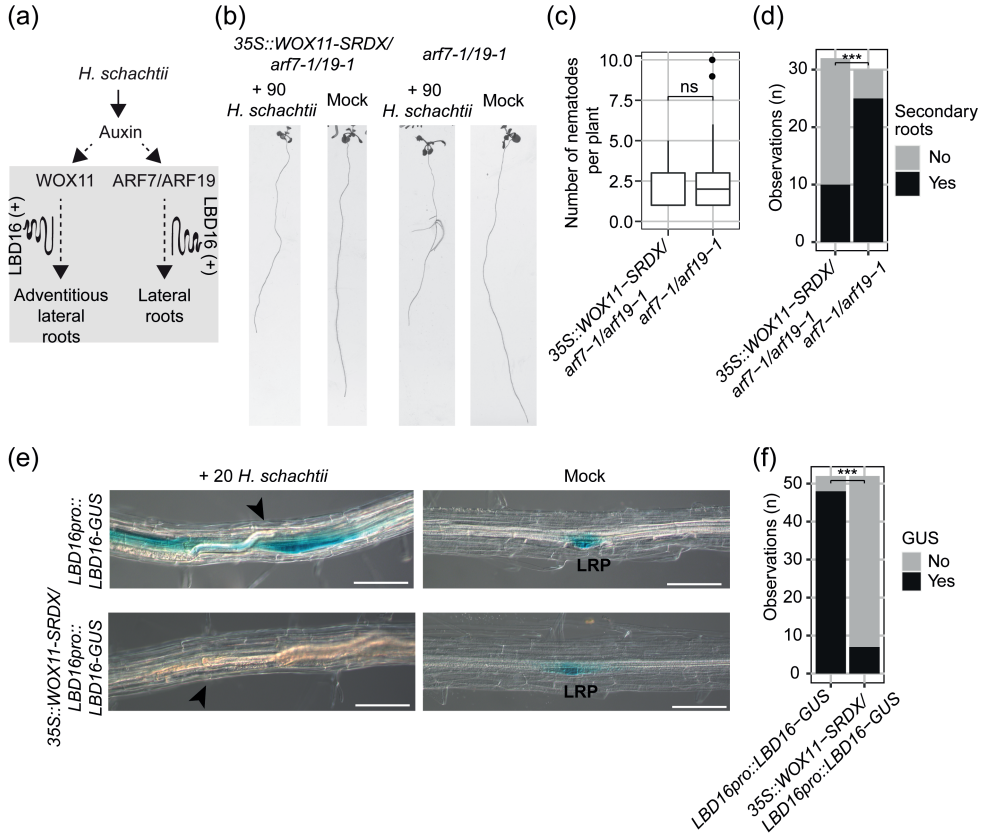

Fig. 1 *Heterodera schachtii* induces adventitious lateral root formation in a WOX11- and LBD16-dependent manner. (a) Schematic diagram of *H. schachtii*-and WOX11-mediated adventitious lateral root emergence. Grey area indicates the tested part of the pathway. Curling line and '+' indicate involvement of multiple proteins, including LBD16. (b-d) Seven-day old *35S::WOX11-SRDX/arf7-1/19-1* and *arf7-1/arf19-1* mutant seedlings were inoculated with 90 *H. schachtii* juveniles or with mock solution. At 7dpi, scans were made of the root system. (b) Representative pictures of *35S::WOX11-SRDX/arf7-1/19-1* and *arf7-1/arf19-1* mutant seedlings inoculated with 90 *H. schachtii* or with mock solution. (c**)** Number of juveniles that invaded the primary roots. (d) Number of seedlings that show secondary roots (Yes) that are associated with *H. schachtii* infection sites or no secondary roots at all (No). Data from three independent biological repeats of the experiment was combined. Statistical significance was calculated by a Pairwise Z-test n=30-32, ***: *P*<0.001). (e-f) Four-day-old Arabidopsis seedlings expressing the *LBD16pro::LBD16-GUS* and *35S::WOX11-SRDX/LBD16pro::LBD16-GUS* reporters were inoculated with 20 *H. schachtii* juveniles. At 4dpi, GUS expression was stained for 3 hours and seedlings were imaged (e**)** *LBD16pro::LBD16-GUS* and *35S::WOX11-SRDX/LBD16pro::LBD16-GUS* expression at nematode infection sites in roots. Black arrowheads indicate the nematode head. LRP indicates lateral root primordia. Scale bar is 100 µm. (**f**) Number of observations with (Yes) or without (No) GUS staining at the nematode infection site in roots of wild-type Col-0 seedlings. Data from three independent biological repeats of the experiment were combined. Statistical significance was calculated by a Pairwise Z-test (n=52, ***: *P*<0.001).

Emergence of adventitious lateral roots correlates with damage in primary roots

Previously, we showed that increasing nematode inoculation densities result in more tissue damage in Arabidopsis leading to a higher number of secondary roots emerging from infected primary roots (Guarneri *et al.*, 2023). To test the hypothesis that WOX11 mediates this quantitative relationship between inoculation density and the number of secondary roots emerging from cyst nematode-infected primary roots (Fig. 2a), we inoculated nine-day-old seedlings of *35S::WOX11-SRDX* and wild-type plants with increasing densities of *H. schachtii* (Fig. 2b). At 7 dpi, the number of nematodes that had successfully penetrated the roots was counted after staining with acid fuchsin (Fig. 2c). The number of infective juveniles in *35S::WOX11-SRDX* plants by inoculation density was significantly higher compared to wild-type Col-0 plants. This indicates that the transcriptional regulation by WOX11 in wild-type Arabidopsis plants reduces susceptibility to penetration by *H. schachtii*. Next, we counted the number of secondary roots to determine whether this correlates with the number of nematodes inside the roots. It should be noted that uninfected *35S::WOX11-SRDX* plants have more secondary roots than wild-type Col-0 plants (Fig. S2). To correct for this background effect of the SRDX-transcriptional repressor construct on root system architecture, we normalized the total number of secondary roots in infected seedlings to the average respective number in uninfected seedlings (Fig. 2d). As expected, after normalization, the number of secondary roots emerging from primary roots increased with the number of successful invasions of *H. schachtii* in wild-type Arabidopsis. However, no such correlation was observed in *35S::WOX11-SRDX* plants. We therefore concluded that the density-dependent adaptations in root system architecture to increasing levels of damage in nematode-infected roots are brought about by WOX11-mediated formation of adventitious lateral roots.

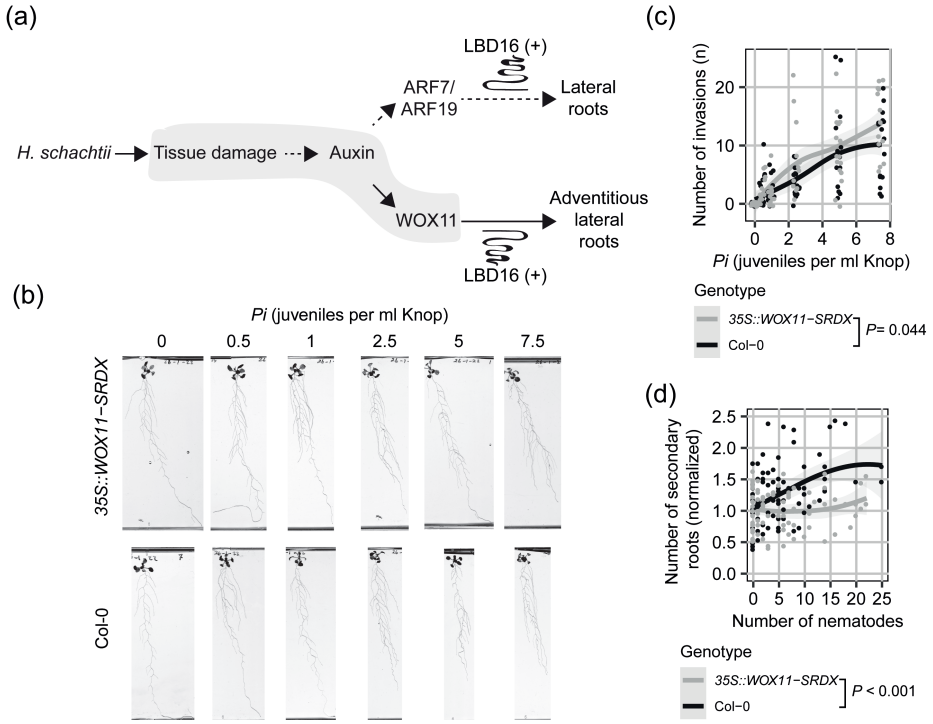

Fig. 2 WOX11 is required in *Heterodera schachtii* induced adventitious lateral root formation in a density-dependent manner. (a) Schematic diagram of *H. schachtii*-and WOX11-mediated adventitious lateral roots emergence. Grey area indicates the tested part of the pathway. Curling line and '+' indicate the involvement of multiple proteins, including LBD16. (b-d) Nine-day-old *35S::WOX11-SRDX* and wild-type Col-0 seedlings were inoculated with nematode densities (P_i) ranging from 0-7.5 *H. schachtii* J2s (ml modified Knop medium). Roots were scanned and nematodes were counted after acid fuchsin staining at 7 dpi. (b) Representative images of Arabidopsis root systems at 7dpi. (c) Number of nematodes that successfully penetrated the roots per plant. (d) Secondary roots formed per number of nematodes inside the roots. The total number of secondary roots of infected seedlings was normalized to the median respective component in mock-inoculated roots. Data from two independent biological repeats of the experiment were combined. Significance of differences between genotypes was calculated by analysis of variance (n=14-18). Grey area indicates the 95% confidence interval.

COI1 and ERF109 modulate damage-induced activation of WOX11 at nematode infection sites

De novo formation of secondary roots on nematode-infected primary roots of Arabidopsis is mediated by damage-induced activation of JA signaling via COI1 and ERF109 (Guarneri *et al.*, 2023). In this study we tested whether COI1 and ERF109 are required for the regulation of *WOX11* in nematode-infection sites (Fig. 3a). Hereto, we imaged nucleus-localized *pWOX11::GFP* expression within single-nematode

infection sites in the *coi1-2* and *erf109* mutants and wild-type Col-0 at 2, 3, 4, and 7 dpi (Fig. 3 and Fig. S3). Cyst nematode infection typically causes tissue autofluorescence in Arabidopsis roots (Hoth *et al.*, 2005). To filter out this autofluorescence from the fluorescent signal emitted by the GFP construct, we subtracted a Gaussian blurred image from the original images (Fig. S4). Hereafter, we observed a gradual increase in the *pWOX11::GFP*-derived fluorescent signal in nematode infection sites over time in *coi1-2, erf109,* and wild-type Col-0 (Fig. S3a-f), with wild-type Col-0 showing the strongest increase (Fig. S3f). For instance, at 4 dpi, wild-type Col-0 plants showed significantly more nuclear GFP fluorescence in and around nematode feeding sites compared to *coi1-2* and *erf109* in the processed images (Fig. 3b-d). We, therefore, concluded that two key components of the damage-induced JA signaling pathway, COI1 and ERF109, modulate *WOX11* expression in infection sites of *H. schachtii* in Arabidopsis.

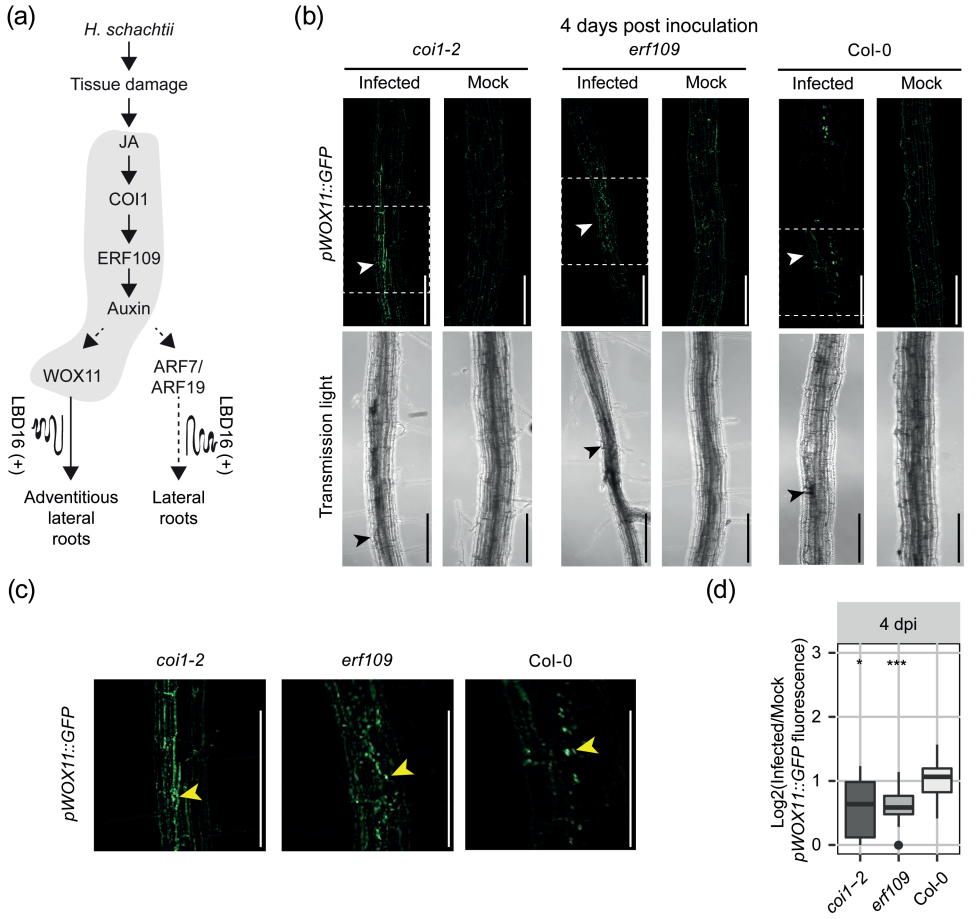

Fig. 3 COI1 and ERF109 modulate *WOX11* expression upon *Heterodera schachtii* infection. (a) Sche-

matic diagram of *H. schachtii*-and WOX11-mediated adventitious lateral root emergence. Grey area indicates the tested part of the pathway. Curling line and '+' indicate involvement of multiple proteins, including LBD16. (b-c) Four-day-old Arabidopsis seedlings were either inoculated with 10 *H.* schachtii second-stage juveniles (J2s) or with mock solution. At 4 dpi, seedlings were mounted in water and then imaged using a fluorescent confocal microscope. Single-nematode infection sites were selected for observation. Images are original. (b) Representative pictures of infected and mock-inoculated seedlings expressing the *pWOX11::GFP* construct with nuclear localization signal in either wild-type Col-0, mutant *coi1-2*, or mutant *erf109* background at 4 dpi. To make the fluorescence more visible, the brightness was enhanced for all the representative pictures in the same way. (c) Zoomed parts of original images fluorescent signal that are indicated by dashed white box in panel (b). Yellow arrowhead indicates true fluorescent signal of *pWOX11::GFP* in the nucleus. (d) Quantification of *pWOX11::GFP* fluorescent intensity induced by infection in wild-type Col-0, *coi1-2,* and *erf109* roots. Values represent $\log_2$ of the fluorescence ratio between the GFP integrated density of infected and noninfected roots. Scale bar is 200 µm. Data from three independent biological repeats of the experiment were combined. Significance of differences between fluorescent intensities in Co-0, *coi1-2,* and *erf109* per timepoint was calculated by a Wilcoxon Rank Sum test. ns = not significant, **P*< 0.05, ***P*< 0.01, ****P*<0.001 (n=15).

Formation of adventitious lateral roots compensates for nematode-induced primary root growth inhibition

Next, we asked whether WOX11-mediated adventitious lateral roots formation compensates for the inhibition of primary root growth due to nematode infections (Fig. 4a). To this end, we quantified root system architecture components (i.e., total root length, primary root length, total secondary root length, and average secondary root length) of nematode-infected roots of both *35S::WOX11-SRDX* and wild-type Col-0 plants (Fig. 2). Initially, we noticed that our measurements of root system architecture components followed a parabolic function with the minimum values at the infection rate of 15 juveniles per root, suggesting the existence of two density dependent counteracting mechanisms (Fig. S5). We, therefore, analysed our data for the lower (Fig. 4) and higher infection rates separately (Fig. S5). For plants infected with 0 to 15 juveniles per root, we found that the total root length was significantly more reduced by nematode infection in *35S::WOX11-SRDX* mutant plants than in wild-type Col-0 plants (Fig. 4b and d). Interestingly, the growth of the primary root was not different between *35S::WOX11-SRDX* mutant plants and wild-type plants upon infection with cyst nematodes (Fig. 4c). However, the total length of the secondary roots of nematode-infected *35S::WOX11-SRDX* mutant plants was significantly smaller as compared to wild-type Col-0 plants (Fig. 4d). As the average secondary root length did not significantly differ between *35S::WOX11-SRDX* and wild-type Arabidopsis plants, WOX11 affects the root system architecture by increasing the number of secondary roots but not by extending secondary root growth (Fig. 5e). For plants infected with 15 to 25 juveniles per plant, we observed no significant differences for the total root length (Fig. S5b) between wild-type Col-0 and *35S::WOX11-SRDX*.

Likewise, we found no differences in the primary root length (Fig. S5c), total secondary root length (Fig. S5d), and average secondary root length (Fig. S5e). Based on our analyses, we concluded that WOX11-mediated formation of adventitious lateral roots compensates for nematode-induced inhibition of primary root growth at lower infection rates.

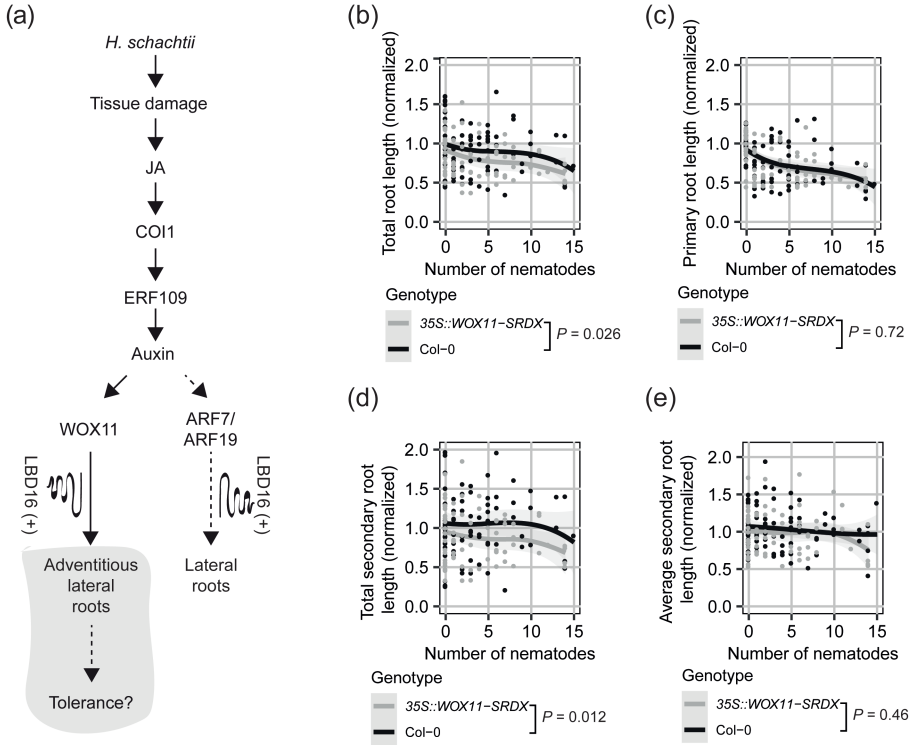

Fig. 4 Formation of adventitious lateral roots compensates for nematode-induced primary root growth inhibition. (a) Schematic diagram of *H. schachtii*-and WOX11-mediated adventitious lateral root emergence. Grey area indicates the tested part of the pathway. Curling line and '+' indicate involvement of multiple proteins, including LBD16. (b-d) Nine-day old *35S::WOX11-SRDX* and wild-type Col-0 seedlings were inoculated densities (P_i) ranging from 0-7.5 *H. schachtii* J2s (ml modified Knop medium). Roots were scanned and nematodes were counted after fuchsine staining at 7 dpi. Root architectural components of infected seedlings were normalized to the median respective component in mock-treated roots. Data of two independent biological repeats of the experiment was combined. (b) Representative images of Arabidopsis root system at 7 dpi. (b) Total root length per number of nematodes inside the roots. (c) Primary root length per number of nematodes inside the roots. (d) Total secondary root length per number of nematodes inside the roots. (e) Average secondary root length per number of nematodes inside the roots. Data from two independent biological repeats of the experiment were combined. Significance of differences between genotypes was calculated by analysis of variance (n=14-18). Grey area indicates the 95% confidence interval of the loess fit.

WOX11 modulates tolerance to cyst nematode infections

The growth of the green canopy area over time reflects the tolerance of Arabidopsis to biotic stress by root-feeding cyst nematodes (Willig *et al.,* 2023b). To assess if WOX11-mediated *de novo* formation of adventitious lateral roots modulates tolerance of Arabidopsis to cyst nematode infection, we monitored the growth of the green canopy area of *35S::WOX11-SRDX* mutant and wild-type Col-0 seedlings for a period of 21 days after inoculation with different numbers of *H. schachtii* (Fig. 5a and b). At the end of the experiment, the green canopy area of the *35S::WOX11-SRDX* mutant was smaller at higher inoculation densities of *H. schachtii* as compared to wild-type Col-0 plants (Fig. 5c and d). Notably, the first significant reduction in green canopy area of *35S::WOX11-SRDX* plants by nematode infection was observed at inoculation densities between P_i 2.5 and 5 J2s per gram sand, while in wild-type Col-0 plants we observed a first significant reduction in green canopy area at P_i 7.5 J2s per gram sand. To quantify more exactly the difference in tolerance of *35S::WOX11-SRDX* and wild-type Col-0 plants, we fitted the growth rates of individual plants (Fig. S6 and S7) to a logistic growth model. From this, we calculated the maximum projected green canopy area and determined the tolerance limit with 95% confidence interval (95% CI) (Fig. 5e). The relationship between maximum canopy area K and the P_i fitted a Gaussian curve, based on which we estimated the tolerance limit for *35S::WOX11-SRDX* at P_i = 2.25 (95% CI: 0.67-3.83) and for wild-type Col-0 at P_i = 4.84 (95% CI: 3.8-5.89). This difference in tolerance limits led us to conclude that WOX11 modulates tolerance of Arabidopsis to cyst nematode infections.

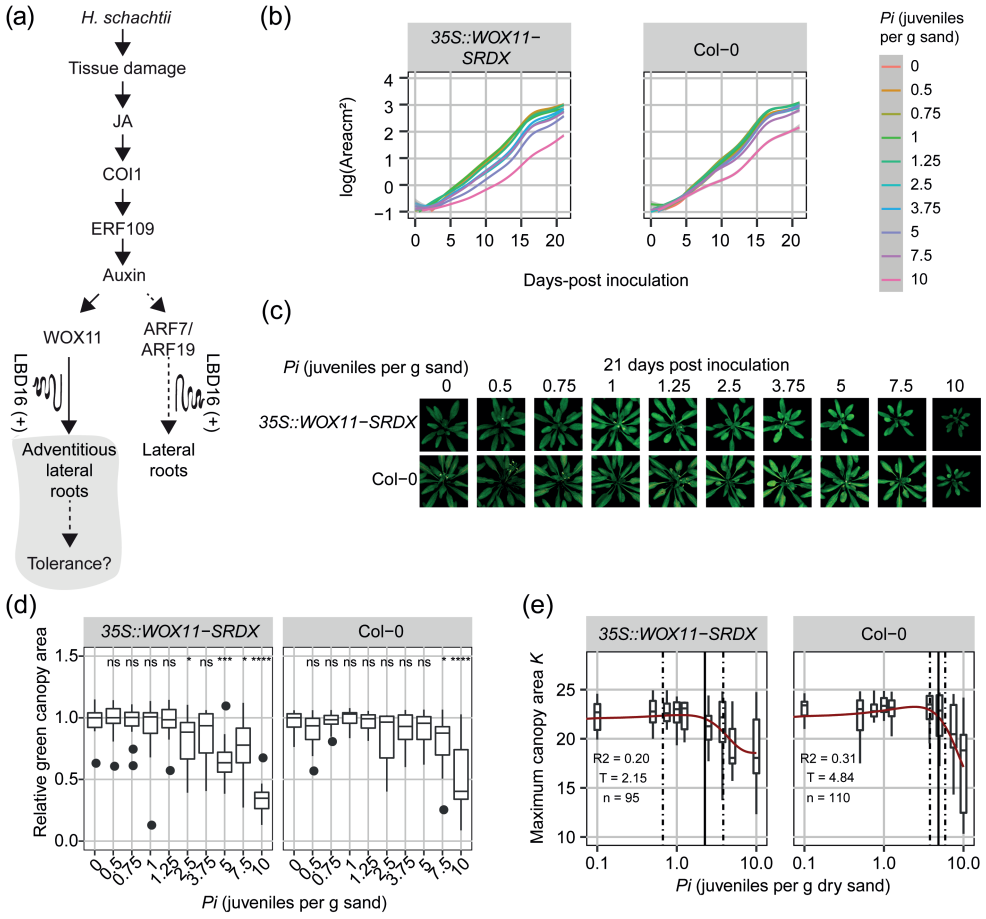

Fig. 5 WOX11 is involved in tolerance to cyst nematode infection. (a) Schematic diagram of *H. schachtii*- and WOX11-mediated adventitious lateral root emergence. Grey area indicates the tested part of the pathway. Curling line and '+' indicate involvement of multiple proteins, including LBD16. Nine-day-old Arabidopsis seedlings were inoculated with 10 densities (P_i) of *H. schachtii* juveniles (0 to 10 J2s per g dry sand) in 200 ml pots containing 200 grams of dry sand. (b) Average growth curve of Arabidopsis plants inoculated with different inoculum densities of *H. schachtii* from 0-21 dpi. Line fitting was based on a LOESS regression. (c) Representative images of plants inoculated with *H. schachtii* at 21-days post inoculation. (d) Relative green canopy area at 21 dpi. For the relative green canopy area, all values were normalized to the median of the measurements of the corresponding mock-inoculated plants. Data was analysed with a Wilcoxon Rank Sum test; ns= not significant, **P*< 0.05, ***P*< 0.01, ****P*<0.001 (n=10-18 plants per treatment). (e) The maximum canopy area *K* per inoculation density of *H. schachtii*. The fitted line is from a Gaussian curve. Solid line indicates the tolerance limit. Dashed line indicates the confidence interval. R^2 is the goodness of the fit, *T* is the tolerance limit, and n is the number of plants used for fitting the data.

Discussion

Excessive root branching is a classical symptom of nematode disease in plants of which the underlying causes nor the functions are well understood. Recently, we showed that endoparasitic cyst nematodes activate a JA-dependent damage signaling pathway leading to local auxin biosynthesis and subsequent *de novo* formation of secondary roots near infection sites (Guarneri *et al.*, 2023). At the outset of this study, it was not clear if nematode-induced secondary roots emerge from primary roots following the canonical auxin-dependent pathway for the formation of acropetal lateral roots, or if they emerge following a different pathway. Our current data supports the alternative hypothesis wherein the emergence of secondary roots in response to nematode damage follows the non-canonical WOX11-dependent pathway leading to the formation of adventitious lateral roots. This induction of adventitious lateral roots near nematode infection sites compensates for the inhibition of primary root growth by root-feeding cyst nematodes. We further show that the WOX11-mediated plasticity of root system architecture contributes to the tolerance of Arabidopsis to cyst nematode infections.

Our observations demonstrate that WOX11 modulates *de novo* root organogenesis near cyst nematode infection sites. Both WOX11- and ARF7/ARF19-mediated rooting pathways are activated by auxin, but they form a divergence point in the differentiation of adventitious lateral root primordia from lateral root primordia. WOX11 responds to auxin signals brought about by external cues, such as wounding (Sheng *et al.*, 2017), and mediates tissue repair and regeneration mechanisms (Liu *et al.*, 2014). In contrast, the auxin signals activating ARF7/ARF19 are thought to be developmentally regulated following endogenous rooting cues. Interestingly, both WOX11- and ARF7/ARF19-mediated root organogenesis pathways converge on LBD16 (Okushima *et al.*, 2007; Sheng *et al.*, 2017). Our findings indeed show that cyst nematodes induce expression of *LBD16* in a WOX11-dependent manner. However, this observation contradicts earlier work wherein *LBD16* expression was not observed in Arabidopsis infected with *H. schachtii* at similar timepoints after inoculation (Cabrera *et al.*, 2014). It should be noted that we used a different *LBD16*$_{pro}$*::LBD16-GUS* reporter line containing a much larger genomic region upstream of *LBD16* (Sheng *et al.*, 2017) compared to previous studies (Okushima *et al.*, 2007; Cabrera *et al.*, 2014). This extended promoter region included in the *LBD16*$_{pro}$*::LBD16-GUS* line harbours multiple WOX11-binding sites, which are absent in previously used *LBD16-GUS* reporter lines and which may thus explain the differences in observed *LBD16* expression in cyst nematode-infected Arabidopsis roots.

Our data further shows that both COI1 and ERF109 modulate *WOX11* expression in response to cyst nematode infection, which positions WOX11 downstream of

ERF109 within the JA-dependent damage signaling pathway. JA-dependent damage signaling induces local auxin biosynthesis, which drives the production of secondary roots (Guarneri *et al.*, 2023). Auxin has been shown to directly activate WOX11 expression, and as such WOX11 connects stress-induced auxin signaling to the establishment of adventitious lateral root founder cells (Sheng *et al.*, 2017). ERF109 most likely modulates WOX11 activity by regulating local YUCCA-mediated biosynthesis of auxin (Cai *et al.*, 2014). However, even in the absence of ERF109 (i.e., *erf109* mutant) we observed some *WOX11-GFP* expression in nematode infection sites. This agrees with our earlier observations demonstrating that besides damage-induced local biosynthesis of auxin, auxin transported from the shoots towards nematode infection sites also contributes to local stress-induced auxin maxima (Guarneri *et al.*, 2023). WOX11 may thus integrate local and systemic auxin-based stress response mechanisms leading to formation of adventitious lateral roots in nematode-infected Arabidopsis.

In our *in vitro* bioassays, WOX11 affected the number of secondary roots emerging from nematode-infected primary roots, but not the average secondary root length. Furthermore, we found that WOX11-mediated adventitious rooting compensated for the inhibition of primary root growth due to nematode infections, which implies that WOX11 mitigates the impact of nematode infections by adapting root system branching. This fits in the current model of wound-induced formation of secondary roots, wherein the activation of WOX11 initiates the cell fate transition of protoxylem cells into adventitious root founder cells (Liu *et al.*, 2014). WOX11 expression is thought to be specific for adventitious root founder cells, where it activates, together with its close homolog WOX12, LBD16- and WOX5-mediated divisions to initiate the formation adventitious root primordia (Liu *et al.*, 2014; Hu and Xu, 2016). During these divisions the expression of WOX11 decreases, because of which it affects the number of secondary roots but is less likely to alter secondary root growth.

Based on the green canopy area as a proxy for measuring the overall impact of belowground stress on plant fitness, we conclude that WOX11-mediated root system plasticity also contributes to the tolerance of Arabidopsis to cyst nematode infections. The estimated tolerance limit of *35S::WOX11-SRDX* plants for cyst nematode infections was significantly lower than for wild-type Col-0 plants. Others have shown that homologs of Arabidopsis WOX11 in rice, apple, and poplar enhance plant tolerance to abiotic stresses, such as drought and low nitrate conditions, by regulating adventitious lateral root formation (Cheng *et al.*, 2016; Wang *et al.*, 2020; Wang, LQ *et al.*, 2021; Tahir *et al.*, 2022). Furthermore, WOX11 functions as a key regulator in the regeneration of primary roots after mechanical injury by inducing the formation of adventitious lateral roots at the cut site (Sheng *et al.*, 2017). Our study provides

a first example of WOX11-mediated mitigation of the impact of belowground biotic stress.

WOX11-mediated adventitious rooting may contribute to tolerance of Arabidopsis to biotic stress by restoring the capacity of the root system to take up and transport water and minerals. Cyst nematodes modify host cells within the vascular cylinder into a permanent feeding structure, which interrupts the continuity of surrounding xylem vessels (Golinowski *et al.*, 1996; Sobczak *et al.*, 1997; Levin *et al.*, 2020). As cyst nematodes develop, their feeding structures expand, consuming a larger part of the vascular cylinder while further impeding the flow of water and minerals (Bohlmann and Sobczak, 2014). This is the reason why aboveground symptoms of cyst nematodes infections are often confused for drought stress. Local and systemic auxin-based stress signals may thus activate WOX11-mediated adventitious lateral rooting to maintain the flow of water and minerals to the xylem vessels above infection sites (Levin *et al.*, 2020). At lower inoculation densities, WOX11-meditated adventitious lateral root formation from cyst nematode infected primary roots may suffice to sustain normal Arabidopsis development and growth resulting in a more tolerant phenotype.

Recent research suggests that the cellular processes targeted by transcriptional activity of WOX11 includes the modulation of reactive oxygen species (ROS)-homeostasis. In poplar, PagWOX11/12a has been shown to regulate the expression of enzymes involved in scavenging ROS under salt stress conditions (Wang, LQ *et al.*, 2021). In crown root meristem cells of rice, WOX11 modulates ROS-mediated post-translational modifications (i.e., protein acetylation) of proteins required for crown root development (Xu *et al.*, 2023). ROS are required for the induction of adventitious root formation from Arabidopsis explants (Shin *et al.*, 2022). There is also evidence that ROS modulate auxin levels during the initiation of adventitious roots from Arabidopsis explants (Huang *et al.*, 2020). Moreover, we have recently linked tolerance of Arabidopsis to cyst nematode infections, ROS-mediated processes, and root system plasticity (Willig *et al.*, 2022). However, further research is needed to investigate if WOX11 influences ROS-related processes, or vice versa, in infection sites of cyst nematodes in Arabidopsis roots, and if such a mechanism plays a role in WOX11-mediated root plasticity and tolerance to nematode infections.

Acknowledgments

We thank Prof. Viola Willemsen for providing the *pWOX11::GFP*, *pWOX11::GFP-coi1-2*, *pWOX11::GFP-erf109* reporter lines, and Lin Xu for providing the *35S::WOX11-SRDX/arf7-1/19-1*, *arf7-1/19-1*, *LBD16pro::LBD16-GUS* and

35S::WOX11-SRDX/LBD16pro::LBD16-GUS mutant lines.This work was supported by the Graduate School Experimental Plant Sciences (EPS). JJW is funded by Dutch Top Sector Horticulture & Starting Materials (TU18152). JLLT was supported by NWO domain Applied and Engineering Sciences VENI (14250) and VIDI (18389) grants. MGS was supported by NWO domain Applied and Engineering Sciences VENI grant (17282).

Author contributions

JJW, NG, JB, and GS conceived the project. JJW, NG, TvL, SW, IEAE designed and performed the experiments. MGS provided scripts for SYLM analysis. Data was analyzed and interpreted by JJW, NG, and MGS. JJW, NG, and GS wrote the article. VW performed crosses of *coi1-2, erf109* with wild-type plants expressing *pWOX11::GFP.* VW and LX provided Arabidopsis mutant and reporter lines. VW, LX, AG, MGS, and JLLT provided critical feedback on the manuscript. All co-authors provided input for the submitted version.

Conflict of interest

The authors declare no conflict of interest.

Supporting information

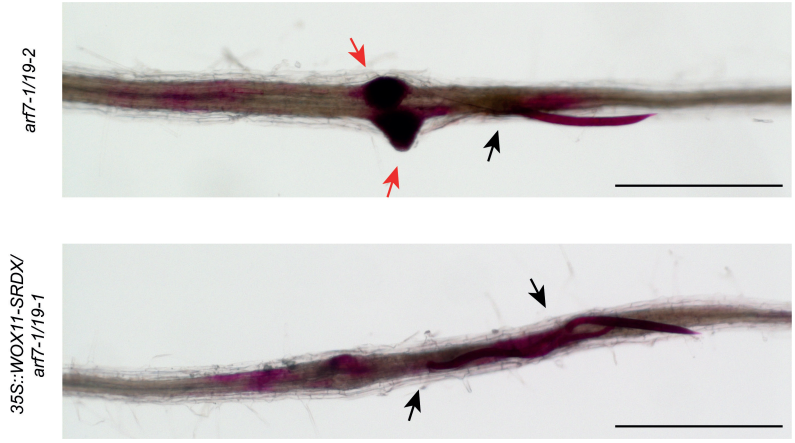

Fig. S1 Primordia formed in response to *H. schachtii* infection in *arf7-1/19-1* mutant seedlings. Seven-day-old *35S::WOX11-SRDX/arf7-1/19-1* and *arf7-1/arf19-1* mutant seedlings were inoculated with 90 *H. schachtii* juveniles or with mock solution. At 7 dpi, nematodes were stained with fuchsin and imaged using a dissection microscope. Black arrowheads indicate the head of the nematode. Red arrowheads indicate

lateral root primordia. Scale bar is 500 µm.

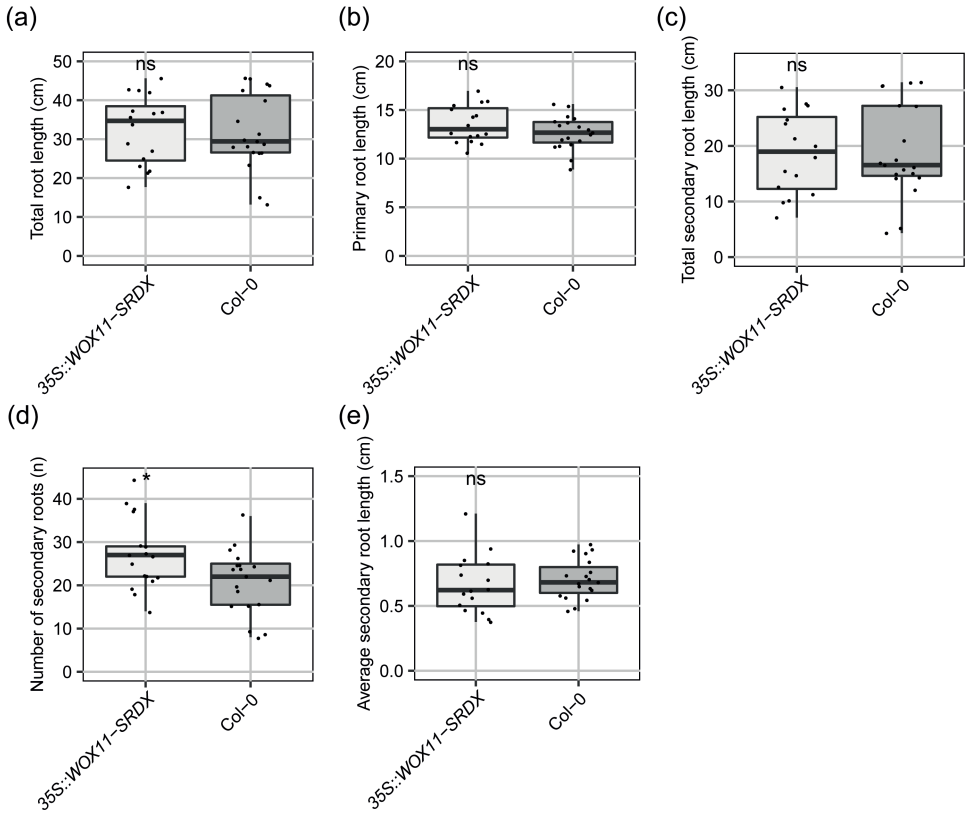

Fig. S2 Root architecture comparison between *35S::WOX11-SRDX* seedlings and wild-type Col-0 seedlings *35S::WOX11-SRDX* and wild-type Col-0 seedlings were grown on modified Knop medium for 16 days. Roots were scanned and root architectural components were measured. (a) Total root length. (b) Primary root length. (c) Total secondary root length. (d) Number of secondary roots. (e) Average secondary root length. Data from two independent biological repeats of the experiment were combined. Significance of differences between genotypes was calculated by a Unpaired Two-Samples Wilcoxon Test (n= 14-18).

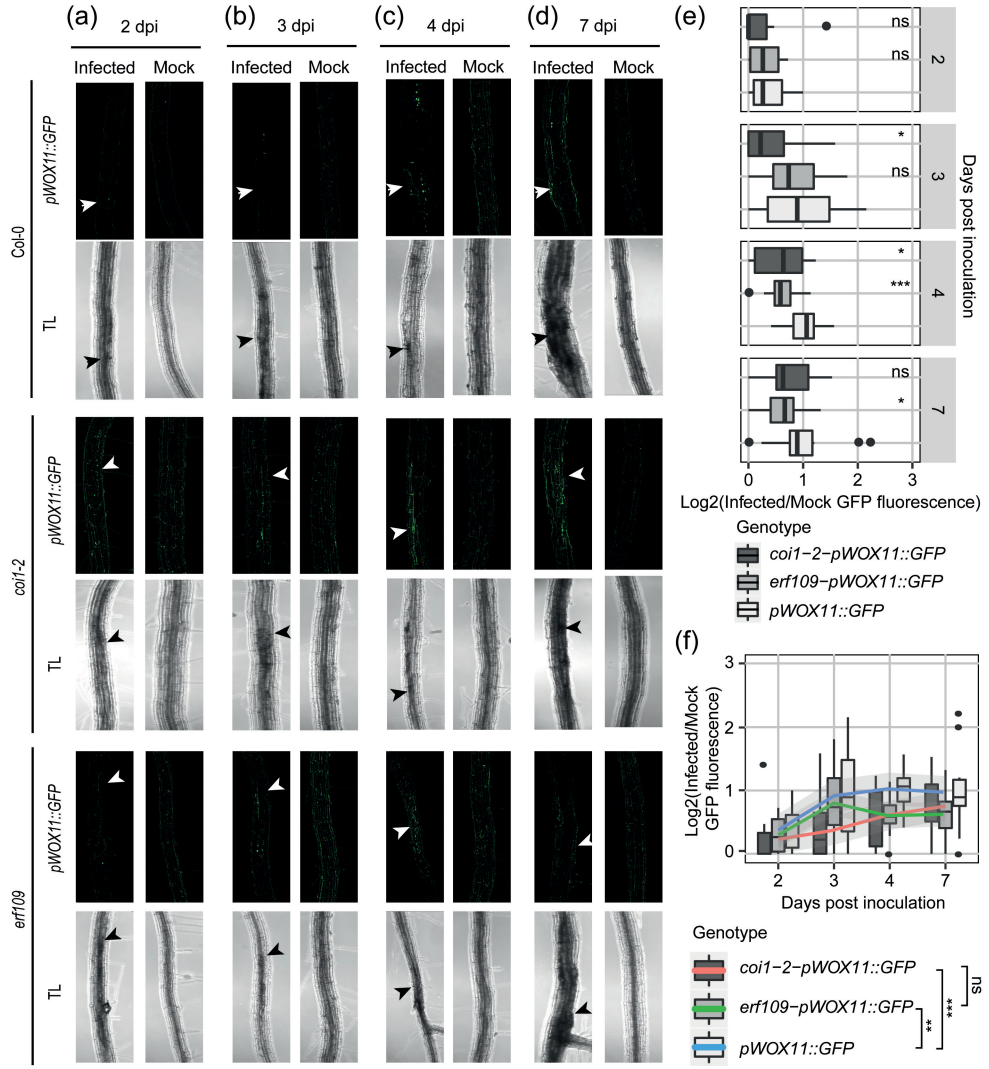

Fig. S3 COI1 and ERF109 contribute to WOX11 expression upon *H. schachtii* infection. (a-f) Four-day-old Arabidopsis seedlings were either inoculated with 10 *H.* schachtii second-stage juveniles (J2s) or with mock solution. At 2, 3, 4, and 7 dpi, seedlings were mounted and then imaged using a fluorescent confocal microscope. Single-nematode infection sites were selected for observation. (a-d) Representative pictures of infected and mock-inoculated seedlings expressing the *pWOX11::GFP* construct in either wild-type Col-0, mutant *coi1-2*, or mutant *erf109* background at **(**a) 2 dpi, (b) 3 dpi, (c) 4 dpi, and (d) 7 dpi. To make the fluorescence more visible, the brightness was enhanced for all the representative pictures in the same way. (e) Quantification of *pWOX11::GFP* fluorescent intensity induced by infection of wild-type Col-0, *coi1-2,* and *erf109* roots. Values represent $\log_2$ of the fluorescence ratio between the GFP integrated density of infected and noninfected roots. Data from three independent biological repeats of the experiment were combined. Significance of differences between fluorescent intensities in Co-0, *coi1-2,*

and *erf109* per timepoint was calculated by a Wilcoxon Rank Sum test. ns = not significant, **P*< 0.05, ***P*< 0.01, ****P*<0.001 (n=15). (f) Values represent $\log_2$ of the fluorescence ratio between the GFP integrated density of infected and noninfected roots. Significance of differences between genotypes was calculated by analysis of variance. Grey area indicates the 95% confidence interval of the loess fit.

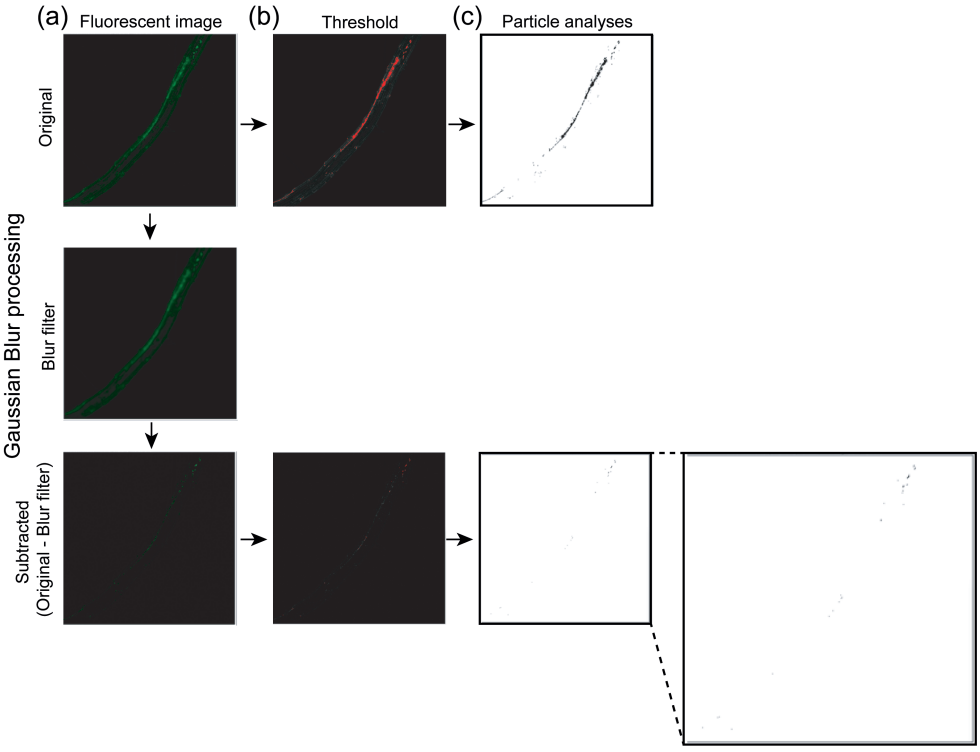

Fig. S4 Noise removal process using Gaussian Blur option in ImageJ. (a) The original images, which gave a lot of noise in the practical analyses (c) after setting the threshold (b) was duplicated and blurred using the Gaussian blur option in ImageJ. The blurred image was subtracted from the original image and the particles were analysed.

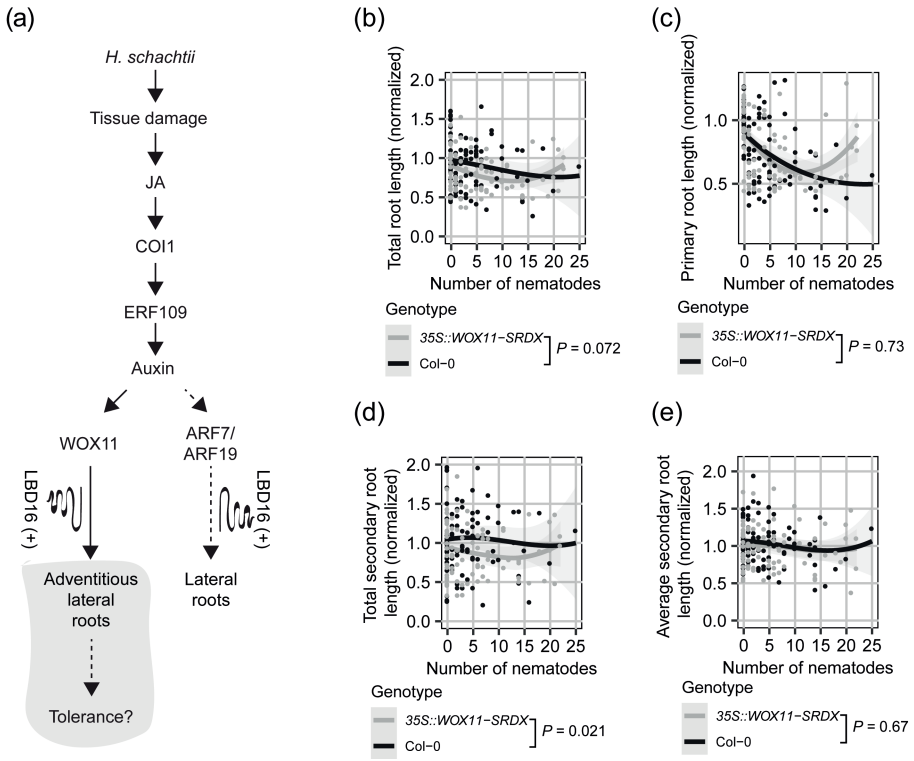

Fig. S5 Adventitious lateral roots increase the total secondary root length upon nematode infection. (a) Schematic diagram of *H. schachtii*- and WOX11-mediated adventitious lateral root emergence. Grey area indicates the tested part of the pathway. Curling line and '+' indicate involvement of multiple proteins, including LBD16. (b-d) Nine-day old *35S::WOX11-SRDX* and wild-type Col-0 seedlings were inoculated with densities (P_i) ranging from 0-7.5 *H. schachtii* J2s (per ml modified Knop medium). Roots were scanned and nematodes were counted after fuchsine staining at 7 dpi. Root architectural components of infected seedlings were normalized to the median respective component in mock-treated roots. Data of two independent biological repeats of the experiment were combined. (b) Total root length per number of nematodes inside the roots. **(**c) Primary root length per number of nematodes inside the roots. (d) Total secondary root length per number of nematodes inside the roots. (e) Average secondary root length per number of nematodes inside the roots. Data from two independent biological repeats of the experiment were combined. Significance of differences between genotypes was calculated by analysis of variance (n=14-18). Grey area indicates the 95% confidence interval of the loess fit.

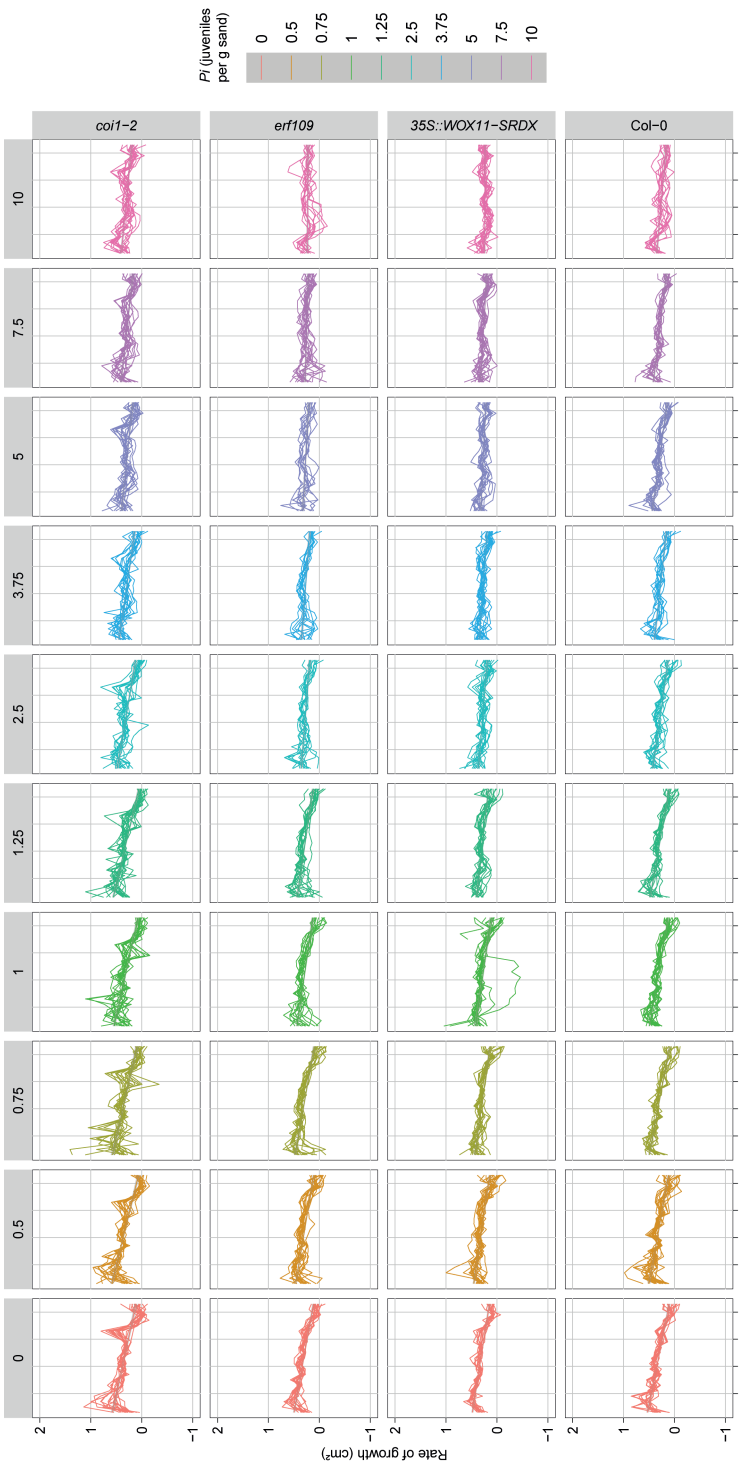

Fig. S6 Growth rates of *35S::WOX11-SRDX* and wild-type Col-0 plants over time. Nine-day-old Arabidopsis seedlings (*35S::WOX11-SRDX* and wild-type Col-0) were inoculated with 10 densities (P_i) of *H. schachtii* juveniles (0 to 2000 juveniles per g dry sand). The growth rates of plants were calculated per day. Lines represent individual plants (n=10-18 plants per treatment).

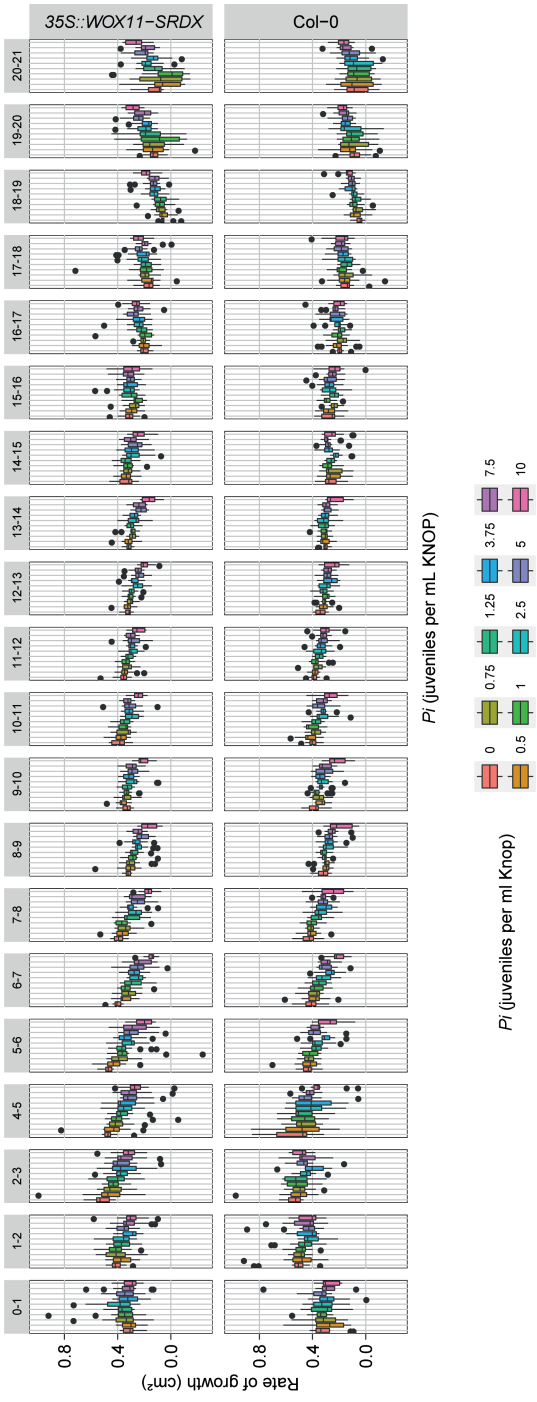

Fig. S7 Growth rates of *35S::WOX11-SRDX* plants are more affected during *H. schachtii* than wild-type Col-0. Nine-day-old Arabidopsis seedlings (*35S::WOX11-SRDX* and wild-type Col-0) were inoculated with 10 densities (P_i) of *H. schachtii* juveniles (0 to 2000 juveniles per g dry sand). The growth rates of plants were calculated per day. Boxplots represent data of x plants, the dots represent outlier measurements (1.5 times the interquartile range). (n = 10-18 plants per treatment).

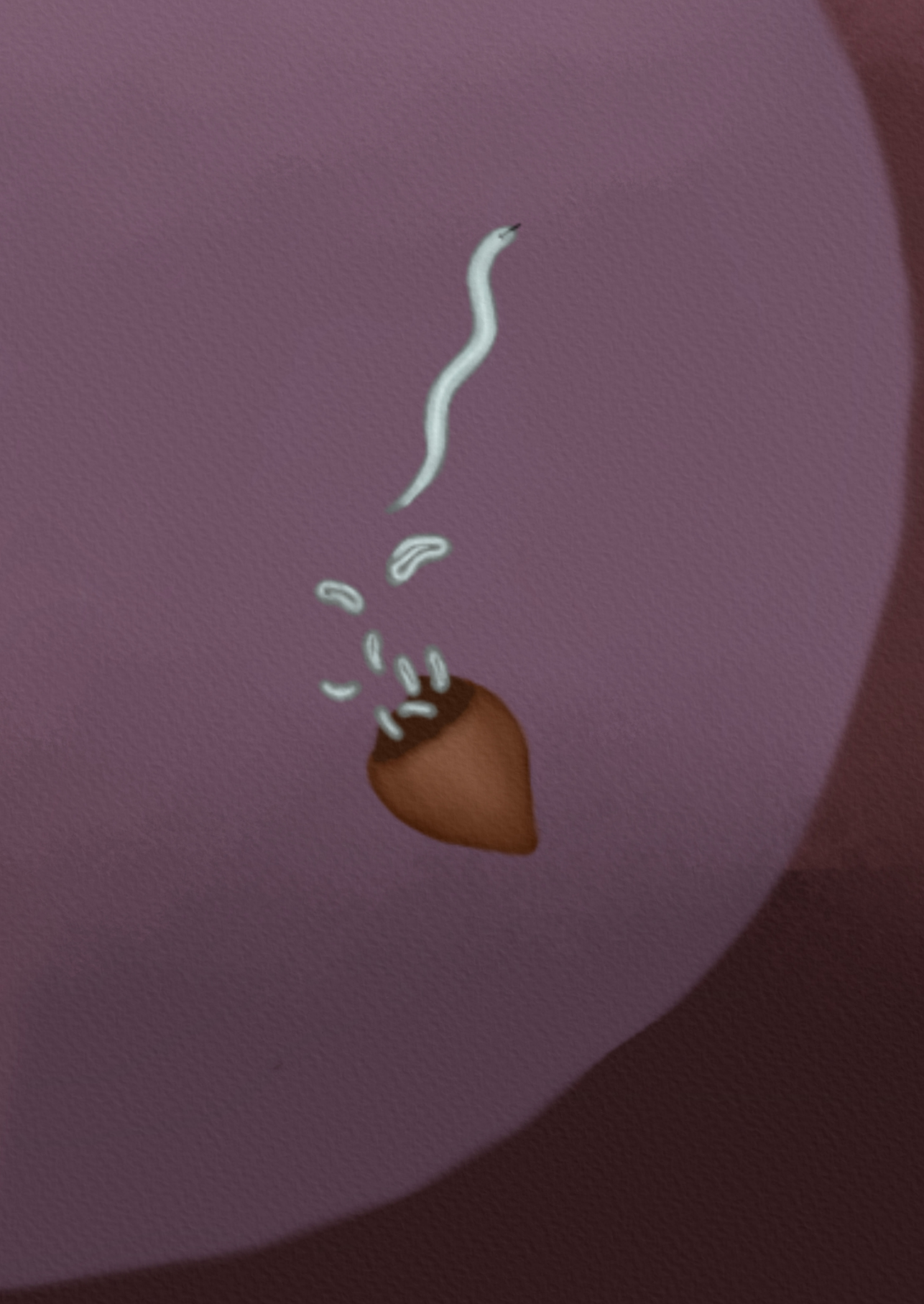

Chapter 4

WOX11-mediated cell size control in Arabidopsis attenuates fecundity of endoparasitic cyst nematodes

Nina Guarneri[1], Jaap-Jan Willig[1], Viola Willemsen[2], Aska Goverse[1], Mark G. Sterken[1], Pieter Nibbering[1], José L. Lozano Torres[1] and Geert Smant[1]

[1] - Laboratory of Nematology, Wageningen University & Research, 6708 PB Wageningen, the Netherlands

[2] - Laboratory of Cell and Developmental Biology, Cluster of Plant Developmental Biology, Wageningen University & Research, 6708 PB Wageningen, the Netherlands

Manuscript submitted; pre-print published on bioRxiv (2023)

Abstract

Cyst nematodes establish permanent feeding structures called syncytia inside host root vasculature, disrupting the flow of water and minerals. In response, plants form WOX11-mediated adventitious lateral roots at nematode infection sites. WOX11-adventitious lateral rooting modulates tolerance to nematode infections, however, whether this also benefits nematode parasitism remains unknown. Here, we report on bioassays using a *35S::WOX11-SRDX* transcriptional repressor mutant to investigate whether WOX11-adventitious lateral rooting promotes syncytium development and thereby female fecundity. Moreover, we chemically inhibited cellulose biosynthesis to verify if WOX11 directly modulates cell-wall plasticity in syncytia. Finally, we performed histochemical analyses to test if WOX11 mediates syncytial cell-wall plasticity via reactive oxygen species (ROS). Repression of WOX11-mediated transcription specifically enhanced the radial expansion of syncytial elements, increasing both syncytium size and female offspring. The enhanced syncytial hypertrophy observed in the *35S::WOX11-SRDX* mutant could be phenocopied by chemical inhibition of cellulose biosynthesis and was associated with elevated levels of ROS at nematode infection sites. We therefore conclude that WOX11 restricts radial expansion of nematode feeding structures and female fecundity, likely by modulating ROS-mediated cell-wall plasticity mechanisms. Remarkably, this novel role of WOX11 in plant cell size control is independent of WOX11-adventitious rooting underlying disease tolerance.

Introduction

Biotic stress by endoparasitic cyst nematodes disrupts plant growth by altering the flow of water and minerals through destructive migration within the roots and feeding (Trudgill *et al.*, 1975; Grundler and Hofmann, 2011; Rodiuc *et al.*, 2014; Levin *et al.*, 2021). In response to nematode infection, plants trigger a damage signaling pathway mediated by *WUSCHEL-RELATED HOMEOBOX11 (WOX11)* that leads to the formation of adventitious lateral roots at nematode infection sites (Guarneri *et al.*, 2023; Willig *et al.*, 2023a). WOX11-adventitious lateral roots compensate for the inhibition of primary root growth caused by cyst nematode infection and contribute to better maintenance of aboveground plant development and growth (Willig *et al.*, 2023a). Thus, WOX11 modulates plant tolerance to cyst nematode infections. Furthermore, WOX11 reduces Arabidopsis susceptibility to cyst nematode penetration. However, whether WOX11 may affect cyst nematode feeding and thereby female fecundity remains unknown.

Cyst nematode females require a permanent feeding structure to reach the adult

stage and produce eggs. Hereto, upon host penetration, the infective second-stage juveniles (J2s) insert their needle-like oral stylet into a cell of the plant vascular cylinder and secrete effector proteins. As a result, this cell undergoes a cascade of structural changes and fuses with hundreds of neighboring cells by partial cell-wall dissolution to form the so-called syncytium. During this process, activation of the endocycle increases the DNA content, while syncytial elements expand radially by hypertrophy (Golinowski *et al.*, 1996). Nematode juveniles feed on syncytia in cycles of continuous ingestion and resting periods, and molt three times until they become adult females and males (Muller *et al.*, 1981). While males stop feeding after the third larval stage and are associated with relatively small syncytia, females ingest food until the adult stage and have large, hypertrophied syncytia (Muller *et al.*, 1981; Hofmann and Grundler, 2006). Syncytial hypertrophy positively correlates with female size, which can be used as an indicator of female fecundity (Urwin *et al.*, 1997; Goverse *et al.*, 2000; Li *et al.*, 2004; Siddique *et al.*, 2012; Ali *et al.*, 2013; Siddique *et al.*, 2014; Siddique *et al.*, 2015; Chopra *et al.*, 2021; Siddique *et al.*, 2022b).

The hypertrophy of female-associated syncytia is thought to depend on the uptake of assimilates, such as sucrose from the phloem (Hofmann and Grundler, 2006). Initially, syncytia are symplastically isolated from surrounding host tissues and sucrose is taken up from phloem companion cells via active transport. Later, when syncytia have reached their maximum expansion, the opening of secondary plasmodesmata allows the passive transport of sucrose from the phloem sieve elements (Hofmann *et al.*, 2007). Increased osmolarity due to the high sucrose concentration causes the passive inflow of water from the xylem, elevating turgor pressure in the syncytia (Böckenhoff and Grundler, 1994). High turgor pressure poses tensile stress on plant cell walls and is thought to drive syncytial hypertrophy (Hofmann and Grundler, 2006; Cosgrove, 2022). At the same time, modifications in the syncytial cell-wall composition likely provide mechanical strength to withstand the turgor pressure, while allowing syncytial elements to expand and thus accommodate the periodic demands imposed by nematode feeding (Zhang *et al.*, 2017a). Indeed, silencing a cell-wall modifying enzyme involved in cellular hypertrophy compromised female fecundity in potato (Catalá *et al.*, 2000; Karczmarek *et al.*, 2008).

The presence of WOX11-mediated adventitious lateral roots at nematode infection sites might interfere with the flow of assimilates and water towards the syncytium, with possible consequences on syncytium hypertrophy and female fecundity. Indeed, similarly to syncytia, adventitious lateral roots constitute a sink of assimilates for the plant (Hofmann *et al.*, 2007; Stitz *et al.*, 2023). As such, adventitious lateral roots may compete with syncytia for the uptake of sucrose. Moreover, root branching depends on the activation of glycolysis in the roots, which increases the demand

for shoot-derived carbon sources (Stitz *et al.*, 2023). Consequently, adventitious lateral root formation may benefit syncytia by enhancing the overall availability of sucrose in the roots. Besides, mature adventitious lateral roots likely increase water flux towards the syncytium (Levin *et al.*, 2020), thereby promoting turgor-driven syncytial hypertrophy. As a result, larger, hypertrophied syncytia may accumulate higher amounts of sucrose, thus better supporting nematode feeding. Therefore, we hypothesize that WOX11 affects syncytium hypertrophy and thus, female fecundity via the induction of adventitious lateral root formation.

WOX11-mediated adventitious lateral root formation requires the transcription factor LATERAL ORGAN BOUNDARIES DOMAIN16 (LBD16). WOX11 directly binds to the promoter of LBD16*,* which induces the asymmetric radial expansion of root founder cells (Goh *et al.*, 2012, Vilches Barro *et al.*, 2019). Subsequently, founder cells divide asymmetrically to initiate an adventitious lateral root primordium. Here, we first investigated whether the transcriptional repressor mutant *35S::WOX11-SRDX* or the knockout *lbd16-2* mutant alter syncytium hypertrophy and female fecundity. Thus, we counted the number of nematodes that successfully established an infection, measured syncytium and female size, and quantified the number of eggs produced by females in the mutants compared to wild-type plants. Next, we conducted a correlation analysis to test for causality between WOX11-mediated adventitious lateral root formation and syncytium hypertrophy and female fecundity. Furthermore, we questioned whether WOX11 could directly affect the capacity of syncytia to accommodate large volumes of water and assimilates by modulating plant cell-wall plasticity. To this end, we analyzed the effect of a chemical inhibitor of cellulose biosynthesis on syncytium hypertrophy in the *35S::WOX11-SRDX* and *lbd16-2* mutants compared to wild-type Arabidopsis. Finally, given that WOX11 has been previously implicated in the regulation of ROS (Liu *et al.*, 2021; Wang, LQ *et al.*, 2021; Xu *et al.*, 2023) and that ROS are known to modulate cell-wall plasticity (Eljebbawi *et al.*, 2021), we researched whether WOX11 modulates ROS homeostasis in nematode syncytia. Our findings indicate that WOX11 attenuates female fecundity by restricting the hypertrophy of syncytial elements. Remarkably, this function of WOX11 in plant cell size control is not causally linked to adventitious lateral root formation. Instead, WOX11 may modulate syncytium hypertrophy via ROS-mediated cell-wall plasticity mechanisms.

Materials and Methods

Plant material and growth conditions

The Arabidopsis (*Arabidopsis thaliana*) lines Col-0, *35S::WOX11-SRDX* (Liu *et al.,* 2014), and *lbd16-2* (Fan *et al.,* 2012) were used. The transcriptional repressor *35S::WOX11-SRDX* mutant was chosen since it was reported to be more strongly impaired in adventitious lateral root formation compared to the double mutant *wox11-2 wox12-1* (Liu *et al.*, 2014; Sheng *et al.*, 2017). For *in vitro* experiments, Arabidopsis seeds were vapor sterilized and grown on modified Knop medium (Sijmons *et al.*, 1991) in a growth chamber with a 16 h : 8 h, light : dark photoperiod at 21°C. Plants were grown horizontally in 12-well plates for the *in vitro* infection assay and vertically in 12x12 cm Petri dishes for microscopy experiments. For pot experiments, non-sterile Arabidopsis seeds were sown on top of silver sand and grown under greenhouse conditions with 19-21°C and a 16 h : 8 h, light : dark photoperiod.

Nematode sterilization

Heterodera schachtii (Woensdrecht population from IRS, The Netherlands) cysts were obtained from infected *Brassica oleracea* roots grown in sand (Baum *et al.*, 2000). The cysts were hatched for seven days in a solution containing 1.5 mg ml^{-1} gentamycin sulfate, 0.05 mg ml^{-1} nystatin, and 3 mM $ZnCl_2$. Next, *H. schachtii* second-stage juveniles (J2s) were separated from debris using a 35% sucrose gradient and incubated in a sterilization solution (0.16 mM $HgCl_2$, 0.49 mM NaN_3, and 0.002% Triton X-100) for 15 minutes. Finally, the J2s were washed three times with sterile tap water and re-suspended in 0.7% Gelrite (Duchefa Biochemie, Haarlem, The Netherlands).

Pot experiment

21-day-old Arabidopsis plants were inoculated with 25 non-sterile J2s per gram of dry sand. This inoculation density was previously found to yield enough cysts (~10) without causing excessive inhibition of plant growth (Fig. S1). Distribution of the pots containing the different genotypes in the trays followed a randomized block design. At 28 days post inoculation (dpi), watering of the plants was discontinued and sand within the pots was allowed to dry for one month. The shoots were cut off and each pot was wrapped in aluminum foil and autoclaved. Samples were sent to the NAK (Emmeloord, The Netherlands) for automated cyst extraction. Cysts were crushed and the number of eggs and J2s per cyst was counted following the protocol by Teklu *et al.* (2018).

Isoxaben treatment

The procedure for the isoxaben treatment was adapted from literature (Chaudhary *et al.*, 2020). Four-day-old Arabidopsis seedlings were inoculated with 15 J2s per seedling or with a mock solution. At 5 dpi, seedlings were transferred to 55 mm round petri dishes containing 10 ml of liquid Knop medium and either 600 nM isoxaben or 0.01% DMSO. After 5 hours of treatment, seedlings were transferred to fresh liquid Knop medium. Nematode syncytia were imaged by brightfield microscopy as described in the next section. Roots were mounted in 10 µg ml^{-1} propidium iodide staining to image the elongation zone of non-infected seedlings and pictures were taken using a Leica SP8 confocal microscope (excitation/emission 488/600-640 nm). For each sample, the one dimension size (maximum width) of five epidermal cells at the elongation zone was measured using Fiji software (Schindelin *et al.*, 2012), after which the average width was calculated.

Measurement of female and syncytium size

Pictures of mature females and syncytia were taken at 28 dpi using an Olympus SZX10 binocular (Olympus, Tokyo, Japan) with a ×1.5 objective and ×2.5 magnification. For the observation of syncytia at 5 dpi, seedlings were mounted in water and imaged with an Axio Imager.M2 light microscope (Zeiss) via a ×20 objective and a differential interference contrast filter. Images were taken with an AxioCam MRc5 camera (Zeiss). The size of females and syncytia was extracted from the pictures by manually measuring the maximum two-dimensional surface areas using Fiji software (Schindelin *et al.*, 2012). The length of syncytia was taken by drawing a longitudinal line in the middle of the syncytium. The width was measured by selecting the widest point of the syncytium.

DAB staining

Five days after inoculation, infected and non-infected Arabidopsis seedlings were stained with DAB as described previously (Siddique *et al.*, 2014). First, seedlings were incubated in a DAB staining solution (10 mg ml^{-1} in water) for 2 hours in the dark. Then, they were bleached using an ethanol: lactic acid: glycerol (3:1:1) solution. Finally, seedlings were mounted in water and imaged with an Axio Imager.M2 light microscope (Zeiss) via a ×20 objective and a differential interference contrast filter. DAB staining intensity was scored on a scale from zero to six as described in Fig. S2.

Statistical analyses

Data was analysed using the R software version 3.6.3 (Windows, x64). The R

packages used were *tidyverse* (https://CRAN.R-project.org/package=tidyverse), ARTool (https://CRAN.R-project.org/package=ARTool) and *multcompView* (https://CRAN.R-project.org/package=multcompView). Correlation between variables was calculated using Spearman Rank-Order Correlation coefficient. The 95% confidence interval of the linear models was calculated using *geom_smooth* in R. For normally distributed data, significance of the differences among means was calculated by ANOVA followed by Tukey's HSD test for multiple comparisons. For non-parametric two-factorial ANOVA, an Aligned Rank Transform followed by an ART-contrast test for multiple comparisons was performed.

Results

WOX11 restricts the radial expansion of nematode syncytia and attenuates female growth

In a previous study, we showed that WOX11 modulates plant tolerance to infections by endoparasitic cyst nematodes (Willig *et al.*, 2023a). Here, we asked whether this also affects nematode parasitism. We first tested whether WOX11 and its downstream target LBD16 affect the number of nematodes that successfully establish an infection. Therefore, we inoculated 14-day-old Col-0, *35S::WOX11-SRDX* (transcriptional repressor), and *lbd16-2* plants with the beet cyst nematode *Heterodera schachtii*. At 28 days post inoculation (dpi), we counted the number of females and males per plant. None of the mutants differed from wild-type Col-0 in the number of females or males (Fig. 1a, b). Next, we investigated whether WOX11 and LBD16 affect syncytium expansion and female growth. For this purpose, pictures of nematode syncytia with only one female were taken from infected Col-0, *35S::WOX11-SRDX*, and *lbd16-2* plants at 28 dpi. The maximum two-dimensional surface area of the adult females and their corresponding syncytia was measured in the focal plane. This showed that the mutant plants *35S::WOX11-SRDX* and *lbd16-2* had significantly larger females and syncytia than wild-type Col-0 (Fig. 1c-e). To further understand in which direction (longitudinal or radial) syncytium expansion in the mutants differed from Col-0, we also measured the width and length maxima of syncytia. We found that *35S::WOX11-SRDX* and *lbd16-2* had significantly wider syncytia compared to wild-type plants (Fig. 1f). In contrast, no difference in syncytium length was observed among the genotypes (Fig. 1g). We concluded that WOX11 and LBD16 restrict the radial expansion of syncytial elements and attenuate female growth.

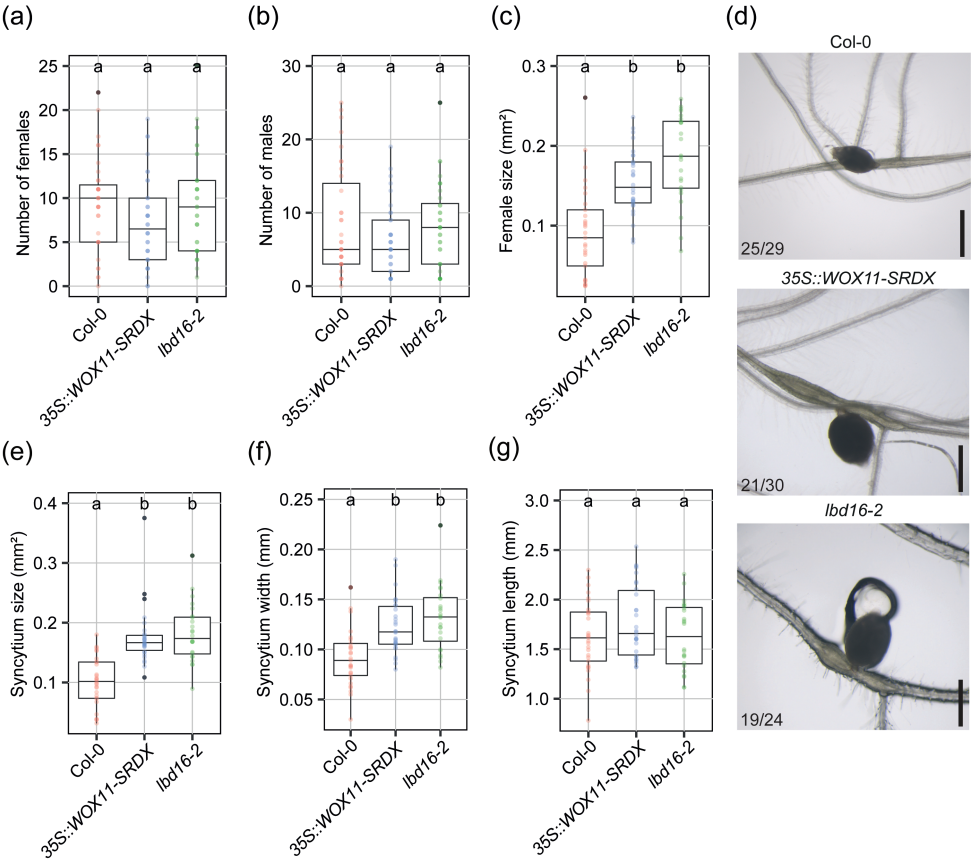

Fig. 1 WOX11 and LBD16 restrict *Heterodera schachtii* syncytium hypertrophy and attenuate female growth. 14-day-old Col-0, *35S::WOX11-SRDX*, and *lbd16-2* Arabidopsis plants were inoculated with 250 J2s per plant. (a) The number of females and (b) the number of males were counted at 28 dpi (n=36). (c) Female size, (e) syncytium size, and (f) syncytium width, and (g) length were measured at 28 dpi (n=24-30). This experiment was performed three times with similar outcomes and data was pooled for statistical analysis. Significance of differences between genotypes was calculated by ANOVA followed by Tukey's HSD test for multiple comparisons. Different letters indicate statistically different groups (P<0.05). (d) Representative pictures of females and syncytia at 28 dpi. Numbers at the bottom left corner indicate how often a similar phenotype as shown in the representative pictures was observed. Scale bar is 0.5 mm.

WOX11 attenuates nematode female fecundity in soil

Nematode assays *in vitro* can yield different results from experiments in soil, where plant growth is subjected to additional stresses and more variable conditions (Grenier *et al.*, 2020). To assess if WOX11 and LBD16 may influence female growth and thus fecundity in soil, we cultivated *35S::WOX11*-SRDX, *lbd16-2,* and wild-type Arabidopsis plants in pots with silver sand and then inoculated them with *H.*

schachtii. At 28 dpi, the sand in the pots was left to dry, after which the dead females, referred to as cysts, were extracted from the sand, counted, and crushed to count the number of eggs or J2s within each cyst (Fig. 2). The number of cysts from *35S::WOX11-SRDX* plants was not significantly different from the wild-type Col-0. However, *lbd16-2* plants had a lower number of cysts per plant compared to Col-0, suggesting that LBD16 may enhance plant susceptibility to nematode infections in pot conditions (Fig. 2a). Interestingly, we found that the average number of eggs or J2s per cyst was significantly higher in *35S::WOX11-SRDX* compared to Col-0 plant. Although *lbd16-2* also showed a higher average number of eggs or J2s per cyst than Col-0, this difference was not significant (Fig. 2b). Thus, we concluded that WOX11 does not affect plant susceptibility to nematode infection but restricts nematode female fecundity in soil.

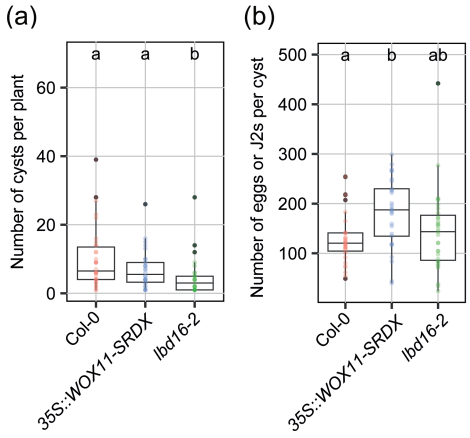

Fig. 2 WOX11 attenuates *Heterodera schachtii* female fecundity in soil. 21 days after growing wild-type Col-0 and *35S::WOX11-SRDX* and *lbd16-2* mutants on silver sand, plants were inoculated with 25 J2s/g of dry sand. Pot disposition in the trays followed a randomized block design. At 28 dpi, cysts were extracted, counted, and crushed to count the number of eggs or J2s contained in each cyst. (a) Number of cysts per plant. (b) Average number of eggs or J2s per cyst. Significance of differences between genotypes was calculated by ANOVA followed by Tukey's HSD test for multiple comparisons. Different letters indicate statistically different groups (P<0.05, n=30-35).

The effect of WOX11 on syncytium hypertrophy and female fecundity is not causally linked to adventitious lateral root formation

WOX11-adventitious lateral roots emerge in proximity or adjacent to nematode syncytia (Golinowski *et al.*, 1996; Willig *et al.*, 2023a). As adventitious lateral roots are both strong sinks of assimilates (Stitz *et al.*, 2023) and an additional source of water and minerals (Levin *et al.*, 2020), we hypothesized that they could either compete or support syncytium hypertrophy and nematode fecundity. To test this, we counted

the number of adventitious lateral roots emerging from 28 dpi syncytia in Col-0, *35S::WOX11*-SRDX, and *lbd16-2* and performed a correlation analysis with female and syncytium size. Interestingly, we found a positive correlation between the number of adventitious lateral roots emerging from syncytia and both syncytium and female size in wild-type Col-0 (Fig. 3a, b). Thus, the emergence of adventitious lateral roots may support syncytium hypertrophy and female fecundity. However, this positive correlation was not observed in the *35S::WOX11*-SRDX and *lbd16-2* mutants (Fig. 3a, b). This indicates that adventitious lateral root formation at nematode syncytia is not causally linked to the role of WOX11 in syncytium hypertrophy and female fecundity.

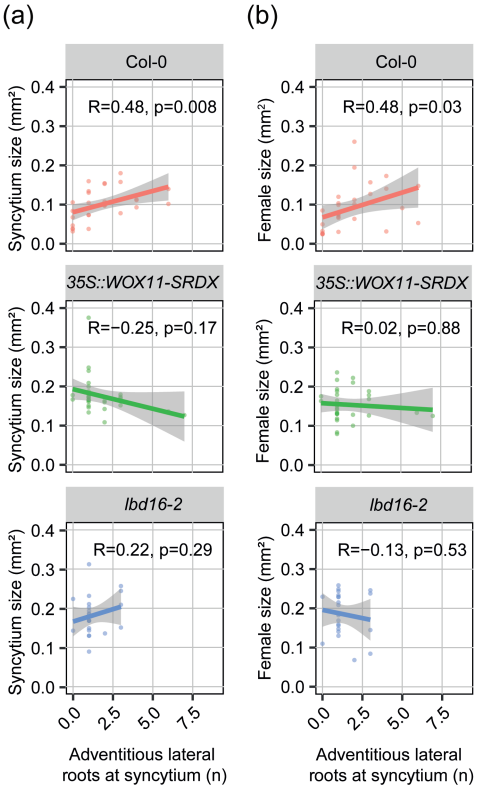

Fig. 3 The effect of WOX11 and LBD16 on *Heterodera schachtii* syncytium hypertrophy and female fecundity is not causally linked to adventitious lateral root formation. 14-day-old Col-0, *35S::WOX11-SRDX*, and *lbd16-2* plants were inoculated with 250 *H. schachtii* J2s per plant. At 28 dpi, the number of adventitious lateral roots in contact with nematode syncytia was counted and the size of females and syncytia was measured. (a) Correlation between the number of adventitious lateral roots and syncytium size. (b) Correlation between the number of adventitious lateral roots and female size. This experiment was performed three times with similar outcomes and data was pooled for statistical analysis. Correlation (R) between two variables was calculated using Spearman's rank-order correlation coefficient (n=24-30). Gray area

indicates 95% confidence interval.

WOX11 restricts the early radial expansion of syncytial elements

Radial expansion of nematode syncytia is mainly determined by the cellular hypertrophy of syncytial elements at 5 dpi (Magnusson and Golinowski, 1991; Golinowski *et al.*, 1996). At this stage, syncytial elements are symplastically isolated from the surrounding host tissue, which likely enables the build op of turgor pressure required for cellular hypertrophy (Ruan *et al.*, 2004; Hofmann *et al.*, 2007). Since we previously observed that WOX11 and LBD16 are expressed between 2 and 7 dpi (Willig *et al.*, 2023a), we asked whether WOX11 and LBD16 play a role in the early phases of syncytium expansion. To this end, we measured syncytium width in *35S::WOX11-SRDX* and *lbd16-2* mutants at 5 dpi. We found that, already at such an early time point, the two mutants displayed wider syncytia compared to the wild-type Col-0 (Fig. 4a, b). Thus, WOX11 and LBD16 limit the early radial expansion of syncytial elements.

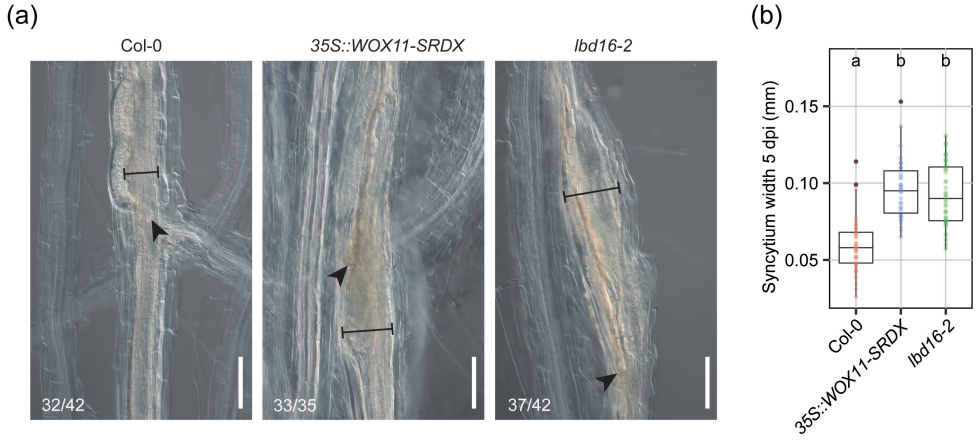

Fig. 4 WOX11 restricts the early radial expansion of *Heterodera schachtii* syncytial elements. Four-day-old Arabidopsis seedlings were inoculated with 15 *H. schachtii* J2s per plant. At 5 dpi, pictures were taken of syncytia and width was measured. (a) Representative pictures of syncytia at 5 dpi. Black arrowheads indicate the nematode head. Black lines indicate syncytium width. Numbers at the bottom left corner indicate how often a similar phenotype as shown in the representative pictures was observed. Scale bar is 100 µm. (b) Syncytium width at 5 dpi. This experiment was performed three times with similar outcomes and data was pooled for statistical analysis. Significance of differences between genotypes was calculated by ANOVA followed by Tukey's HSD test for multiple comparisons. Different letters indicate statistically different groups (P<0.001, n=35-42).

WOX11 restricts the cell-wall extensibility of syncytial elements

Root cells in the maturation zone are typically long and narrow. This is because root

cells elongate longitudinally in the root elongation zone before completing differentiation and entering the maturation zone (Verbelen *et al.*, 2006). The orientation of cellulose microfibrils and the properties of other cell-wall components increase the stiffness of the lateral cell walls, thus guiding the expansion in the longitudinal direction (Chaudhary *et al.*, 2020). However, plant developmental processes and environmental stresses can cause changes in cell-wall structure and composition, leading to enhanced radial expansion of root cells (Gigli-Bisceglia *et al.*, 2020). It was previously shown that LBD16 regulates the asymmetric radial expansion of founder cells, which involves the differential organization of cortical microtubules driving the deposition of cellulose microfibrils (Vilches Barro *et al.*, 2019). Here, we hypothesized that WOX11 and LBD16 restrict the radial expansion of syncytial elements by modulating cell-wall plasticity mechanisms.

To test this, we inhibited cellulose biosynthesis using isoxaben, a chemical that causes the internalization of cellulose synthase complexes from the plasma membrane to cytosolic vesicles (Tateno *et al.*, 2016). Disruption of cellulose biosynthesis or changes in cellulose microfibril alignment affects the directional growth of plant cells, which causes the cells to become radially swollen. Hence, four-days-old Arabidopsis *35S::WOX11-SRDX, lbd16-2,* and wild-type Col-0 seedlings were inoculated with *H. schachtii.* At 5 dpi, seedlings were treated either with isoxaben or DMSO as a negative control. Isoxaben treatment led to a significant increase in syncytium width in wild-type Col-0 plants, which phenocopied the DMSO-treated syncytia in the *35S::WOX11-SRDX* and *lbd16-2* mutants (Fig. 5a, b). Thus, inhibition of cellulose biosynthesis causes similar effects on radial expansion of syncytial elements as a disruption in WOX11- and LBD16-mediated pathways.

Interestingly, isoxaben treatment did not have a visible additive effect on the radial expansion of syncytia in *35S::WOX11-SRDX* and *lbd16-2* (Fig. 5a, b), suggesting that the syncytial cell walls in the mutants already reached their maximum extensibility. Therefore, we hypothesized that WOX11 and LBD16 attenuate plant cell-wall extensibility. We verified this by treating nine-day-old non-infected seedlings with isoxaben, which is known to cause the radial expansion of root epidermal cells at the elongation zone (Chaudhary *et al.*, 2020). After 5 hours of treatment with isoxaben, we found that the width of epidermal cells at the elongation zone of *35S::WOX11-SRDX* and *lbd16-2* increased dramatically compared to wild-type Col-0 (Fig. 6a, b). Notably, the width of epidermal cells in all genotypes was similar upon treatment with the negative control (Fig. 6a, b). Altogether, our data suggests that WOX11 and LBD16 restrict cell-wall extensibility of both isoxaben-treated epidermal cell at the elongation zone and syncytial elements in the mature zone.

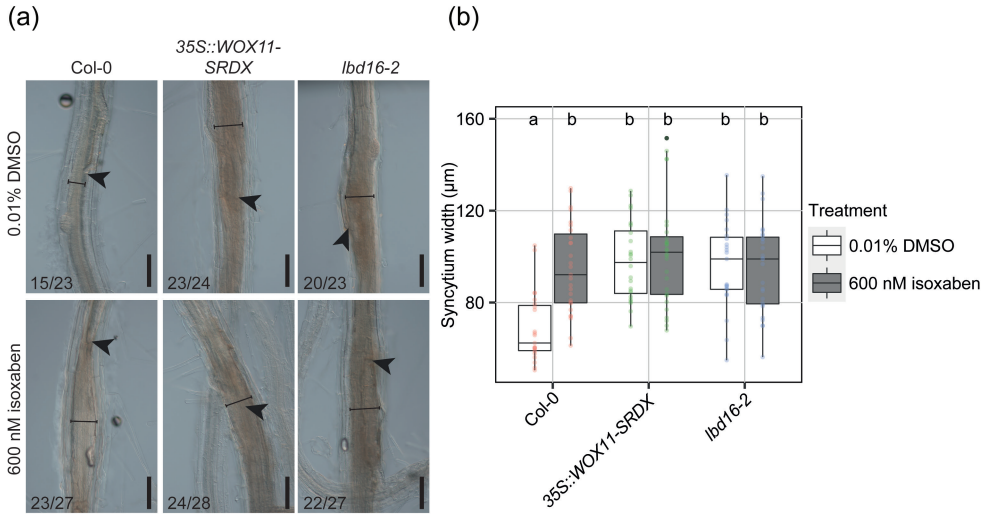

Fig. 5 Chemical inhibition of cellulose biosynthesis in Col-0 phenocopies the enhanced radial expansion of syncytial elements observed in *35S::WOX11-SRDX* and *lbd16-2*. Four-day-old Col-0, *35S::WOX11-SRDX,* and *lbd16-2* Arabidopsis seedlings were inoculated with 15 *H. schachtii* J2s. At 5 dpi, seedlings were transferred to liquid Knop medium containing either 600 nM isoxaben (ISX) or 0.01% DMSO. (a) Representative pictures of nematode syncytia. Black arrowheads indicate the nematode head. Black lines indicate syncytium width. Numbers at the bottom left corner indicate how often a similar phenotype as shown in the representative pictures was observed. Scale bar is 100 µm. (b) Quantification of syncytium width. This experiment was performed two times with similar outcomes and data was pooled for statistical analysis. Significance of differences between genotypes was calculated by ANOVA followed by Tukey's HSD test for multiple comparisons (P<0.05, n=23-27). Different letters indicate statistically different groups.

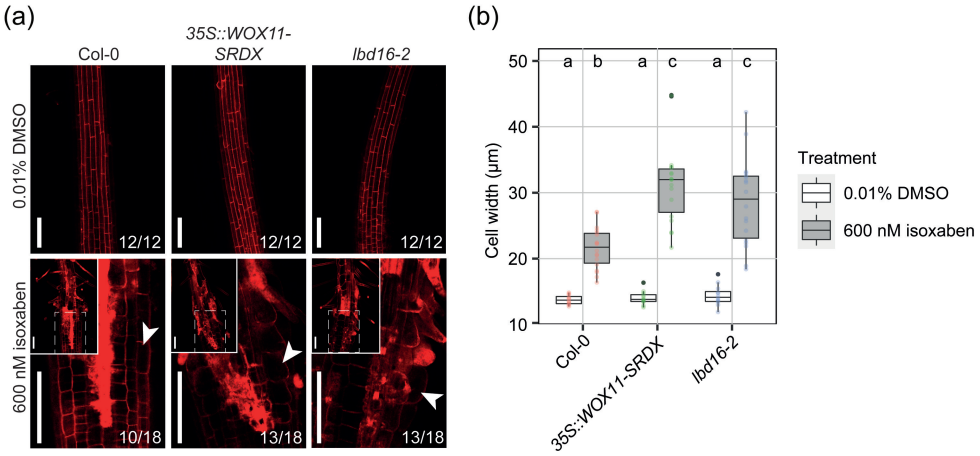

Fig. 6 WOX11 restricts the radial expansion of epidermal cells at the elongation zone in response to isoxaben treatment. Nine-day-old Col-0, *35S::WOX11-SRDX,* and *lbd16-2* Arabidopsis seedlings were transferred to liquid Knop medium containing either 600 nM isoxaben or 0.01% DMSO. After 5 hours, seedlings were mounted in 10 µg ml−1 propidium iodide for imaging. (a) Representative pictures of the elongation zone. White arrowheads indicate a radially expanded epidermal cell. The top-left inserts represent the original zoomed-out pictures. Numbers at the bottom left corner indicate how often a similar phenotype as shown in the representative pictures was observed. Scale bar is 100 µm. (b) Quantification of epidermal cells width. Each data point corresponds to the average width of five epidermal cells for each root sample. This experiment was performed two times with similar outcomes and data was pooled for statistical analysis. Significance of differences between genotypes was calculated by ANOVA followed by Tukey's HSD test for multiple comparisons (P<0.0001, n=12-18). Different letters indicate statistically different groups.

WOX11 modulates ROS homeostasis in nematode syncytia

ROS homeostasis is important in determining plant cell-wall plasticity (Eljebbawi *et al.*, 2021). WOX11 was previously found to regulate ROS homeostasis for crown root development in rice (Xu *et al.*, 2023) and during drought and salt stress in poplar (Liu *et al.*, 2021; Wang, LQ *et al.*, 2021). Therefore, we hypothesized that WOX11-mediated plant cell-wall plasticity involves the regulation of ROS. First, we stained 5 dpi syncytia in the *35S::WOX11-SRDX* and *lbd16-2* mutants with a DAB solution, which is oxidized by peroxidases in the presence of H_2O_2 (Eljebbawi *et al.*, 2021). This revealed that nematode syncytia in the *35S::WOX11-SRDX* and *lbd16-2* mutants have significantly lower ROS compared to wild-type Col-0 (Fig. 7a, b). Thus, we concluded that WOX11 modulates ROS homeostasis at nematode syncytia.

To verify whether WOX11-mediated ROS burst is linked to cell-wall plasticity responses, we treated non-infected nine-day-old Col-0, *35S::WOX11-SRDX*, and *lbd16-2* seedlings with 600 nM isoxaben or 0.01% DMSO for 5 hours, followed by

DAB staining. Isoxaben treatment caused an increase in ROS at the elongation zone in all genotypes. However, the levels of ROS in the *35S::WOX11-SRDX* and *lbd16-2* mutants were significantly lower compared to Col-0 (Fig. 6a, b). Thus, we concluded that modulation of ROS homeostasis is a plausible mechanism underlying WOX11-mediated cell-wall plasticity at nematode syncytia.

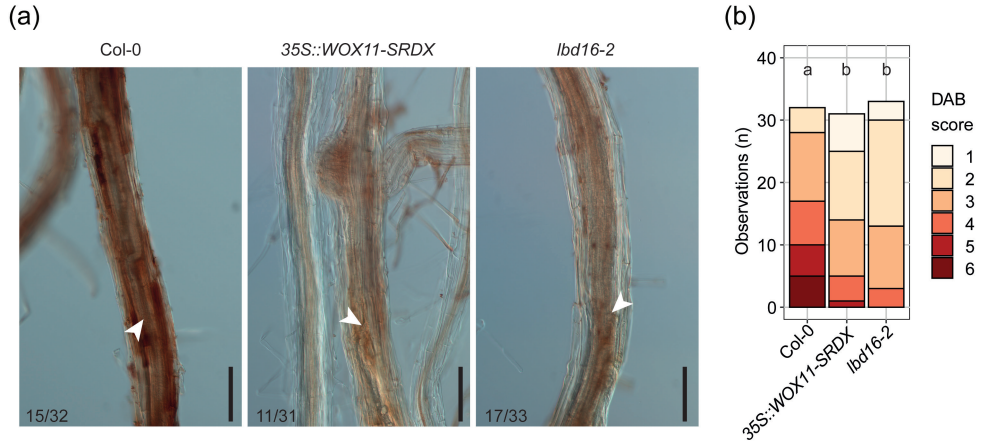

Fig. 7 WOX11 and LBD16 increase ROS levels in *Heterodera schachtii* syncytia. Four-day-old Col-0, *35S::WOX11-SRDX* and *lbd16-2* Arabidopsis seedlings were inoculated with 15 *H. schachtii* J2s. At 5 dpi, seedlings were incubated in a DAB staining solution for 2 hours in the dark. (a) Representative pictures of nematode syncytia. White arrowheads indicate the nematode head. Numbers at the bottom left corner indicate how often a similar phenotype as shown in the representative pictures was observed. Scale bar is 100 µm. (b) Scoring of DAB staining intensity on a scale from 1 to 6, based on the pictures shown in Fig. S2. Bar graphs indicate how often a certain DAB score is observed in each genotype. This experiment was performed three times with similar outcomes and data was pooled for statistical analysis. Significance of differences between genotypes was calculated by and Aligned Ranks Transform (ART) non-parametric ANOVA followed by an ART-contrast test for multiple comparisons (P<0.0001, n=31-35). Different letters indicate statistically different groups.

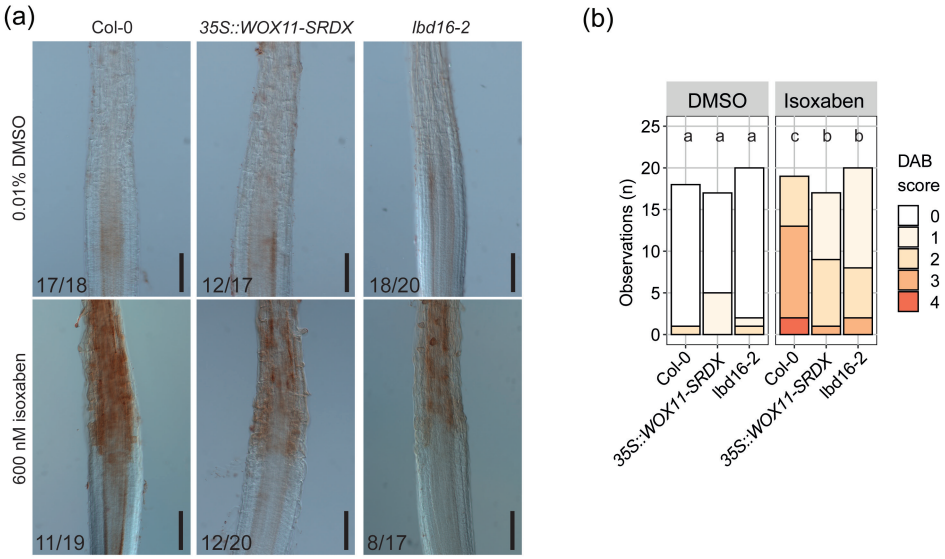

Fig. 8 WOX11 and LBD16 increase ROS levels at the elongation zone in response to cellulose biosynthesis inhibition. 9-day-old Col-0, *35S::WOX11-SRDX* and *lbd16-2* Arabidopsis seedlings were transferred to liquid KNOP medium containing either 600 nM isoxaben or 0.01% DMSO. After 5 hours, seedlings were incubated in a DAB staining solution for 2 hours in the dark. (a) Representative pictures of the elongation zone. Numbers at the bottom left corner indicate how often a similar phenotype as shown in the representative pictures was observed. Scale bar is 100 µm. (b) Scoring of DAB staining intensity on a scale from 0 to 4, based on the pictures shown in Fig. S2. Bar graphs indicate how often a certain DAB score is observed in each genotype. This experiment was performed two times with similar outcomes and data was pooled for statistical analysis. Significance of differences between genotypes was calculated by and Aligned Ranks Transform (ART) non-parametric ANOVA followed by an ART-contrast test for multiple comparisons (P<0.0001, n=18-20). Different letters indicate statistically different groups.

Discussion

Plant developmental plasticity mitigates the negative impacts of cyst nematode infections on growth, yet its potential impact on nematode parasitism remains largely unknown. We recently reported that plant perception of cyst nematode invasion induces the formation of WOX11-adventitious lateral roots at nematode infection sites (Guarneri *et al.*, 2023; Willig *et al.*, 2023a). Through this local root plasticity response, WOX11 compensates for the inhibition of primary root growth caused by nematode infection, which benefits overall plant growth and development (Willig *et al.*, 2023a). In this study, we shift perspective from the plant to the nematode and investigate whether WOX11-mediated developmental plasticity has an impact on nematode fecundity. Our findings support a model where WOX11 modulates ROS

homeostasis and cell-wall plasticity mechanisms that attenuate syncytial cell size and nematode fecundity.

We provide evidence that WOX11 restricts cyst nematode female growth and egg production. Although it was previously found that WOX11 decreases host invasion by infective juveniles (Willig *et al.*, 2023a), the repressor *35S::WOX11-SRDX* did not alter the number of nematodes successfully establishing an infection. Yet, Arabidopsis roots of the *35S::WOX11-SRDX* repressor displayed bigger females compared to wild-type Col-0 *in vitro.* When plants cultivated in soil were inoculated with *H. schachtii*, the cysts extracted from *35S::WOX11-SRDX* contained a higher number of eggs and J2s as compared to the cysts obtained from wild-type Col-0.

Consistently, the downstream target of WOX11, LBD16, similarly decreased female fecundity. *In vitro, lbd16-2* showed the same trend as the repressor *35S::WOX11-SRDX,* displaying bigger females compared to wild-type Col-0. Additionally, LBD16 had no effect on the number of nematodes that successfully established an infection. This is in agreement with a previous study, where the repressor mutant *35S::LBD16-SRDX* did not alter the number of nematode-induced syncytia after inoculation with *H. schachtii in vitro* (Cabrera *et al.*, 2014). In soil, *lbd16-2* showed a lower number of eggs or J2s per cyst compared to Col-0, albeit that this difference was not statistically significant. However, the number of cysts extracted from *lbd16-2* plants was lower compared to Col-0 and *35S::WOX11-SRDX*. LBD16 does not only regulate adventitious rooting but also lateral root formation (Sheng *et al.*, 2017). Thus, the disruption of both rooting pathways in the *lbd16-2* may have decreased the chances of nematodes locating or penetrating the roots in our pot experiment. Moreover, the outcomes of nematode bioassays in soil are generally more variable and have a lower resolution than *in vitro* assays. Thus, the overall low infection rates of *lbd16-2* plants may underly the absence of statistical significance in the difference between the average number of eggs or J2s per cysts in *lbd16-2* and Col-0.

We found that WOX11-induced adventitious lateral root formation is not causally linked to WOX11-mediated syncytium hypertrophy and nematode fecundity. Our data showed that adventitious lateral roots nonetheless support syncytium hypertrophy and female growth. This is in line with a previous hypothesis that adventitious lateral roots may increase water influx towards nematode syncytia (Levin *et al.*, 2020). However, the positive correlation between the number of adventitious lateral roots and syncytium and female size was disrupted in the repressor *35S::WOX11-SRDX* and in the *lbd16-2* mutants. This suggested that the role of WOX11 in modulating syncytium hypertrophy and female fecundity is separate from its role in adventitious lateral root formation.

WOX11 may attenuate female offspring size by directly restricting the availability of plant assimilates in nematode syncytia. We found that the repressor *35S::WOX11-SRDX* and *lbd16-2* enhanced the radial expansion of syncytia at 5 dpi, a stage where syncytial elements are symplastically isolated from the surrounding host tissue (Hofmann *et al.*, 2007). During symplastic isolation, nematode syncytia take up sucrose from the phloem via the apoplast through active transporters, which attracts water from the xylem and builds up turgor pressure (Hofmann *et al.*, 2007; Grundler and Hofmann, 2011). The cyclic feeding behavior of nematodes likely causes fluctuations of sucrose levels and turgor pressure that are accommodated by changes in cell-wall plasticity and syncytium expansion (Zhang *et al.*, 2017a). If WOX11 restricts the radial expansion of syncytial elements, it could interfere with the ability of syncytia to accumulate assimilates and support the cyclic food demands of female nematodes.

Furthermore, our data suggests that WOX11 modulates the plasticity of syncytial cell walls. We found that inhibition of cellulose biosynthesis using isoxaben increased the radial expansion of syncytial elements similarly to the disruption of WOX11-mediated pathways. Moreover, in non-infected plants, WOX11 limited the radial expansion of epidermal cells at the elongation zone in response to isoxaben treatment. This indicates that WOX11 limits the extensibility of syncytial elements in the radial direction. Syncytial cell-wall plasticity plays an important role in cyst nematode parasitism. Indeed, the silencing of two plant cell-wall modifying endo-B-1,4-glucanases reduced the number of females and their egg content in potato (Karczmarek *et al.*, 2008). Endo-B-1,4-glucanases loosen the cell wall by modifying amorphous cellulose structures (Glass *et al.*, 2015), which likely affects the expansion of syncytial elements. Moreover, the upregulation of many expansin proteins in nematode syncytia at 5 dpi suggests that syncytium expansion involves mechanisms of cell-wall loosening (Wieczorek *et al.*, 2006). It is possible that WOX11 mediates cell-wall plasticity in nematode syncytia by regulating the expression of expansin genes. Indeed, WOX11 was found to directly bind the promoter of an expansin gene and thereby modulate grain width in rice (Xiong *et al.*, 2023).

Plant cell-wall plasticity is a tightly regulated process involving many interacting components (Cosgrove, 2022). Organization and biosynthesis of cellulose microfibrils, the major load bearing components of the cell wall, are strongly influenced by cortical microtubules and by the properties and abundance of different polymers in the cell-wall matrix (Li *et al.*, 2015; Xiao *et al.*, 2015; Du *et al.*, 2020). Cortical microtubules guide cellulose synthase complexes, determining the organization of cellulose microfibrils (Li *et al.*, 2015). In turn, cellulose deposition regulates microtubule organization through a positive feedback loop (Vilches Barro *et al.*, 2019). Moreover,

pectin methylation and hemicellulose were found to affect both cellulose biosynthesis and cortical microtubule organization (Xiao *et al.*, 2015; Du *et al.*, 2020). Due to this complex network, isoxaben treatment does not only cause internalization of cellulose synthase complex but also alters the organization of cortical microtubules (Vilches Barro *et al.*, 2019). We observed that isoxaben treatment did not result in a measurable radial expansion of nematode syncytia in the *35S::WOX11-SRDX* and *lbd16-2* mutants. Interestingly, syncytium expansion is known to involve the disorganization of cortical microtubules (De Almeida Engler *et al.*, 2004). Thus, one plausible explanation for our observation is that WOX11 and LBD16 mediate plant cell-wall plasticity mechanisms that alter the organization of cortical microtubules. In this scenario, the level of microtubule organization in *35S::WOX11-SRDX* and *lbd16-2* syncytia would be too low to be further affected by isoxaben. Consistently, cortical microtubule organization was found to play an important role in LBD16-mediated asymmetric radial expansion of root founder cells (Vilches Barro *et al.*, 2019).

Our study suggests that WOX11 modulates ROS homeostasis in nematode syncytia. We found that WOX11 and LBD16 increase ROS accumulation in 5 dpi nematode syncytia. This is in line with a recent study where WOX11 directly activates peroxidase activity to induce ROS production and regulate crown root development in rice (Xu *et al.*, 2023). Besides, WOX11 was found to reduce cytotoxic levels of ROS in response to salt and drought stress in poplar (Liu *et al.*, 2014; Wang, LQ *et al.*, 2021). Thus, WOX11 modulates ROS homeostasis in different plant species and in response to multiple stresses. However, how WOX11-mediated ROS homeostasis affects plant developmental plasticity still remains unclear.

WOX11-mediated ROS homeostasis could modulate the extensibility of plant cell walls. ROS regulate both cell-wall loosening and cell-wall stiffening (Schmidt *et al.*, 2016; Eljebbawi *et al.*, 2021). H_2O_2 can be converted by peroxidases into OH^-, which catalyzes the oxidative cleavage of hemicellulose and pectins in the apoplast and loosens the cell wall (Eljebbawi *et al.*, 2021). Additionally, when H_2O_2 levels are high, peroxidases promote the oxidation and thereby cross-linking of extensins and phenolic compounds, leading to cell-wall stiffness (Magliano and Casal, 1998; Brownleader *et al.*, 2000; Eljebbawi *et al.*, 2021). Furthermore, ROS homeostasis regulates tubulin polymerization during microtubule formation (Livanos *et al.*, 2012), which could affect the orientation of cellulose biosynthesis and hereby change the cell-wall structural properties (Li *et al.*, 2015). We have observed that WOX11 induces ROS production at the elongation zone in response to cellulose biosynthesis inhibition by isoxaben. Moreover, WOX11 attenuates the radial expansion of epidermal cells at the elongation zone upon isoxaben treatment. Thus, we suggest that WOX11-mediated ROS homeostasis increases cell-wall stiffness in response to

cellulose biosynthesis inhibition. Similarly, WOX11 could modulate ROS to restrict syncytial cell-wall extensibility. Whether this involves the regulation of cortical microtubules, the cross-linking of extensins and phenolics, or other cell-wall plasticity mechanisms needs to be investigated.

We found that WOX11 increases ROS accumulation and attenuates female fecundity. However, previous research showed that the decreased ROS production in the *rboh*D/F mutant resulted in smaller syncytia and females compared to wild-type plants (Siddique *et al.*, 2014; Chopra *et al.*, 2021). While too high or too low levels of ROS can be deleterious for plants, modulation of ROS homeostasis within non-deleterious levels can regulate many cellular and physiological processes (Mittler, 2017; Willig *et al.*, 2022). For instance, modulation of ROS homeostasis via WOX11 could possibly mediate changes in syncytial cell-wall extensibility in response to the fluctuations in sucrose and turgor pressure due to nematode cyclic feeding behavior. This may regulate the volumes of water and assimilates available for nematode feeding and thereby affect female fecundity.

In conclusion, we showed that WOX11 controls cell size likely by modulating ROS homeostasis and cell-wall plasticity. Furthermore, we demonstrated that as a result WOX11 attenuates female growth and offspring size. Our results point at a novel role of WOX11 in the plant response to nematode infection, which is distinct from WOX11-mediated adventitious rooting. Importantly, our findings provide evidence that plant developmental plasticity can modulate nematode parasitism.

Acknowledgments

This work was supported by the Graduate School Experimental Plant Sciences (EPS). JJW is funded by Dutch Top Sector Horticulture & Starting Materials (TU18152). MGS was supported by NWO domain Applied and Engineering Sciences VENI grant (17282). JLLT was supported by NWO domain Applied and Engineering Sciences VENI (14250) and VIDI (18389) grants. No conflict of interest declared.

Competing interests

None declared.

Author contributions

GS, NG, and JJW conceived the project. NG and JJW designed the experiments and performed data collection. Data was analyzed and interpreted by NG, GS, JJW,

JJLT, MGS, and PN. NG and GS wrote the article with inputs from AG, JJLT, JJW, MGS, PN, and VW.

Data availability

The data that supports the findings of this study are available in the supplementary material of this article.

Supporting information

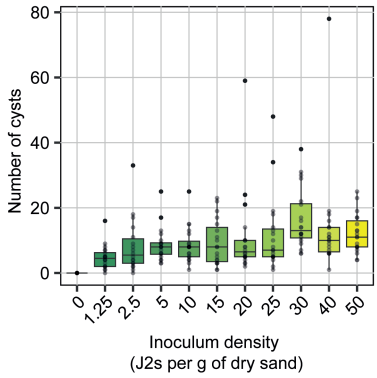

Fig. S1 Number of *Heterodera schachtii* cysts at increasing inoculation densities in wild-type Col-0 grown in pots. 21-day-old Arabidopsis Col-0 plants were inoculated with increasing nematode densities ranging from 0 to 50 juveniles per g of dry sand. At 28 dpi, cysts were extracted and counted.

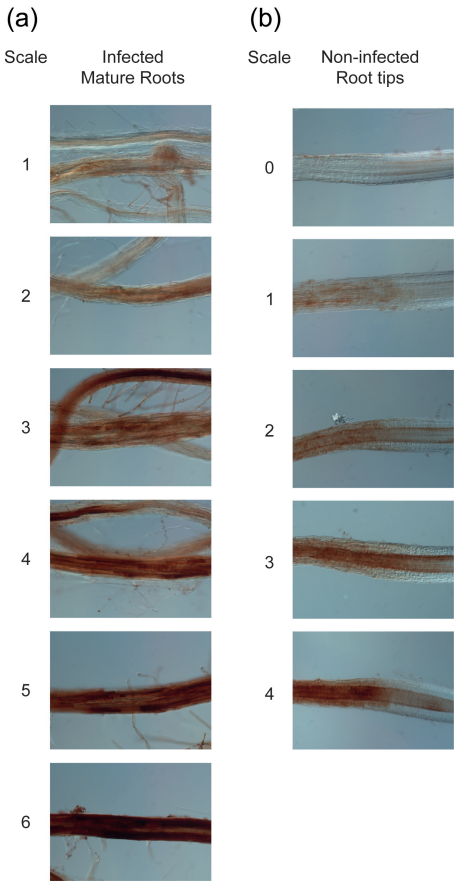

Fig. S2 Scale used for scoring the DAB staining of Arabidopsis roots. Four-day-old Arabidopsis seedlings were inoculated with 15 *Heterodera schachtii* J2s or a mock solution. At 5 dpi, seedlings were incubated in a DAB staining solution for 2 hours in the dark. (a) DAB staining of nematode infection sites on a scale from 1 to 6. (b) DAB staining of non-infected root tips on a scale from 0 to 4.

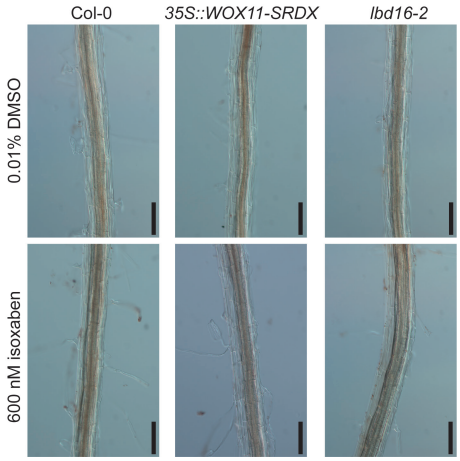

Fig. S3 DAB staining of the mature zone in non-infected roots treated with 600nM isoxaben or 0.01% DMSO. Nine-day-old Col-0, *35S::WOX11-SRDX*, and *lbd16-2* Arabidopsis seedlings were transferred to liquid Knop medium containing either 600 nM isoxaben or 0.01% DMSO. After 5 hours, seedlings were incubated in a DAB staining solution for 2 hours in the dark. Scale bar is 100 µm.

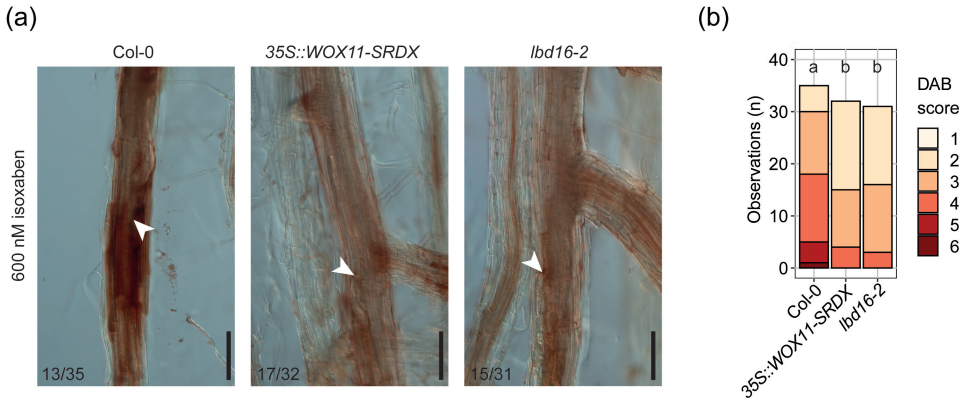

Fig. S4 DAB staining of *Heterodera schachtii* infected roots treated with 600nM isoxaben. Four-day-old Col-0, *35S::WOX11-SRDX*, and *lbd16-2* Arabidopsis seedlings were inoculated with 15 *H. schachtii* J2s. At 5 dpi, seedlings were transferred to liquid Knop medium containing 600 nM isoxaben. After 5 hours, DAB staining was performed for 2 hours in the dark. (a) Representative pictures of nematode syncytia. White arrowheads indicate the nematode head. Numbers at the bottom left corner indicate how often a similar phenotype as shown in the representative pictures was observed. Scale bar is 100 µm. (b) Scoring of DAB staining intensity on a scale from 1 to 6, based on the pictures shown in Figure S2. Bar graphs indicate how often a certain DAB score is observed in each genotype. This experiment was performed three times with similar outcomes and data was pooled for statistical analysis. Significance of differences between genotypes was calculated by and Aligned Ranks Transform (ART) non-parametric ANOVA followed by an ART-contrast test for multiple comparisons (P<0.0001, n=31-35). Different letters indicate statistically different groups.

Chapter 5

Shifting perspectives: the roles of plant cellular reprogramming during nematode parasitism

Nina Guarneri[1], Arne Schwelm[1,2], Aska Goverse[1] and Geert Smant[1]

[1] Laboratory of Nematology, Wageningen University & Research, 6708 PB Wageningen, the Netherlands

[2]Department of Environment, Soils and Landuse, Teagasc, Johnstown Castle, Wexford, Ireland

Manuscript submitted

Introduction

Biotrophic endoparasitism by root-knot nematodes (*Meloidogyne spp.*) and cyst nematodes (*Globodera* and *Heterodera* spp.) entails a prolonged and intimate interaction between the nematode and the plant (Yu and Steele, 1981; Gheysen and Mitchum, 2011). During this process, plant tissues at the site of infection undergo cellular reprogramming (Kyndt *et al.*, 2013). It is generally accepted that nematodes induce plant cellular reprogramming to establish permanent feeding structures providing them access to plant assimilates (Magnusson and Golinowski, 1991; de Almeida Engler *et al.*, 2012; Levin *et al.*, 2020). However, recent findings suggest that it is also a plant response to mitigate the impact of biotic stress by endoparasitism (Guarneri *et al.*, 2023; Willig *et al.*, 2023a). In our view, these outcomes of plant cellular reprogramming during nematode parasitism are two sides of the same coin (Fig. 1). Here, we take four examples where it can either benefit the nematode or its host or both (Fig. 2). Thus, we demonstrate how shifting from a pathogen-centered to a plant-centered perspective and vice versa can inspire new hypotheses and change our understanding of the function and regulation of plant cellular reprogramming during nematode parasitism. Furthermore, we apply this two-point perspective to another biotrophic plant-pathogen interaction that causes clubroot disease. This parallelism raises new questions on the evolution of plant cellular reprogramming during biotrophic parasitism in general. We aim to stimulate further research in this underexplored area, thereby advancing our comprehension of parallel adaptations to biotrophy in unrelated pathogens and common stress mitigation strategies in plants. We believe that such a two-pronged approach will lead to the identification of plant traits that not only decrease plant susceptibility to diseases but also increase plant tolerance to biotic stresses.

Nematode endoparasitism and its impact on the plant host

The infective juveniles of endoparasitic nematodes hatch from eggs in the soil and move to the surface of plant roots, guided by chemical cues released by the host (Sikder and Vestergard, 2019). Using their needle-like oral stylet, juveniles penetrate host roots and secrete salivary compounds known as effectors, which aid nematode parasitism (Jones *et al.*, 2013). During migration within the root tissue, juveniles release plant cell-wall-degrading enzymes in the apoplast, to loosen or break plant cells (Davis *et al.*, 2011). Cyst nematodes invade the mature root zone and migrate intracellularly, creating a necrotic track (Wyss and Zunke, 1986; Grundler *et al.*, 1994). Root-knot nematodes enter the root behind the root cap and migrate intercellularly towards the apical meristem. Here, they make a U-turn and move upwards towards the vascular cylinder in the differentiation zone (Jones *et al.*, 2013). Nema-

tode-induced cell-wall degradation, stylet thrusts, and pressure from the nematode body are likely to activate plant defense responses. In turn, nematodes secrete effector proteins that suppress the plant immune system (Siddique *et al.*, 2022a). The first symptom of nematode host invasion is an inhibition of the primary root growth, likely due to tissue damage and the allocation of resources by the plant toward defense (Zhou *et al.*, 2019; Willig *et al.*, 2022).

Upon reaching the vascular cylinder, infective juveniles secrete effectors into chosen host cells, prompting their differentiation into feeding structures (Abad and Williamson, 2010). Cyst nematodes induce the partial fusion of hundreds of cells to form multinucleated syncytia. In contrast, root-knot nematode feeding structures appear as five to seven separate and multinucleated giant cells surrounded by highly proliferating tissue (Jones *et al.*, 2013). Both syncytia and giant cells are characterized by an increase in DNA content through endopolyploidy, which is coupled to cell expansion by hypertrophy (de Almeida Engler *et al.*, 2012). Hypertrophy of feeding sites disrupts plant vascular connectivity (Yu and Steele, 1981; Bartlem *et al.*, 2014). However, a network of phloem and xylem elements is created by *de novo* vascularization embedding nematode feeding structures (Hoth *et al.*, 2005; Melnyk, 2017; Levin *et al.*, 2020). Additionally, the cell walls at the interface between the feeding structures and the plant vasculature thicken and form ingrowths to enhance water uptake and phloem unloading (Rodiuc *et al.*, 2014; Zhao *et al.*, 2018). As a result, nematode feeding structures become root-associated pseudo-organs that constitute a strong metabolic sink for the plant. The development of nematode feeding structures corresponds to a further inhibition in primary root growth and causes plant stunting, yellowing of leaves, and wilting (Jones *et al.*, 2013; Willig *et al.,* 2023b). Infected plants, however, can form *de novo* secondary roots that emerge either adjacent or near nematode feeding sites (Golinowski *et al.*, 1996; Olmo *et al.*, 2017; Guarneri *et al.*, 2023).

In conclusion, nematode endoparasitism intricately influences plant root tissue, triggering processes of cellular reprogramming and *de novo* organogenesis. In the next sections, we will illustrate four examples where these processes can be interpreted differently from both a nematode-centered and a plant-centered perspective.

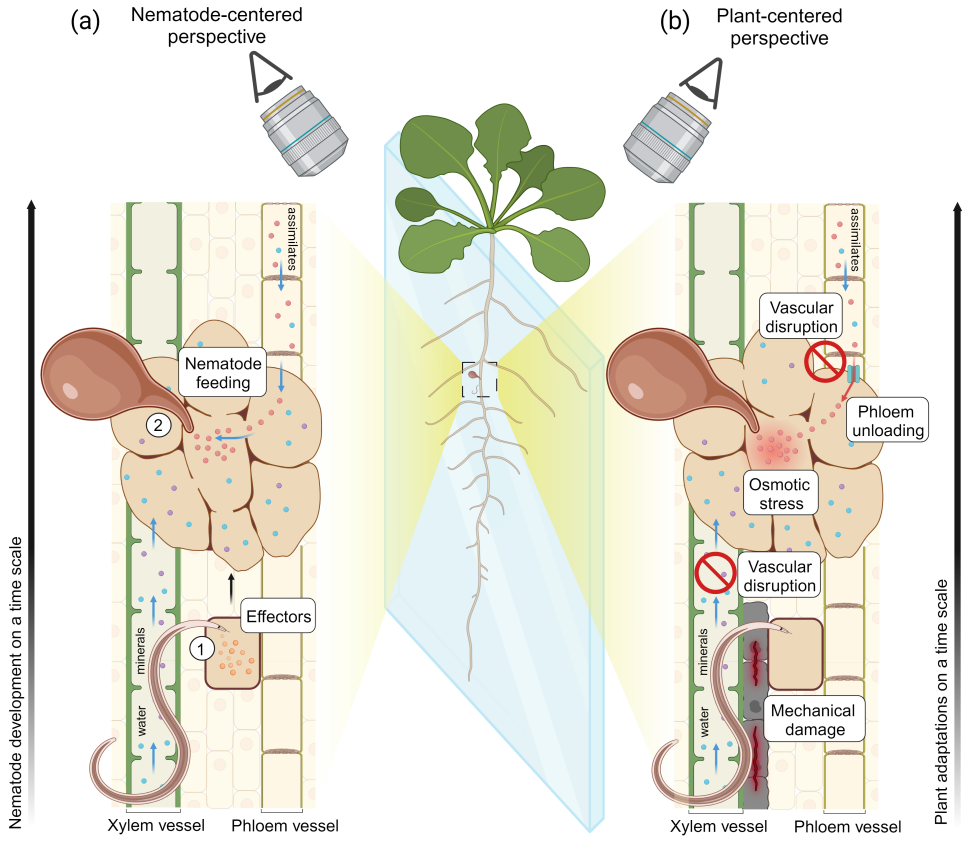

Fig 1. Nematode parasitism from a two-point perspective. An infected seedling on a microscopy glass is observed either from a nematode-centered perspective (a) or from a plant-centered perspective (b). The nematode-centered perspective in (a) describes how infective juveniles (1) secrete effectors that manipulate plant developmental pathways to induce a permanent feeding structure. Water and assimilates are taken up by the feeding structure from the plant vasculature and support nematode development into an adult female (2). The plant-centered perspective in (b) highlights the consequences of nematode parasitism for the plant host. Host invasion by infective juveniles cause mechanical damage to plant cells and feeding site development disrupts vascular connectivity. Plant assimilates are lost due to phloem unloading and high sucrose concentrations cause osmotic stress. Image created in Biorender.

Endopolyploidy

Endopolyploidy is the increase in genome copies within nuclei of somatic cells (Lang and Schnittger, 2020). It is the result of a modified mitotic cell cycle, where chromosomes multiply without a subsequent nuclear or cell division. These two variants of the cell cycle are called endocycle and acytokinetic mitosis, respectively. In angio-

sperms, high ploidy levels are typically found in plant tissues that grow rapidly and have high metabolic activity (Lang and Schnittger, 2020). Besides, endopolyploidy is present in several root cell types, where it accompanies the switch from cell proliferation to differentiation (Bhosale *et al.*, 2018). Recent studies suggest that endopolyploidy enables high cell growth rates by increasing the levels of cell-wall modifying genes. Vice versa, a reduced endoploidy level that cannot sustain the high metabolism needed for cell expansion, mediates cell-wall stiffening and slower growth (Bhosale *et al.*, 2018; Ma *et al.*, 2022). Thus, endopolyploidy is a mechanism inherent to plant development and involved in the regulation of cell growth and organ shape.

In nematode feeding sites, down-regulation or overexpression of genes regulating the endocycle impaired nematode development (de Almeida Engler *et al.*, 2012), suggesting that endocycling sustains nematode feeding. To date, nematode effectors initiating the endocycle in host cells have not been identified. However, some effectors potentially target the cell cycle and could thereby promote endopolyploidy. For example, the *Globodera pallida* effector GpIA7 interacts and interferes with the function of the potato EBP1, a plant growth regulator that modulates key cell cycle components such as CYCD3;1 and RBR1 (Coke *et al.*, 2021). Both CYCD3;1 and RBR1 repress the endocycle and thus their down-regulation by GpIA7 could induce endopolyploidy in *G. pallida* syncytia.

Yet, endopolyploidy-mediated cell expansion is also considered a plant response to mitigate the negative impact of abiotic and biotic stresses (Van de Peer *et al.*, 2020). For instance, endopolyploidy regulates fast hypocotyl elongation in response to low light and promotes plant growth upon shoot apical damage by herbivores (Paige, 2018). Furthermore, salt, osmotic, temperature, nutrient, and DNA stresses were all predicted to stimulate the endocycle in Arabidopsis roots (Bhosale *et al.*, 2018). This raises the question of whether endopolyploidy is a plant response to mitigate biotic stress by parasitic nematodes. Indeed, high endoploidy levels were found in feeding sites of plant-parasitic nematodes from distinct lineages, suggesting it may be a generic cellular response to the increased metabolic activity due to nematode feeding (Smant *et al.*, 2018). Additionally, cellular hypertrophy induced by endopolyploidy is thought to enhance water intake thereby mitigating osmotic stress caused by the high concentration of assimilates in nematode feeding sites (Grundler and Hofmann, 2011). Thus, investigating endopolyploidy from a plant-centered perspective could reveal novel mechanisms underlying plant tolerance to endoparasitic nematodes.

Root meristem regeneration

The root apical meristem ensures the continuous production of cells that drive root

growth (Zhou *et al.*, 2019). The meristem contains mitotically less active organizer cells forming the quiescent center, surrounded by mitotically active stem cells that originate root tissues. When the root meristem is damaged, a process of regeneration restores the quiescent center and stem cell niche to resume root growth within a few days (Zhou *et al.*, 2019). Upon injury, the plant hormone jasmonate induces the transcription factor *ERF109*, which in turn up-regulates *ERF115* and the cell-cycle regulator *CYCD6;1*. ERF115 establishes a new quiescent center by activating a molecular network that involves RBR1 and the stem cell transcription factor SCR. Additionally, CYCD6;1 promotes restorative cell divisions that replenish the site of injury.

Although root-knot nematodes migrate intracellularly without breaking plant cells, the pressure of their body and possibly the interference with symplastic continuity are sufficient to damage the root meristem and inhibit root growth (Zhou *et al.*, 2019). Interestingly, host invasion by root-knot nematodes was found to activate regeneration of the root apical meristem. Furthermore, transcriptional repression downstream of ERF115 (in the Arabidopsis *35S::ERF115-SRDX* mutant) resulted in a more severe primary root growth inhibition by nematode host invasion compared to wild-type plants (Zhou *et al.*, 2019). This suggests that plants deploy root regeneration mechanisms to mitigate the negative impact of nematodes on root growth.

Nevertheless, regeneration might be beneficial also for nematodes. The *35S::ERF115-SRDX* repressor mutant showed a delay in feeding site formation (Zhou *et al.*, 2019). Consistently, *scr* mutants displayed a lower number of feeding sites compared to wild-type plants (Olmo *et al.*, 2020). Additionally, MP/ARF5, a regulator of root regeneration, is highly expressed in *M. javanica* galls and fewer feeding sites can develop on the *35S::ARF5-SRDX* repressor mutant than on wild-type (Olmo *et al.*, 2020). If regeneration promotes nematode development, nematodes may have evolved effector proteins to induce regeneration. In 2006, an *M. incognita* effector called 16D10 was found to enhance root growth and target SCR-like protein SCL6 and SCL21, the function of which was unknown at the time. Ten years later, SCL21 was observed to interact with ERF115 and recently it was discovered to regulate wound-induced restorative cell divisions downstream of ERF115 (Heyman *et al.*, 2016; Bisht *et al.*, 2023). It would be informative to test if the root-knot nematode effector 16D10 enhances plant regeneration. This would suggest that nematodes may use effectors to reinforce or stabilize the plant-induced regeneration pathway. If so, could that mean that nematodes promote root growth to compensate for the damage inflicted on their host? Here, taking a pathogen-centered perspective on a typically plant-centered field of research such as meristem regeneration may reveal novel aspects regulating plant interactions with biotrophic pathogens.

De novo vascularization

Vascular development in plants occurs in two phases. During the primary phase, vascular cells formed in the root meristem undergo periclinal divisions to form a xylem axis flanked by two opposite phloem poles (Shimadzu *et al.*, 2022). In the secondary phase, the cells surrounding the vasculature divide to form multiple ring-shaped cell layers called the vascular cambium. The vascular cambium includes a layer of stem cells, which divide into vascular precursors that later differentiate into phloem and xylem elements. Vascular stem cell maintenance is regulated by small, secreted CLE peptides that upon detection by cell surface receptors promote cell division and/or inhibit phloem and xylem differentiation (Ren *et al.*, 2019; Carbonnel *et al.*, 2023).

Nematode infection disrupts vascular connectivity and induces the *de novo* formation of phloem and xylem elements (Yu and Steele, 1981; Hoth *et al.*, 2005; Melnyk, 2017; Levin *et al.*, 2020). *De novo* vascularization at nematode feeding sites is thought to be induced by nematode-secreted peptides that mimic plant CLEs (Bartlem *et al.*, 2014). *Heterodera schachtii* secretes CLE peptides that are recognized by the plant secretory machinery and transported from the cytoplasm to the apoplast (Wang *et al.*, 2021). In the apoplast, HsCLEs are perceived by the cell surface receptors CLV2-CRN and TDR (Replogle *et al.*, 2011; Guo *et al.*, 2017; Wang *et al.*, 2021). Exogenous treatment of hypocotyls with a combination of HsCLEs induced a TDR-dependent proliferation of the vascular cambium (Guo et al., 2017). Furthermore, the plant CLEs receptor mutants *clv2-1*, *crn-1*, and *tdr-1* displayed a decreased syncytium size compared to wild-type plants (Replogle *et al.*, 2011). Thus, it was proposed that cyst nematodes secrete CLEs to promote vascular cambium proliferation to their benefit (Guo *et al.*, 2017).

However, *de novo* vascularization is also a process that plants initiate when vascular connectivity is lost due to an injury. During wound healing and grafting, parenchyma cells first form a proliferating cambium and then differentiate into *de novo* phloem and xylem elements (Melnyk *et al.*, 2015; Shimadzu *et al.*, 2022). Since the xylem elements found at nematode infection sites are asymmetric and form irregular networks like wound-induced xylem, it is thought that they are induced as a plant response to nematode infection (Bartlem et al., 2014, Melnyk, 2017). The phloem around giant cells, however, appears different from the phloem formed in response to wounding in the stems or mature root zone, as it does not have companion cells (Bartlem *et al.*, 2014). This suggests either that root-knot nematodes manipulate *de novo* phloem formation or that wound-induced phloem at the root tip does not involve the development of companion cells. Companion cells form when protophloem sieve elements are fully elongated and functional and thus they are observed only

at around 500 µm from the root tip (Stadler *et al.*, 2005; Graeff and Hardtke, 2021). Thus, *de novo* vascularization could be induced by plants as a response to the damage associated with nematode infection.

Recently, EVG1, a positive regulator of cambium proliferation and a negative regulator of vascular differentiation was found to be induced both by wounding and cyst nematode infection (Mazumdar *et al.*, 2023). The *evg1-1* mutant enhanced xylem and phloem connectivity during grafting. Moreover, *evg1-1* displayed bigger syncytia compared to wild-type plants, whereas EVG1 overexpression decreased the size of syncytia as well as of *H. schachtii* females. These results suggest that enhanced vascular differentiation benefits both the plant, by promoting vascular reconnection after injury, and the nematode, possibly by increasing the flow of water and assimilates towards the syncytium. Yet, both wounding and nematode infection upregulate EVG1, which inhibits vascular differentiation. One possible explanation for this is that, when injured, plants induce EVG1 to promote cell division in the vascular cambium and restore the wounded tissue before re-establishing a vascular connection. Consequently, EVG1 may delay vascular reconnection during nematode infection and thus decrease the transport of water and assimilates to nematode syncytia. It would be interesting to test whether EVG1 may also decrease the ability of nematode-infected roots to transport water to the other plant tissues.

In conclusion, *de novo* vascularization during nematode infection could be modulated both by the plant and by the nematode. On one hand, plant responses to nematode damage may activate a molecular network that tightly regulates vascular proliferation and differentiation to heal the wounded tissue and restore vascular conductivity. On the other hand, nematode effectors may induce vascular cambium proliferation to enhance nutrient uptake. However, whether nematode-induced cambium proliferation interferes with plant-induced vascular reconnection remains to be investigated.

Secondary root formation

Cyst nematode infection has for long been reported in association with secondary root formation (Yu and Steele, 1981). These secondary roots emerge from nematode feeding sites but are also found in their proximity (Grymaszewska and Golinowski, 1991). Until recently, secondary roots have been proposed to benefit nematode parasitism. It was observed that nematode syncytia could extend into lateral roots, by incorporating cells of the lateral root xylem parenchyma (Magnusson and Golinowski, 1991). This led to the conclusion that secondary roots were not a secondary plant response, but a primary response induced by the nematode to increase

syncytium expansion. In line with this perspective, the *H. schachtii* effector Hs19C07 was found to interact with the auxin influx transporter LAX3, an important regulator of secondary root emergence (Lee *et al.*, 2011). However, Arabidopsis auxin influx mutants *lax3aux1* and *aux1lax1lax2lax3* infected with *H. schachtii* showed an enhanced lateral root emergence from syncytia. One given explanation for this unexpected result was that nematodes may induce auxin accumulation independently from LAX3 or that they may by-pass the auxin requirement to induce secondary root formation.

This latter example demonstrates how taking a plant perspective would have generated a different hypothesis. While secondary roots may increase the water and solute supply of nematode syncytia, they may as well be a response of the plant to mitigate the impact of biotic stress (Levin *et al.*, 2020). Indeed, potato and soybean cultivars that were able to form secondary roots in response to nematode infection better maintained their shoot growth (Trudgill and Cotes, 1983; Miltner et al., 1991). Furthermore, we previously found that the nematode density-dependent formation of secondary roots in Arabidopsis is controlled by the jasmonate-responsive ERF109 and WOX11 transcription factors, typically induced by mechanical damage (Guarneri *et al.*, 2023; Willig *et al.*, 2023a). Damage signaling by ERF109 partially regulates local auxin biosynthesis at nematode infection sites and thereby induces secondary root formation. This would explain why a mutation in LAX3 did not decrease the number of secondary roots at nematode infection sites. Moreover, WOX11-mediated root plasticity modulates plant tolerance to cyst nematode infection (Willig *et al.*, 2023a). This means that secondary root formation at cyst nematode infection sites benefits the plant.

Root-knot nematode feeding sites have a transcriptional profile that is very similar to secondary root formation (Cabrera *et al.*, 2014; Olmo *et al.*, 2017; Olmo *et al.*, 2020). Interestingly, the application of nematode secretions to Arabidopsis protoplasts induces the expression of LBD16, an important regulator of root primordium formation (Cabrera *et al.*, 2014). Moreover, mutation of genes involved in secondary root formation impaired gall formation and decreased plant susceptibility to nematodes (Olmo *et al.*, 2017; Olmo *et al.*, 2020). Additionally, the *M. incognita* effector MiIDL1 mimics the Arabidopsis IDA, a regulator of cell separation during root primordium emergence (Kim *et al.*, 2018). These results suggested that root-knot nematodes may hijack the pathways leading to secondary root formation to their benefit (Cabrera *et al.*, 2014; Kim *et al.*, 2018; Olmo *et al.*, 2020).

However, these results do not exclude that secondary roots are induced as a plant response to root-knot nematode infection. Indeed, root-knot nematode host invasion triggers wound responses that are known to induce local auxin biosynthesis and

thereby secondary root formation (Zhou *et al.*, 2019). It would be interesting to test whether secondary root formation at root-knot nematode infection sites can benefit the plant similarly to what was observed for cyst nematode infections.

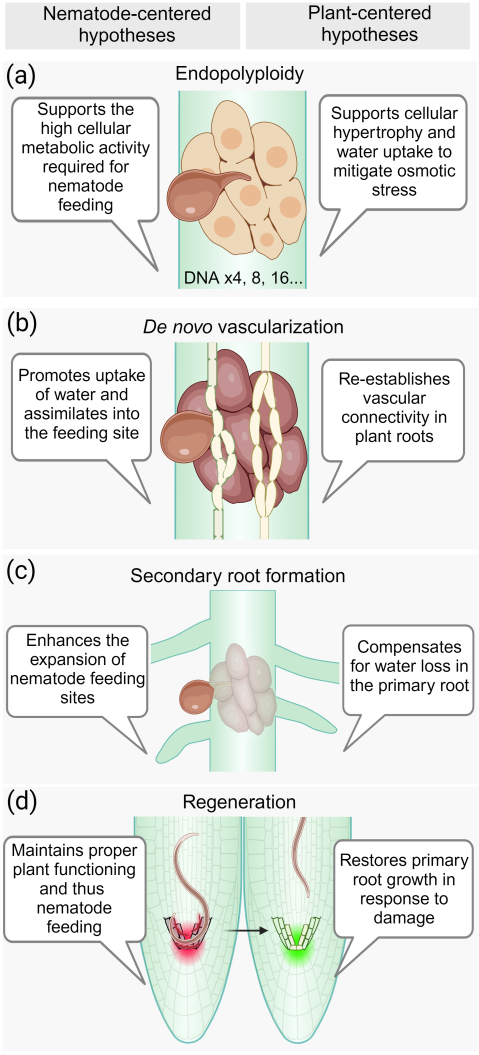

Fig.2 Hypotheses on nematode-associated cellular reprogramming from a two-point perspective. Four examples of nematode-associated cellular reprogramming (a-d) are observed from either a nematode-centered or a plant-centered perspective, generating different research questions. (a) Endopolyploidy increases DNA copy numbers, nuclear size and cellular hypertrophy. (b) Nematode feeding site development disrupts the existing plant vasculature. However, a network of xylem and phloem elements is created by *de novo* vascularization. (c) Secondary roots emerge from the primary root adjacent or near nematode feeding sites. (d) Nematode host invasion damages the root meristem, inhibiting root growth. Nevertheless, a regeneration mechanism replenishes the root with new cells. Speech boxes illustrate the

major research questions mentioned in this opinion paper. Image created in Biorender.

Shifting evolutionary perspectives: parallel adaptations in pathogens or common plant responses?

Parallelisms in host cellular reprogramming between nematode endoparasitism and other plant-biotroph interactions have been described several times (Wildermuth, 2010; Galindo-Gonzalez *et al.*, 2020; Harris and Pitzschke, 2020; Ichihashi *et al.*, 2020). Thus, we advocate that a plant-centered perspective can be adopted to study biotrophic interactions in general. Such an approach could reveal conserved plant mechanisms to mitigate the negative impact of biotrophic infections on fitness. Moreover, it may provide new insights into the ecological role and evolution of biotrophic parasitism. To support our opinion, we take the example of the protist *Plasmodiophora brassicae,* the causal agent of clubroot (Fig. 3), a devastating disease of Brassica crops (Javed *et al.*, 2023). This interaction is interesting because it shows how failure of the host to activate cellular reprogramming can lead to a collapse of the biotrophic relationship, which has detrimental effects both for the host and the parasite (Malinowski *et al.*, 2012).

The life cycle of *P. brassicae* consists of two phases. In the first phase, *P. brassicae* zoospores attach to root hair cells and epidermal cells in the root elongation zone and inject themselves into the host cytosol (Javed *et al.*, 2023). Inside the host cell, *P. brassicae* forms a primary plasmodium, which produces secondary zoospores that are released into the soil. In the second phase, the secondary zoospores infect the root cortex and develop into secondary plasmodia. At the site of secondary infection, cells expand by hypertrophy coupled to endopolyploidy. Additionally, the activation of existing meristematic activity in the plant vascular cambium causes plant cell proliferation. As a result, infected hypocotyls and roots become swollen, deformed and form galls, which causes the characteristic clubroot phenotype (Javed *et al.*, 2023). Gall formation is associated with the disruption of the existing plant vasculature and the appearance of *de novo* fragmented xylem elements and phloem parenchyma (Malinowski *et al.*, 2012). Moreover, increased expression of SWEET sucrose permeases redirects the flow of sugars to the pathogen infection site, creating a strong carbohydrate sink (Walerowski *et al.*, 2018). *P. brassicae* feeds on these carbohydrate-rich host cells by phagocytosis (Garvetto *et al.*, 2023) before producing resting spores, which are released into the soil upon disintegration of the gall (Javed *et al.*, 2023).

Although gall formation may benefit *P. brassicae* by providing extended space for its reproduction, it is not required by *P. brassicae* to complete its life cycle (Malinowski

et al., 2012; Olszak *et al.*, 2019). The secondary phase of clubroot disease involves initially activated vascular cambium proliferation, which later transitions to endocycle activation and increased cellular hypertrophy (Olszak *et al.*, 2019). Inhibition of the cell cycle using an inducible Arabidopsis line expressing the inhibitor KRP1 compromised the ability of plants to form galls. Similarly, disruption in cambium activity in the *cle41-1* mutant showed reduced gall formation compared to wild-type plants (Malinowski *et al.*, 2012). Moreover, infected hypocotyls in the Arabidopsis endocycle mutant *ccs52a1* displayed lower cellular hypertrophy compared to wild-type plants (Olszak *et al.*, 2019). Thus, both vascular cambium divisions and activation of the endocycle seem to be required for gall development. However, interference with these two processes in the aforementioned Arabidopsis mutants did not compromise *P. brassicae* ability to produce resting spores. This suggests that vascular cambium proliferation and endopolyploidy most likely are a plant response to the presence of the parasite.

In support of this hypothesis, the inability of infected plants to induce vascular proliferation results in the premature death and disintegration of plants (Malinowski *et al.*, 2012; Walerowski *et al.*, 2018). Specifically, infection of the *cle41-1* mutant led to almost 100% plant death compared to 20% of Col-0 at 32 days post-inoculation. Moreover, three early phloem development mutants (*ops-2*, *cvp2-1 cvl1-1*, and *brx-2*) that were unable to induce *de novo* formation of phloem elements in response to *P. brassicae* infection also showed premature plant death (Malinowski *et al.*, 2012). Therefore, the *de novo* vascularization observed in clubroot may be a plant response to compensate for the decreased availability of water and nutrients due to *P. brassicae* infection. Besides, endocycling coupled with hypertrophy in the plant cells containing secondary plasmodia could enable an increased water intake to mitigate the osmotic stress caused by the high sucrose concentrations. Alternatively, endocycling could be induced by the plant to maintain cell-wall integrity in response to the mechanical pressure caused by the growing plasmodium (Hittorf et al., 2023).

Although *P. brassicae* and endoparasitic nematodes belong to completely different eukaryotic supergroups, they trigger similar processes of plant cellular reprogramming. One explanation for this is that the targeting by biotrophic pathogens of common and limited plant processes resulted in the convergent evolution of similar effector activities. Alternatively, biotrophic plant pathogens may share effectors that evolved from a common ancestor. Additionally, secretion by biotrophic pathogens of bioactive non-proteinaceous compounds common to most eukaryotes (e.g., auxin) may trigger similar signaling pathways in plants. While these hypotheses on the evolution of biotrophic parasitism may all be true, it is important to consider an alternative more parsimonious scenario. Hence, we propose an additional perspective

where plant cellular reprogramming during biotrophic parasitism may be the result of conserved plant responses to mitigate biotic stress independent of molecular cues deriving from the pathogens.

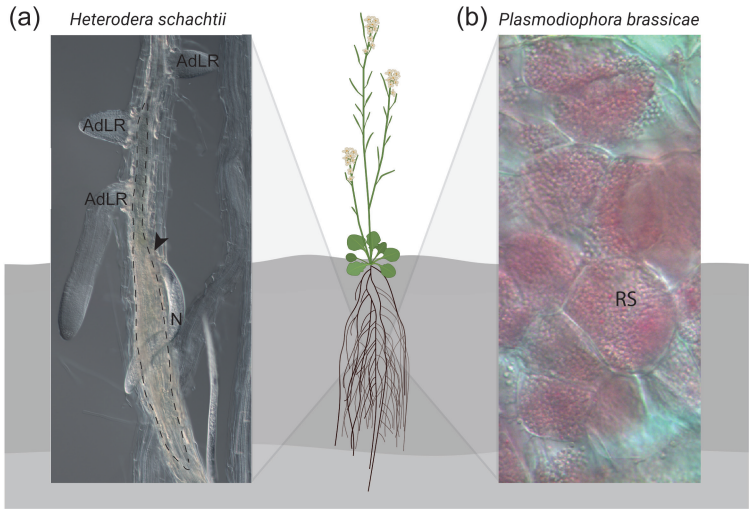

Fig.3 Plant interaction with two unrelated biotrophic pathogens. (a) Roots infected by the cyst nematode *Heterodera schachtii.* adLR=adventitious lateral roots. N=nematode. The dotted line indicates the nematode feeding site. (b) Root cells containing *Plasmodiophora brassicae* resting spores (RS), stained with nile red. Image partially created in BioRender.

Conclusions

We have illustrated how adopting a two-point perspective reveals that cellular reprogramming regulating biotrophic parasitism can benefit both the pathogen and the plant. This is in contrast with the commonly accepted definition of parasitic interactions, where the host typically experiences detrimental effects. Recent research showed how the line between parasitism and mutualism is thinner than previously thought, and that the consequences for the host are dictated by cost and benefit trade-offs specific to different environmental conditions. In fact, under critical environments, parasites can become mutualists (Goutte and Molbert, 2022) and mutualists can become parasites (Wang *et al.*, 2018). This highlights the plasticity of biotrophic interactions, modulated by a balance between biotroph-induced and host-induced mechanisms.

Acknowledgments

This work was supported by the Graduate School Experimental Plant Sciences (EPS). AS has received funding from the Research Leaders 2025 program co-funded by Teagasc and the European Union's Horizon 2020 research and innovation program under the Marie Skłodowska-Curie (grant agreement number 754380).

Conflict of interest

The authors declare no conflict of interest.

Chapter 6

General discussion

Introduction

Plant-parasitic nematodes pose a serious threat to food security. The damage of plant-parasitic nematodes to agriculture is estimated at 12.3% of global yield losses (Abad *et al.*, 2008, Jones *et al.*, 2013). In addition, climate change is increasing the spread and abundance of plant-parasitic nematodes and will likely exacerbate the severity of nematode-associated plant diseases (Dutta and Phani, 2023). Management of plant-parasitic nematodes is very challenging, due to the bans on chemical nematicides and the limited efficacy of other more environmentally friendly control measures (Nicol *et al.*, 2011, Desaeger *et al.*, 2020). Besides, the durability of crop resistance based on a limited number of resistance(R)-genes is undermined by the emergence of new virulent nematode populations (Davies and Elling, 2015). Therefore, alternative strategies are needed to limit the damage of plant-parasitic nematodes to agriculture.

Endoparasitic cyst nematodes are one of the most damaging groups of plant-parasitic nematodes (Jones *et al.*, 2013). They hatch from eggs in the soil and penetrate host roots by means of a needle-like oral stylet and salivary secretions that degrade plant cell walls (Bohlmann and Sobczak, 2014). Host invasion is followed by a migratory phase, in which the juveniles breach through plant cells to reach the vascular cylinder (Grundler *et al.*, 1994). Here, they secrete effector proteins that reprogram plant cells to induce a feeding site called syncytium (Gheysen and Mitchum, 2011). The syncytium is formed by partial cell-wall dissolution and protoplast fusion of hundreds of neighboring cells (Siddique *et al.*, 2012). These partially fused cells, here referred to as syncytial elements, increase in size by hypertrophy, resulting in the radial expansion of the syncytium (Golinowski *et al.*, 1996). Cyst nematodes feed on the syncytium for several weeks and develop into adult males and females (Muller *et al.*, 1981). After fertilization, the females lay eggs and become cysts, which are the remains of dead females with a hardened cuticle (Lilley *et al.*, 2005).

Plant growth is severely affected by cyst nematode infections. The destructive migration of the juveniles disrupts the flow of water and minerals in the roots (Grundler and Hofmann, 2011). Besides, nematode feeding creates a strong sink of assimilates for the plant (Hofmann *et al.*, 2007). As a result, the growth of the primary root is inhibited, negatively impacting aboveground growth and development (Willig *et al.*, 2023b). Nevertheless, infected plants can produce secondary roots at nematode infection sites, thereby compensating for the loss of water and minerals (Levin *et al.*, 2020). Indeed, the formation of secondary roots upon nematode infection promoted the maintenance of shoot growth in some soybean and potato cultivars (Trudgill and Cotes, 1983, Miltner *et al.*, 1991). Thus, root architecture plasticity is a possible mechanism underlying plant tolerance to cyst nematodes (Trudgill, 1991). However,

root developmental plasticity in response to biotic stress remains a largely unexplored field of research.

In this thesis I investigated the contribution of root developmental plasticity to plant-cyst nematode interactions. Specifically, I demonstrated that secondary root formation at nematode infection sites is regulated by a damage-signaling pathway, activated upon nematode host invasion of Arabidopsis primary roots (Chapter 2). Moreover, I showed that this root plasticity response to nematode host invasion is mediated by the transcription factor WOX11 and increases the overall plant tolerance to cyst nematode infections (Chapter 3). Furthermore, I provided evidence that besides modulating root architecture plasticity, WOX11 plays a separate role in plant cell size control during nematode parasitism. Remarkably, WOX11 attenuated syncytial hypertrophy and female fecundity, likely by modulating reactive oxygen species (ROS) homeostasis and plant cell-wall plasticity mechanisms (Chapter 4). Finally, in this chapter, I will discuss the main findings of this thesis in the context of a broader scientific and societal perspective and provide recommendations for future research.

Auxin: the core regulator of *de novo* organogenesis during cyst nematode endoparasitism

Auxin is a signaling molecule present in more than 80% of prokaryotes and in many eukaryotes such as fungi, algae, and land plants (Carrillo-Carrasco *et al.*, 2023). In land plants, auxin is a core regulator of growth and development. At the cellular level, auxin controls elongation, division, and identity (Caumon and Vernoux, 2023). Yet, at the tissue level, its action affects many different developmental processes e.g., regulation of embryo polarization, organ formation, shoot and root growth and tropism, stem cell maintenance, and vascular development. This pleiotropism of auxin is not yet fully understood. However, it is thought that auxin responses are highly dependent on cellular and developmental contexts, as well as on the spatial distribution and timing of auxin signaling (Caumon and Vernoux, 2023).

A large pool of auxin is synthesized in source organs (e.g., young leaves and root tips) and transported actively to other organs by transporters (Peer *et al.*, 2011). Active auxin transport is polar and is directed by AUX1/LAX influx carriers and PIN efflux carriers that are asymmetrically distributed on the plant cellular membrane. Auxin acts on plant cells by signaling through a canonical and a non-canonical pathway (Caumon and Vernoux, 2023). The canonical auxin sensing pathway occurs in the nucleus. Here, the F-box protein TIR1 binds to auxin and degrades AUX/IAA proteins. AUX/IAA proteins bind to the promoter of AUXIN RESPONSE FACTORS (ARFs) genes and repress their expression. Thus, by activating ARFs, auxin per-

ception induces the transcription of thousands of genes in a cell-specific manner. In contrast, the non-canonical pathway of auxin perception triggers non-transcriptional responses, such as protein phosphorylation, cytosolic calcium influx, acidification or alkalinization of the apoplast, plasma membrane depolarization, and changes in the actin network (Carrillo-Carrasco *et al.*, 2023).

Auxin regulates the formation of organs through auxin maxima. For example, periodic oscillations of auxin maxima at the primary root tip of Arabidopsis prime pericycle cells to form lateral roots with a regular spacing (Perianez-Rodriguez *et al.*, 2021). Moreover, auxin levels and its spatial distribution are crucial for the emergence of lateral root primordia (Zhao *et al.*, 2023). Polar auxin transport plays a major role in the accumulation of auxin. Furthermore, local auxin biosynthesis is required to generate auxin maxima, both during physiological processes and in the plant response to stress (Brumos *et al.*, 2018, Matosevich *et al.*, 2020).

Biotic stress by endoparasitic cyst nematodes induces the formation of auxin maxima at the site of infection (Grunewald *et al.*, 2009). In this thesis, we found that auxin maxima at cyst nematode infection sites are partially dependent on local auxin biosynthesis (Chapter 2) (Guarneri *et al.*, 2023). However, this is likely not the only mechanism regulating auxin accumulation at nematode infection sites. In fact, cyst nematode infection is known to interfere with polar auxin transport. Specifically, PIN1 and PIN7 proteins are downregulated around the nematode head, while PIN3 and PIN4 are redistributed from the basal to the lateral cell membrane of syncytial elements (Grunewald *et al.*, 2009). Thus, it is hypothesized that auxin efflux from the syncytium is blocked and that the auxin traveling from the shoot is redistributed laterally to the cells surrounding the syncytial elements. Finally, another source of auxin could be produced by the nematodes themselves. Indeed, auxin has been detected in nematode secretions (De Meutter *et al.*, 2005), and a possibly functional auxin biosynthesis pathway was found in the genome of potato cyst nematodes (Oosterbeek *et al.*, 2021).

Auxin maxima are crucial in *de novo* organogenesis at nematode infection sites. The development of syncytia involves the specific reprogramming of plant tissues, as if the plant underwent a regulated program of *de novo* organogenesis (Kyndt *et al.*, 2013). Unsurprisingly, auxin is required for the development of functional syncytia. Indeed, it was found that both auxin-insensitive mutants and the chemical inhibition of auxin polar transport negatively affect syncytium radial expansion (Goverse *et al.*, 2000). Moreover, the *pin1* mutant decreased the number of cysts by 40%, and *pin1, pin3,* and *pin4* mutants showed smaller cysts compared to wild-type Col-0 plants (Grunewald *et al.*, 2009). Besides, auxin accumulation also regulates *de novo* formation of adventitious lateral roots at nematode infection sites. We found that inhi-

bition of local auxin biosynthesis at nematode infection sites abolishes the formation of adventitious lateral roots (Chapter 2) (Guarneri *et al.*, 2023). This is in line with a previous study, where auxin-insensitive mutants showed fewer adventitious lateral roots at nematode infection sites (Goverse *et al.*, 2000). However, the auxin influx mutants *aux1lax3* and *aux1lax1lax2lax3* showed an increased adventitious lateral rooting in response to nematode infection compared to wild-type plants (Lee *et al.*, 2011). One explanation for this contrasting result could be that the upregulation of auxin influx via AUX/LAX3 at nematode infection sites may alter the distribution and levels of auxin required for root primordium formation and emergence (Zhao *et al.*, 2023).

Jasmonates integrate cyst nematode mechanical damage into an auxin response

Jasmonates regulate plant responses to wounding, herbivory, and some pathogens (Zhang *et al.*, 2017). Jasmonate signaling is mediated by the F-box protein receptor COI1, a close relative of the auxin receptor TIR1 (Wang *et al.*, 2015). Research has shown that jasmonate and auxin signaling likely originated from a common hormone signaling pathway after the duplication of an ancient receptor in the last common ancestor of land plants. Plant colonization of land likely subjected plants to new biotic and abiotic stresses. Therefore, it is possible that jasmonate signaling provided an evolutionary advantage in adapting to this new combination of stresses.

Jasmonate signaling has been observed to induce auxin biosynthesis, mediating plant developmental plasticity in response to stress. Using Arabidopsis leaf explants, researchers have demonstrated that jasmonate signaling via COI1 activates the transcription factor ERF109 (Zhang *et al.*, 2019). In turn, ERF109 induces auxin accumulation by directly binding to the promoter of auxin biosynthesis genes (Cai *et al.*, 2014, Zhang *et al.*, 2019). Jasmonate-responsive ERF109 has been implied in lateral root formation in response to drought stress and in the re-adjustment of ROS homeostasis in leaves exposed to high light stress (Cai *et al.*, 2014). Moreover, ERF109 regulates *de novo* root organogenesis in response to wounding in leaf explants, and root meristem regeneration upon soil penetration and root-knot nematodes host invasion (Zhang *et al.*, 2019, Zhou *et al.*, 2019). In this thesis, we found that jasmonate signaling via ERF109 mediates local auxin biosynthesis and adventitious lateral root formation in response to cyst nematode host invasion (Chapter 2 and 3) (Guarneri *et al.*, 2023, Willig *et al.*, 2023a). This finding further supports the role of ERF109 in integrating plant perception of biotic and abiotic stresses into jasmonate-mediated developmental plasticity.

Jasmonate-mediated root plasticity may require local changes in auxin transport.

Indeed, chemical inhibition of auxin transport in leaf explants abolished *de novo* root organogenesis (Liu *et al.*, 2014). This suggested that following auxin biosynthesis at the wound site, auxin is concentrated in the regeneration-competent cells via auxin carriers. In Chapter 2, we observed that adventitious lateral root formation at nematode infection sites is dependent on local auxin biosynthesis. However, we did not verify whether changes in polar auxin transport at nematode infection sites may also be required. Auxin influx and efflux carriers are known to be differentially regulated at nematode infection sites (Grunewald *et al.*, 2009, Lee *et al.*, 2011). Therefore, we hypothesize that ERF109-mediated auxin biosynthesis at nematode infection sites is followed by a change in polar auxin transport that redirects auxin to the regeneration-competent cells to form a root primordium. This could be tested by applying a chemical inhibitor of auxin transport to the nematode-infected wild-type and *erf109* Arabidopsis roots, followed by scoring the number of adventitious lateral roots at nematode infection sites.

WOX11 translates local and systemic auxin signaling into plant plasticity responses to biotic stress by endoparasitic cyst nematodes

Members of the WOX protein family regulate essential plant developmental processes, such as stem-cell maintenance, embryonic patterning, and organogenesis (van der Graaff *et al.*, 2009). Although WOX genes are present in all green plants, WOX11 and its homologue WOX12 are only found in seed plants (Wan *et al.*, 2023). Seed plants have the highest phenotypic plasticity of all green plants (Motte and Beeckman, 2018). Their root system is made of three main components: 1) a primary root; 2) lateral roots, which are determined by oscillations of auxin at the primary root tip (Perianez-Rodriguez *et al.*, 2021); and 3) adventitious lateral roots, which form *de novo* in the mature root zone in response to environmental stimuli (Wan *et al.*, 2023). The ability to form adventitious lateral roots resides in the presence of xylem-pole pericycle cells that are in a division-competent state (Motte and Beeckman, 2018). Interestingly, WOX11 regulates the cell fate transition of xylem-pole pericycle cells into root primordium founder cells, thereby regulating adventitious lateral root formation (Wan *et al.*, 2023). Additionally, WOX11 mediates light-induced seed germination by suppressing dormancy, allowing seeds to survive in harsh environments and germinate in favorable conditions (Liao *et al.*, 2022). Thus, the evolution of the WOX11/12 subclade may have conferred on angiosperms the ability to adapt to changing environmental conditions by regulating plant developmental plasticity.

WOX11-mediated root plasticity modulates plant tolerance to biotic and abiotic stresses. In poplar, WOX11 promotes root biomass and scavenges cytotoxic levels of ROS, thereby mediating tolerance to drought and salt stress (Liu *et al.*, 2021, Wang *et al.*, 2021). In rice, WOX11 prevents water loss during drought stress by reg-

ulating crown root development and root hair formation (Cheng *et al.*, 2016). Finally, in Chapter 3, we showed that WOX11 modulates tolerance to endoparasitic cyst nematodes (Willig *et al.*, 2023a). Specifically, WOX11 induced adventitious lateral root formation at nematode infection sites in a nematode-density dependent manner. This local response allowed plants to compensate for the primary root growth inhibition caused by nematode damage. WOX11 has been previously implicated in the systemic regulation of ROS homeostasis, which is known to play a role in plant tolerance to cyst nematodes (Liu *et al.*, 2021, Wang *et al.*, 2021, Willig *et al.*, 2022). Thus, it would be informative to test if WOX11-mediated tolerance to cyst nematodes also involves systemic ROS signaling.

Auxin maxima regulate WOX11-mediated root plasticity. The promoter of WOX11 has multiple auxin response elements bound by ARF proteins (Wan *et al.*, 2023). The presence of an auxin maximum in regeneration-competent cells induces WOX11, which determines the reprogramming of cell fate. Here, WOX11 binds to the promoter of LBD16, another auxin-response transcription factor. LBD16 regulates the asymmetric expansion of founder cells, which involves the reorganization of cortical microtubules and structural changes in the plant cell walls. This asymmetric radial expansion is needed for the asymmetric division of founder cells and the formation of a root primordium (Vilches Barro *et al.*, 2019). We observed that infection by endoparasitic cyst nematodes upregulates WOX11 and WOX11-dependent LBD16, likely due to the presence of auxin maxima at nematode infection sites (Chapter 3) (Willig *et al.*, 2023a). Moreover, we found that WOX11 expression is dependent on jasmonate-responsive ERF109, suggesting that local auxin biosynthesis is responsible for WOX11 induction at nematode infection sites (Chapter 3). However, a low WOX11 expression could still be detected at nematode infection sites in the *erf109* Arabidopsis mutant. Besides, it was previously shown that long-distance transport of auxin from the shoot is required for WOX11 expression upon mechanical damage at the primary root (Sheng *et al.*, 2017). Therefore, we propose that both systemic and local auxin signaling are necessary for WOX11 expression in cyst nematode-infected roots.

Besides inducing adventitious lateral roots, WOX11 plays a role in cellular hypertrophy. In rice, WOX11 regulates the transcription of multiple genes involved in cell expansion and directly binds the promoter of *OsEXPB7* expansin gene (Xiong *et al.*, 2023). Interestingly, knock-out mutations of WOX11 resulted in a smaller cellular width, leading to more slender grains compared to wild-type plants. In Chapter 4, we found that in Arabidopsis WOX11 restricts the radial expansion of syncytial elements, likely by mediating cell-wall plasticity mechanisms. This role of WOX11 was not causally linked to WOX11-mediated adventitious lateral root formation. Notably,

syncytia are initiated close to protoxylem poles from a pericycle or procambium cell that expands by hypertrophy and later fuses to neighboring cells (Golinowski *et al.*, 1997). Since WOX11 is typically expressed in the xylem-pole pericycle, it is tempting to speculate that WOX11 may restrict the expansion of the initial syncytial cell (ISC). Interestingly, syncytia induced from a pericycle ISC associate with males, whereas a procambium ISC correlates with the development of females. This raises the question of whether WOX11 expression in the pericycle may be responsible for the lower hypertrophy of male-induced syncytia.

WOX11-mediated developmental plasticity is modulated by the nutritional status of the plant. Plants can perceive energy availability through sensor kinases and thereby initiate developmental programs (Stitz *et al.*, 2023). For instance, the presence of sucrose activates the kinase TOR, which in turn regulates the translation of ARF7, ARF19, and LBD16 to promote lateral root formation. Moreover, chemically induced knock-down of TOR results in both the upregulation of WOX11 and the repression of WOX11-mediated adventitious lateral root formation upon wounding. This latter effect of TOR knock-down is probably the result of a decrease in TOR-mediated LBD16 expression, which is required for adventitious lateral root formation. Thus, sucrose-sensitive TOR kinase tightly regulates WOX11-mediated root plasticity.

In this thesis, we found that WOX11 attenuates female growth and, thereby, female fecundity (Chapter 4). Nematode females feed in cycles of rest and ingestion phases, which likely cause fluctuations in sucrose. Therefore, we hypothesize that WOX11 expression at nematode infection sites is modulated by these fluctuations in sucrose, possibly via TOR. In this scenario, WOX11 could function as a metabolic gatekeeper that limits nematode female growth and promotes adventitious lateral root formation upon perception of low sucrose concentrations at nematode infection sites. This role of WOX11 may have evolved as a plant strategy to regulate energy allocation to processes that promote the overall plant growth in stress conditions.

ROS homeostasis underlies WOX11-mediated plant plasticity responses to cyst nematode infection

Reactive oxygen species ($O_2^{\bullet-}$, H_2O_2, $OH^{\bullet}$, $^1O_2$) are excited or partially reduced derivatives of molecular oxygen that can oxidize cellular components (Mittler, 2017). ROS are thought to have been present on Earth for 2.4–3.8 billions of years, and to have evolved as signaling molecules before unicellular and multicellular organisms diverged (Fichman *et al.*, 2023). If at first ROS may have served to sense critical levels of atmospheric oxygen or to monitor metabolic processes, they later evolved into a complex network regulating almost all aspects of life in most eukaryotic organisms (Mittler, 2017). In plants, ROS are actively produced in the apoplast by mem-

brane-bound enzymes such as NADPH oxidases and peroxidases. Additionally, they are formed in multiple plant organelles as a byproduct of aerobic metabolism. ROS vary in levels of reactivity, migration distances, production sites, and scavenging systems, which makes them highly versatile signaling molecules.

In principle, elevated levels of ROS may be cytotoxic, as they can damage proteins, membranes, and nucleic acids. However, recent studies suggest that ROS levels in plants are mostly physiological, as plants possess mechanisms to maintain ROS within a certain range, above cytostatic and below cytotoxic levels (Mittler, 2017). Moreover, modulation of ROS homeostasis within this range allows plants to regulate processes of growth, development, and defense. Indeed, the production of different ROS in multiple cellular compartments combined to the scavenging activity of plant enzymes and antioxidants creates cell-specific ROS signatures that mediate both local and systemic signals. ROS signaling in response to environmental stimuli has been shown to be critical for plants to adapt to their surrounding environment. For instance, ROS homeostasis confers plants tolerance to high salinity (Bose *et al.*, 2013), drought (Liu *et al.*, 2021), and cyst nematode infection (Willig *et al.*, 2022).

ROS homeostasis is an important mechanism underlying WOX11-mediated developmental plasticity. WOX11 was found to promote ROS scavenging in response to drought and salt stress in poplar, and thereby mitigate the negative impacts of these stresses on plant growth (Liu *et al.*, 2021, Wang *et al.*, 2021). Moreover, WOX11 regulates crown root development in rice by increasing ROS production via peroxidases (Xu *et al.*, 2023). Finally, in this thesis we showed that WOX11 restricts the radial expansion of nematode syncytia, which correlated with an increased ROS production at nematode infection sites (Chapter 4). The exact mechanisms through which WOX11-mediated ROS homeostasis specifically regulates cellular and developmental plasticity remain unclear. In rice, it was observed that WOX11 induces a ROS-mediated protein acetylation (Xu *et al.*, 2023). Furthermore, our data suggests that WOX11-mediated ROS homeostasis regulates plant cell-wall plasticity mechanisms (Chapter 4). Besides having a direct effect on cellular processes, WOX11-induced ROS could also reinforce auxin signal in a feed-forward loop, like it has been observed during lateral root formation in Arabidopsis (Biswas *et al.*, 2019).

Plant modulation of ROS homeostasis has consequences for cyst nematode fitness. Indeed, knock-out mutation of the NADPH oxidase RBOH D/F caused a reduction in the number of females per plant as well as in the size of females and syncytia (Chopra *et al.*, 2021). In this study, RBOH D/F was shown to upregulate the auxin transporter WAT1 and induce auxin accumulation at nematode infection sites. Thus, ROS likely benefits nematode fitness by regulating the formation of auxin maxima. Yet, in Chapter 4, we found that WOX11-induced ROS production attenuates syncy-

tium radial expansion and female fecundity. This suggests that cyst nematodes benefit from ROS levels within a certain range and that an increase or decrease of ROS beyond that range negatively affects cyst nematode fitness. This raises the intriguing question of whether plants may modulate nematode fitness via ROS signaling.

Current view of how plant developmental plasticity contributes to nematode parasitism

In conclusion, this thesis supports a model where root plasticity responses to cyst nematode infection affect plant growth and nematode fitness (Fig.1). We found that cyst nematode host invasion causes mechanical damage, triggering a jasmonate-dependent pathway. Specifically, jasmonate signaling via the receptor COI1 induces the transcription factor ERF109, which upregulates auxin biosynthesis genes (Chapter 2). Local auxin biosynthesis and likely polar auxin transport cause the formation of auxin maxima at nematode infection sites, inducing the auxin-sensitive transcription factor WOX11 and its downstream target LBD16 (Chapter 3). In turn, WOX11 and LBD16 modulate ROS homeostasis and cell-wall extensibility at nematode infection sites (Chapter 4). In xylem-pole pericycle cells, this leads to asymmetric radial expansion and cell division, resulting in the formation of adventitious lateral root primordia. Adventitious lateral roots compensate for the loss of water and minerals due to nematode damage and thus mediate plant tolerance to biotic stress by endoparasitic cyst nematodes (Chapter 3). Additionally, WOX11-mediated ROS homeostasis modulates cell-wall plasticity in nematode syncytial elements, restricting their radial expansion. This possibly limits the space available for the uptake of plant assimilates and thus attenuates female growth and fecundity (Chapter 4).

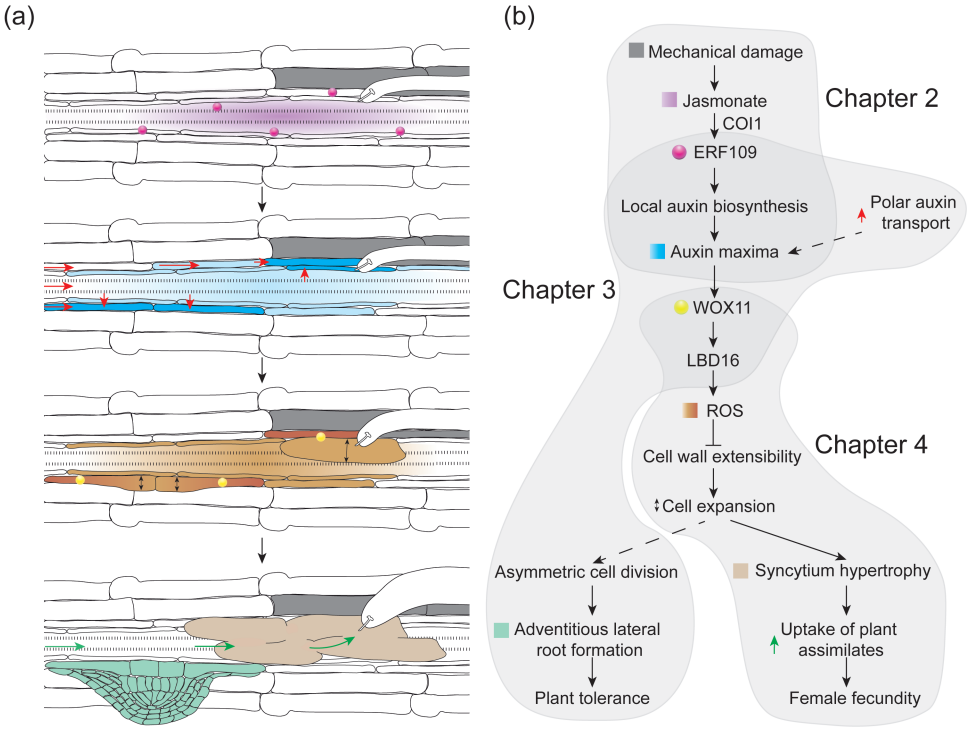

Fig. 1 Thesis overview: how plant developmental plasticity contributes to nematode parasitism and plant tolerance to biotic stress. (a) Graphical model illustrating the molecular and cellular processes investigated in this thesis. (b) Schematic model showing how the pathways studied in this thesis are connected to each other. Color-codes and shapes link the pathway in panel (b) to the processes in panel (a): mechanical damage (grey fill), jasmonate signaling (lilac gradient fill), ERF109 expression (pink spheres), auxin accumulation (light blue gradient fill), polar auxin transport (red arrows), WOX11 expression (yellow spheres), ROS levels (brown gradient fill), cell expansion (double black arrows), syncytium hypertrophy (beige fill), transport of assimilates (green arrows), adventitious lateral root formation (aquamarine fill). The grey areas in (b) highlight the contribution of each experimental chapter to the model.

Future perspectives

The findings within this thesis unveil intricate molecular mechanisms underlying root plasticity responses to cyst nematode infection, profoundly impacting plant growth and nematode parasitism. To advance these discoveries, it is crucial to explore their translation into practical applications addressing current societal challenges.

The WOX11 pathway investigated in this thesis influences a wide range of plant traits, including rice grain morphology, root system architecture, and plant tolerance to biotic and abiotic stresses (Sheng *et al.*, 2017, Liu *et al.*, 2021, Wang *et al.*, 2021,

Willig *et al*., 2023a, Xiong *et al*., 2023, Xu *et al*., 2023). Therefore, this pathway holds potential for improving plant performance in breeding programs. However, deeper insights into the specificity of WOX11 downstream signaling are necessary. For instance, investigating the interaction of WOX11 with other proteins could shed light on the tissue specificity of WOX11-mediated developmental plasticity. This specificity would enable the improvement of specific traits (e.g., root architecture) without unintentionally affecting other commercially valuable traits (e.g., grain morphology). Importantly, WOX11 expression is regulated by both environmental conditions and the nutritional status of the plant. Thus, gaining further insights on the upstream regulation of WOX11 may reveal how plants integrate environmental cues into appropriate developmental responses. This knowledge may pave the way for increasing plant resilience to varying environmental conditions by enhancing their ability to perceive and respond adequately.

In a world where human activities are contributing to a constant increase in greenhouse gas emissions and a subsequent rise in global temperatures, addressing multifactorial stress combinations becomes increasingly urgent. This is especially true as the intensive use of land to meet the food demands of a growing population has resulted in soil impoverishment and pollution (Zandalinas *et al.*, 2021). Additionally, the combined effect of climate change and global food trade is facilitating the spread of plant pathogens and pests to new geographical areas, adding new stress combinations to native and agricultural plant species (Ristaino *et al.*, 2021). To tackle these challenges, it is crucial to explore strategies that enhance plant tolerance to multifactorial stresses.

Crop varieties are typically selected for commercially desirable traits, yield, and uniformity (Schneider and Lynch, 2020). However, plant developmental plasticity is an often-disregarded trait in breeding programs, possibly due to the lack of understanding of its complex genetic architecture (Trudgill, 1991, Schneider and Lynch, 2020). In this thesis, I have provided evidence that plants utilize root architecture plasticity as a coping strategy to mitigate biotic stress by root feeding nematodes. Moreover, I elucidated a molecular pathway that modulates root architecture plasticity by regulating the formation of secondary roots at nematode infection sites. Finally, I showed that this pathway does not only modulate root plasticity but also restricts the expansion of nematode feeding structures, thereby attenuating nematode offspring size. To translate this knowledge into a possible solution to plant diseases, further research should further investigate the role of root plasticity in the interaction between plants and other biotrophic pathogens. Importantly, shifting between a plant-centered perspective and a pathogen-centered perspective, as discussed in Chapter 5, will provide a better understanding of how plants and pathogens mutually influence

one another during biotrophic interactions. Finally, studying the natural variation of root plasticity in response to combinations of biotic and abiotic stresses could reveal valuable insights for breeders aiming to develop climate-proof crop varieties.

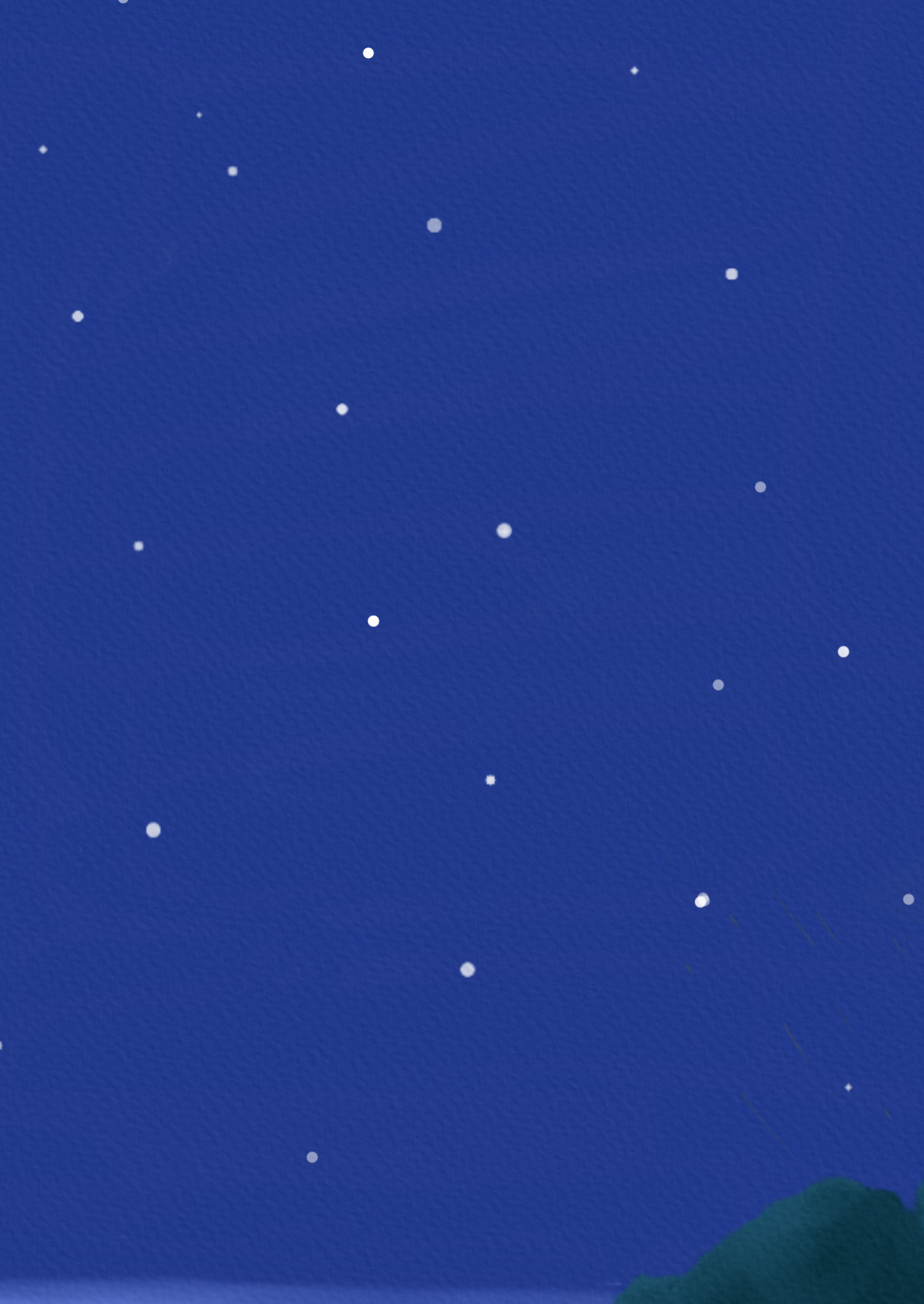

Appendix

References

Abad P, Gouzy J, Aury JM, Castagnone-Sereno P, Danchin EG, Deleury E, Perfus-Barbeoch L, Anthouard V, Artiguenave F, Blok VC, et al. 2008. Genome sequence of the metazoan plant-parasitic nematode Meloidogyne incognita. *Nat Biotechnol* **26**(8): 909-915.

Abad P, Williamson VM 2010. Plant Nematode Interaction: A Sophisticated Dialogue. In: Kader J-C, Delseny M eds. *Advances in Botanical Research*: Academic Press, 147-192.

Absmanner B, Stadler R, Hammes UZ. 2013. Phloem development in nematode-induced feeding sites: the implications of auxin and cytokinin. *Front Plant Sci* **4**: 241.

Ali MA, Abbas A, Kreil DP, Bohlmann H. 2013. Overexpression of the transcription factor RAP2.6 leads to enhanced callose deposition in syncytia and enhanced resistance against the beet cyst nematode Heterodera schachtii in Arabidopsis roots. *BMC Plant Biol* **13**: 47.

Ali MA, Azeem F, Li H, Bohlmann H. 2017. Smart Parasitic Nematodes Use Multifaceted Strategies to Parasitize Plants. *Front Plant Sci* **8**: 1699.

Bartlem DG, Jones MG, Hammes UZ. 2014. Vascularization and nutrient delivery at root-knot nematode feeding sites in host roots. *J Exp Bot* **65**(7): 1789-1798.

Baty F, Ritz C, Charles S, Brutsche M, Flandrois J-P, Delignette-Muller M-L. 2015. A toolbox for non-linear regression in R: the package nlstools. *Journal of Statistical Software* **66**: 1-21.

Baum TJ, Wubben MJ, Hardyy KA, Su H, Rodermel SR. 2000. A screen for *Arabidopsis thaliana* mutants with altered susceptibility to *Heterodera schachtii*. *J Nematol* **32**(2): 166-173.

Bebber D, Ramotowski M, Gurr S. 2013. Crop pests and pathogens move poleward in a warming world. *Nature Climate Change* **3**.

Bebber DP, Holmes T, Gurr SJ. 2014. The global spread of crop pests and pathogens. *Global Ecology and Biogeography* **23**(12): 1398-1407.

Beziat C, Kleine-Vehn J, Feraru E. 2017. Histochemical staining of beta-glucuronidase and its spatial quantification. *Methods Mol Biol* **1497**: 73-80.

Bhosale R, Boudolf V, Cuevas F, Lu R, Eekhout T, Hu Z, Van Isterdael G, Lambert GM, Xu F, Nowack MK, et al. 2018. A Spatiotemporal DNA Endoploidy Map of the Arabidopsis Root Reveals Roles for the Endocycle in Root Development and Stress Adaptation. *Plant Cell* **30**(10): 2330-2351.

Bisht A, Eekhout T, Canher B, Lu R, Vercauteren I, De Jaeger G, Heyman J, De Veylder L. 2023. PAT1-type GRAS-domain proteins control regeneration by activating DOF3.4 to drive cell proliferation in Arabidopsis roots. *The Plant Cell* **35**(5): 1513-1531.

Biswas MS, Fukaki H, Mori IC, Nakahara K, Mano J. 2019. Reactive oxygen species and reactive carbonyl species constitute a feed-forward loop in auxin signaling for lateral root formation. *Plant J* **100**(3): 536-548.

Böckenhoff A, Grundler FMW. 1994. Studies on the nutrient uptake by the beet cyst nematode Heterodera schachtii by in situ microinjection of fluorescent probes into the feeding structures in Arabidopsis thaliana. *Parasitology* **109**(2): 249-255.

Bohlmann H, Sobczak M. 2014. The plant cell wall in the feeding sites of cyst nematodes. *Front Plant Sci* **5**: 89.

Bose J, Rodrigo-Moreno A, Shabala S. 2013. ROS homeostasis in halophytes in the context of salinity stress tolerance. *Journal of Experimental Botany* **65**(5): 1241-1257.

Brooker R, Brown LK, George TS, Pakeman RJ, Palmer S, Ramsay L, Schöb C, Schurch N, Wilkinson MJ. 2022. Active and adaptive plasticity in a changing climate. *Trends in Plant Science* **27**(7): 717-728.

Brownleader MD, Hopkins J, Mobasheri A, Dey PM, Jackson P, Trevan M. 2000. Role of extensin peroxidase in tomato (*Lycopersicon esculentum* Mill.) seedling growth. *Planta* **210**(4): 668-676.

Brumos J, Robles LM, Yun J, Vu TC, Jackson S, Alonso JM, Stepanova AN. 2018. Local Auxin Biosynthesis Is a Key Regulator of Plant Development. *Developmental Cell* **47**(3): 306-318.e305.

Burns AR, Baker RJ, Kitner M, Knox J, Cooke B, Volpatti JR, Vaidya AS, Puumala E, Palmeira BM, Redman EM, et al. 2023. Selective control of parasitic nematodes using bioactivated nematicides. *Nature* **618**(7963): 102-109.

Cabrera J, Diaz-Manzano FE, Sanchez M, Rosso MN, Melillo T, Goh T, Fukaki H, Cabello S, Hofmann J, Fenoll C, et al. 2014. A role for *LATERAL ORGAN BOUNDARIES-DOMAIN 16* during the interaction Arabidopsis-*Meloidogyne* spp. provides a molecular link between lateral root and root-knot nematode feeding site development. *New Phytol* **203**(2): 632-645.

Cai XT, Xu P, Zhao PX, Liu R, Yu LH, Xiang CB. 2014. Arabidopsis ERF109 mediates cross-talk between jasmonic acid and auxin biosynthesis during lateral root formation. *Nat Commun* **5**: 5833.

Carbonnel S, Cornelis S, Hazak O. 2023. The CLE33 peptide represses phloem differentiation via autocrine and paracrine signaling in Arabidopsis. *Communications Biology* **6**(1): 588.

Carrillo-Carrasco VP, Hernandez-Garcia J, Mutte SK, Weijers D. 2023. The birth of a giant: evolutionary insights into the origin of auxin responses in plants. *The EMBO Journal* **42**(6): e113018.

Castagnone-Sereno P. 2006. Genetic variability and adaptive evolution in parthenogenetic root-knot nematodes. *Heredity (Edinb)* **96**(4): 282-289.

Catalá C, Rose JKC, Bennett AB. 2000. Auxin-Regulated Genes Encoding Cell Wall-Modifying Proteins Are Expressed during Early Tomato Fruit Growth. *Plant Physiology* **122**(2): 527-534.

Caumon H, Vernoux T. 2023. A matter of time: auxin signaling dynamics and the regulation of auxin responses during plant development. *Journal of Experimental Botany* **74**(14): 3887-3902.

Chaudhary A, Chen X, Gao J, Lesniewska B, Hammerl R, Dawid C, Schneitz K. 2020. The Arabidopsis receptor kinase STRUBBELIG regulates the response to cellulose deficiency. *PLoS Genet* **16**(1): e1008433.

Chen L, Tong J, Xiao L, Ruan Y, Liu J, Zeng M, Huang H, Wang JW, Xu L. 2016. YUCCA-mediated auxin biogenesis is required for cell fate transition occurring during *de novo* root organogenesis in Arabidopsis. *J Exp Bot* **67**(14): 4273-4284.

Cheng S, Zhou DX, Zhao Y. 2016. WUSCHEL-related homeobox gene WOX11 increases rice drought resistance by controlling root hair formation and root system development. *Plant Signal Behav* **11**(2): e1130198.

Cheng YT, Zhang L, He SY. 2019. Plant-Microbe Interactions Facing Environmental Challenge. *Cell Host Microbe* **26**(2): 183-192.

Chopra D, Hasan MS, Matera C, Chitambo O, Mendy B, Mahlitz SV, Naz AA, Szumski S, Janakowski S, Sobczak M, et al. 2021. Plant parasitic cyst nematodes redirect host indole metabolism via NADPH oxidase-mediated ROS to promote infection. *New Phytol* **232**(1): 318-331.

Coke MC, Mantelin S, Thorpe P, Lilley CJ, Wright KM, Shaw DS, Chande A, Jones JT, Urwin PE. 2021. The GpIA7 effector from the potato cyst nematode *Globodera pallida* targets potato EBP1 and interferes with the plant cell cycle. *Journal of Experimental Botany* **72**(20): 7301-7315.

Cosgrove DJ. 2022. Building an extensible cell wall. *Plant Physiol* **189**(3): 1246-1277.

Davies LJ, Elling AA. 2015. Resistance genes against plant-parasitic nematodes: a durable control strategy? *Nematology* **17**(3): 249-263.

Davis EL, Haegeman A, Kikuchi T 2011. Degradation of the Plant Cell Wall by Nematodes. In: Jones J, Gheysen G, Fenoll C eds. *Genomics and Molecular Genetics of Plant-Nematode Interactions*. Dordrecht: Springer Netherlands, 255-272.

de Almeida Engler J, Kyndt T, Vieira P, Van Cappelle E, Boudolf V, Sanchez V, Escobar C, De Veylder L, Engler G, Abad P, et al. 2012. CCS52 and DEL1 genes are key components of the endocycle in nematode-induced feeding sites. *The Plant Journal* **72**(2): 185-198.

De Almeida Engler J, Van Poucke K, Karimi M, De Groodt R, Gheysen G, Engler G, Gheysen G. 2004. Dynamic cytoskeleton rearrangements in giant cells and syncytia of nematode-infected roots. *The Plant Journal* **38**(1): 12-26.

De Meutter J, Tytgat T, Prinsen E, Gheysen G, Van Onckelen H, Gheysen G. 2005. Production of auxin and related compounds by the plant parasitic nematodes *Heterodera schachtii* and *Meloidogyne incognita*. *Commun Agric Appl Biol Sci* **70**(1): 51-60.

Desaeger J, Wram C, Zasada I. 2020. New reduced-risk agricultural nematicides - rationale and review. *J Nematol* **52**.

Du J, Kirui A, Huang S, Wang L, Barnes WJ, Kiemle SN, Zheng Y, Rui Y, Ruan M, Qi S, et al. 2020. Mutations in the Pectin Methyltransferase QUASIMODO2 Influence Cellulose Biosynthesis and Wall Integrity in Arabidopsis. *The Plant Cell* **32**(11): 3576-3597.

Dubrovsky JG, Sauer M, Napsucialy-Mendivil S, Ivanchenko MG, Friml J, Shishkova S, Celenza J, Benkova E. 2008. Auxin acts as a local morphogenetic trigger to specify lateral root founder cells. *Proc Natl Acad Sci U S A* **105**(25): 8790-8794.

Dutta TK, Phani V. 2023. The pervasive impact of global climate change on plant-nematode interaction continuum. *Front Plant Sci* **14**: 1143889.

Eljebbawi A, Guerrero Y, Dunand C, Estevez JM. 2021. Highlighting reactive oxygen species as multitaskers in root development. *iScience* **24**(1): 101978.

Fichman Y, Rowland L, Oliver MJ, Mittler R. 2023. ROS are evolutionary conserved cell-to-cell stress signals. *Proceedings of the National Academy of Sciences* **120**(31): e2305496120.

Fleming TR, McGowan NE, Maule AG, Fleming CC. 2016. Prevalence and diversity of plant parasitic nematodes in Northern Ireland grassland and cereals, and the influence of soils and rainfall. *Plant Pa-*

thology **65**(9): 1539-1550.

Fukaki H, Tasaka M. 2009. Hormone interactions during lateral root formation. *Plant Mol Biol* **69**(4): 437-449.

Galindo-Gonzalez L, Manolii V, Hwang SF, Strelkov SE. 2020. Response of Brassica napus to Plasmodiophora brassicae Involves Salicylic Acid-Mediated Immunity: An RNA-Seq-Based Study. *Front Plant Sci* **11**: 1025.

Garvetto A, Murúa P, Kirchmair M, Salvenmoser W, Hittorf M, Ciaghi S, Harikrishnan SL, Gachon CMM, Burns JA, Neuhauser S. 2023. Phagocytosis underpins the biotrophic lifestyle of intracellular parasites in the class Phytomyxea (Rhizaria). *New Phytologist* **238**(5): 2130-2143.

Gheysen G, Mitchum MG. 2011. How nematodes manipulate plant development pathways for infection. *Curr Opin Plant Biol* **14**(4): 415-421.

Gigli-Bisceglia N, Engelsdorf T, Hamann T. 2020. Plant cell wall integrity maintenance in model plants and crop species-relevant cell wall components and underlying guiding principles. *Cell Mol Life Sci* **77**(11): 2049-2077.

Glass M, Barkwill S, Unda F, Mansfield SD. 2015. Endo-β-1,4-glucanases impact plant cell wall development by influencing cellulose crystallization. *Journal of Integrative Plant Biology* **57**(4): 396-410.

Golinowski W, Grundler FMW, Sobczak M. 1996. Changes in the structure ofArabidopsis thaliana during female development of the plant-parasitic nematode *Heterodera schachtii*. *Protoplasma* **194**(1): 103-116.

Golinowski W, Sobczak M, Kurek W, Grymaszewska G. 1997. The structure of syncytia. *Cellular and molecular aspects of plant-nematode interactions*: 80-97.

Goverse A, Overmars H, Engelbertink J, Schots A, Bakker J, Helder J. 2000. Both induction and morphogenesis of cyst nematode feeding cells are mediated by auxin. *Mol Plant Microbe Interact* **13**(10): 1121-1129.

Graeff M, Hardtke CS. 2021. Metaphloem development in the Arabidopsis root tip. *Development* **148**(18).

Grenier E, Kiewnick S, Smant G, Fournet S, Montarry J, Holterman M, Helder J, Goverse A. 2020. Monitoring and tackling genetic selection in the potato cyst nematode *Globodera pallida*. *EFSA Supporting Publications* **17**(6): 1874E.

Grundler FMW, Böckenhoff A, Schmidt K-P, Sobczak M, Golinowski W, Wyss U 1994. *Arabidopsis thaliana* and *Heterodera schachtii*: a versatile model to characterize the interaction between host plants and cyst nematodes. In: Lamberti F, De Giorgi C, Bird DM eds. *Advances in Molecular Plant Nematology*. Boston, MA: Springer US, 171-180.

Grundler FMW, Hofmann J 2011. Water and Nutrient Transport in Nematode Feeding Sites. In: Jones J, Gheysen G, Fenoll C eds. *Genomics and Molecular Genetics of Plant-Nematode Interactions*. Dordrecht: Springer Netherlands, 423-439.

Grunewald W, Cannoot B, Friml J, Gheysen G. 2009. Parasitic nematodes modulate PIN-mediated auxin transport to facilitate infection. *PLoS Pathog* **5**(1): e1000266.

Grymaszewska G, Golinowski W. 1991. Structure of syncytia Induced by *Heterodera avenae* Woll. in roots of susceptible and resistant wheat (*Triticum aestivum L.*). *Journal of Phytopathology* **133**(4): 307-

319.

Guarneri N, Willig JJ, Sterken MG, Zhou W, Hasan MS, Sharon L, Grundler FMW, Willemsen V, Goverse A, Smant G, et al. 2023. Root architecture plasticity in response to endoparasitic cyst nematodes is mediated by damage signaling. *New Phytol* **237**(3): 807-822.

Guo X, Wang J, Gardner M, Fukuda H, Kondo Y, Etchells JP, Wang X, Mitchum MG. 2017. Identification of cyst nematode B-type CLE peptides and modulation of the vascular stem cell pathway for feeding cell formation. *PLoS Pathog* **13**(2): e1006142.

Hanson MR, Kohler RH. 2001. GFP imaging: methodology and application to investigate cellular compartmentation in plants. *J Exp Bot* **52**(356): 529-539.

Harris MO, Pitzschke A. 2020. Plants make galls to accommodate foreigners: some are friends, most are foes. *New Phytol* **225**(5): 1852-1872.

Hasan MS, Chopra D, Damm A, Koprivova A, Kopriva S, Meyer AJ, Muller-Schussele S, Grundler FMW, Siddique S. 2022. Glutathione contributes to plant defence against parasitic cyst nematodes. *Mol Plant Pathol* **23**(7): 1048-1059.

He W, Brumos J, Li H, Ji Y, Ke M, Gong X, Zeng Q, Li W, Zhang X, An F, et al. 2011. A small-molecule screen identifies L-kynurenine as a competitive inhibitor of TAA1/TAR activity in ethylene-directed auxin biosynthesis and root growth in Arabidopsis. *Plant Cell* **23**(11): 3944-3960.

Hewezi T, Piya S, Richard G, Rice JH. 2014. Spatial and temporal expression patterns of auxin response transcription factors in the syncytium induced by the beet cyst nematode *Heterodera schachtii* in Arabidopsis. *Mol Plant Pathol* **15**(7): 730-736.

Heyman J, Cools T, Canher B, Shavialenka S, Traas J, Vercauteren I, Van den Daele H, Persiau G, De Jaeger G, Sugimoto K, et al. 2016. The heterodimeric transcription factor complex ERF115–PAT1 grants regeneration competence. *Nature Plants* **2**(11): 16165.

Hiratsu K, Matsui K, Koyama T, Ohme-Takagi M. 2003. Dominant repression of target genes by chimeric repressors that include the EAR motif, a repression domain, in Arabidopsis. *The Plant Journal* **34**(5): 733-739.

Hittorf, M., Garvetto, A., Magauer, M., Kirchmair, M., Salvenmoser, W., Murúa, P. and Neuhauser, S. (2023) Local endoreduplication of the host is a conserved process during Phytomyxea-host interaction. *bioRxiv*, 2023.2009.2021.558765.

Hofmann J, Grundler FM. 2006. Females and males of root-parasitic cyst nematodes induce different symplasmic connections between their syncytial feeding cells and the phloem in *Arabidopsis thaliana*. *Plant Physiol Biochem* **44**(5-6): 430-433.

Hofmann J, Wieczorek K, Blochl A, Grundler FM. 2007. Sucrose supply to nematode-induced syncytia depends on the apoplasmic and symplasmic pathways. *J Exp Bot* **58**(7): 1591-1601.

Holterman M, Karssen G, van den Elsen S, van Megen H, Bakker J, Helder J. 2009. Small subunit rDNA-based phylogeny of the *Tylenchida* sheds light on relationships among some high-impact plant-parasitic nematodes and the evolution of plant feeding. *Phytopathology* **99**(3): 227-235.

Hoth S, Schneidereit A, Lauterbach C, Scholz-Starke J, Sauer N. 2005. Nematode infection triggers the de novo formation of unloading phloem that allows macromolecular trafficking of green fluorescent

protein into syncytia. *Plant Physiol* **138**(1): 383-392.

Hu X, Xu L. 2016. Transcription factors WOX11/12 directly activate WOX5/7 to promote root primordia initiation and organogenesis. *Plant Physiol* **172**(4): 2363-2373.

Huang A, Wang Y, Liu Y, Wang G, She X. 2020. Reactive oxygen species regulate auxin levels to mediate adventitious root induction in Arabidopsis hypocotyl cuttings. *Journal of Integrative Plant Biology* **62**(7): 912-926.

Ichihashi Y, Hakoyama T, Iwase A, Shirasu K, Sugimoto K, Hayashi M. 2020. Common Mechanisms of Developmental Reprogramming in Plants-Lessons From Regeneration, Symbiosis, and Parasitism. *Front Plant Sci* **11**: 1084.

Javed MA, Schwelm A, Zamani-Noor N, Salih R, Silvestre Vañó M, Wu J, González García M, Heick TM, Luo C, Prakash P, et al. 2023. The clubroot pathogen Plasmodiophora brassicae: A profile update. *Molecular Plant Pathology* **24**(2): 89-106.

Jones JT, Haegeman A, Danchin EG, Gaur HS, Helder J, Jones MG, Kikuchi T, Manzanilla-Lopez R, Palomares-Rius JE, Wesemael WM, et al. 2013. Top 10 plant-parasitic nematodes in molecular plant pathology. *Mol Plant Pathol* **14**(9): 946-961.

Kammerhofer N, Radakovic Z, Regis JM, Dobrev P, Vankova R, Grundler FM, Siddique S, Hofmann J, Wieczorek K. 2015. Role of stress-related hormones in plant defence during early infection of the cyst nematode *Heterodera schachtii* in Arabidopsis. *New Phytol* **207**(3): 778-789.

Karczmarek A, Fudali S, Lichocka M, Sobczak M, Kurek W, Janakowski S, Roosien J, Golinowski W, Bakker J, Goverse A, et al. 2008. Expression of two functionally distinct plant endo-beta-1,4-glucanases is essential for the compatible interaction between potato cyst nematode and its hosts. *Mol Plant Microbe Interact* **21**(6): 791-798.

Karczmarek A, Overmars H, Helder J, Goverse A. 2004. Feeding cell development by cyst and root-knot nematodes involves a similar early, local and transient activation of a specific auxin-inducible promoter element. *Mol Plant Pathol* **5**(4): 343-346.

Kim J, Yang R, Chang C, Park Y, Tucker ML. 2018. The root-knot nematode *Meloidogyne incognita* produces a functional mimic of the Arabidopsis INFLORESCENCE DEFICIENT IN ABSCISSION signaling peptide. *J Exp Bot* **69**(12): 3009-3021.

Koevoets IT, Venema JH, Elzenga JT, Testerink C. 2016. Roots withstanding their environment: exploiting root system architecture responses to abiotic atress to improve crop tolerance. *Front Plant Sci* **7**: 1335.

Kong X, Tian H, Yu Q, Zhang F, Wang R, Gao S, Xu W, Liu J, Shani E, Fu C, et al. 2018. PHB3 maintains root stem cell niche identity through ROS-responsive AP2/ERF transcription factors in Arabidopsis. *Cell Rep* **22**(5): 1350-1363.

Kyndt T, Vieira P, Gheysen G, de Almeida-Engler J. 2013. Nematode feeding sites: unique organs in plant roots. *Planta* **238**(5): 807-818.

Lang L, Schnittger A. 2020. Endoreplication — a means to an end in cell growth and stress response. *Current Opinion in Plant Biology* **54**: 85-92.

Larrieu A, Champion A, Legrand J, Lavenus J, Mast D, Brunoud G, Oh J, Guyomarc'h S, Pizot M,

Farmer EE, et al. 2015. A fluorescent hormone biosensor reveals the dynamics of jasmonate signalling in plants. *Nat Commun* **6**: 6043.

Lee C, Chronis D, Kenning C, Peret B, Hewezi T, Davis EL, Baum TJ, Hussey R, Bennett M, Mitchum MG. 2011. The novel cyst nematode effector protein 19C07 interacts with the Arabidopsis auxin influx transporter LAX3 to control feeding site development. *Plant Physiol* **155**(2): 866-880.

Levin KA, Tucker MR, Bird DM, Mather DE. 2020. Infection by cyst nematodes induces rapid remodelling of developing xylem vessels in wheat roots. *Sci Rep* **10**(1): 9025.

Levin KA, Tucker MR, Strock CF, Lynch JP, Mather DE. 2021. Three-dimensional imaging reveals that positions of cyst nematode feeding sites relative to xylem vessels differ between susceptible and resistant wheat. *Plant Cell Rep* **40**(2): 393-403.

Li S, Lei L, Yingling YG, Gu Y. 2015. Microtubules and cellulose biosynthesis: the emergence of new players. *Current Opinion in Plant Biology* **28**: 76-82.

Li Y, Chen S, Young ND. 2004. Effect of the rhg1 gene on penetration, development and reproduction of *Heterodera glycines* race 3. *Nematology* **6**(5): 729-736.

Liao J, Deng B, Cai X, Yang Q, Hu B, Cong J, Zhang Y, Wang G, Xin G, Li Y, et al. 2022. Time-course transcriptome analysis reveals regulation of Arabidopsis seed dormancy by the transcription factors WOX11/12. *Journal of Experimental Botany* **74**(3): 1090-1106.

Lilley CJ, Atkinson HJ, Urwin PE. 2005. Molecular aspects of cyst nematodes. *Mol Plant Pathol* **6**(6): 577-588.

Liu J, Sheng L, Xu Y, Li J, Yang Z, Huang H, Xu L. 2014. WOX11 and 12 are involved in the first-step cell fate transition during de novo root organogenesis in Arabidopsis. *Plant Cell* **26**(3): 1081-1093.

Liu R, Wang R, Lu MZ, Wang LQ. 2021. WUSCHEL-related homeobox gene PagWOX11/12a is involved in drought tolerance through modulating reactive oxygen species scavenging in poplar. *Plant Signal Behav* **16**(3): 1866312.

Liu R, Wen S-S, Sun T-T, Wang R, Zuo W-T, Yang T, Wang C, Hu J-J, Lu M-Z, Wang L-Q. 2022. PagWOX11/12a positively regulates the PagSAUR36 gene that enhances adventitious root development in poplar. *Journal of Experimental Botany* **73**(22): 7298-7311.

Livanos P, Galatis B, Quader H, Apostolakos P. 2012. Disturbance of reactive oxygen species homeostasis induces atypical tubulin polymer formation and affects mitosis in root-tip cells of *Triticum turgidum* and *Arabidopsis thaliana*. *Cytoskeleton* **69**(1): 1-21.

Ma Y, Jonsson K, Aryal B, De Veylder L, Hamant O, Bhalerao RP. 2022. Endoreplication mediates cell size control via mechanochemical signaling from cell wall. *Science Advances* **8**(49): eabq2047.

Magliano TMA, Casal JJ. 1998. In vitro cross-linking of extensin precursors by mustard extracellular isoforms of peroxidase that respond either to phytochrome or to wounding. *Journal of Experimental Botany* **49**(326): 1491-1499.

Magnusson C, Golinowski W. 1991. Ultrastructural relationships of the developing syncytium induced by *Heterodera schachtii* (Nematoda) in root tissues of rape. *Canadian Journal of Botany* **69**(1): 44-52.

Malinowski R, Smith JA, Fleming AJ, Scholes JD, Rolfe SA. 2012. Gall formation in clubroot-infected Arabidopsis results from an increase in existing meristematic activities of the host but is not essential for

the completion of the pathogen life cycle. *Plant J* **71**(2): 226-238.

Marhavy P, Kurenda A, Siddique S, Denervaud Tendon V, Zhou F, Holbein J, Hasan MS, Grundler FM, Farmer EE, Geldner N. 2019. Single-cell damage elicits regional, nematode-restricting ethylene responses in roots. *EMBO J* **38**(10).

Matosevich R, Cohen I, Gil-Yarom N, Modrego A, Friedlander-Shani L, Verna C, Scarpella E, Efroni I. 2020. Local auxin biosynthesis is required for root regeneration after wounding. *Nat Plants* **6**(8): 1020-1030.

Mazumdar, S., Zhang, A., Musseau, C., Anjam, M.S., Marhavy, P. and Melnyk, C.W. (2023) Damage activates *EVG1* to suppress vascular differentiation during regeneration in *Arabidopsis thaliana*. *bioRxiv*, 2023.2002.2027.530175.

Melnyk CW. 2017. Connecting the plant vasculature to friend or foe. *New Phytol* **213**(4): 1611-1617.

Melnyk CW, Schuster C, Leyser O, Meyerowitz EM. 2015. A Developmental Framework for Graft Formation and Vascular Reconnection in *Arabidopsis thaliana*. *Curr Biol* **25**(10): 1306-1318.

Mendy B, Wang'ombe MW, Radakovic ZS, Holbein J, Ilyas M, Chopra D, Holton N, Zipfel C, Grundler FM, Siddique S. 2017. Arabidopsis leucine-rich repeat receptor-like kinase NILR1 is required for induction of innate immunity to parasitic nematodes. *PLoS Pathog* **13**(4): e1006284.

Miltner E, Karnok KJ, Hussey RS. 1991. Root response of tolerant and intolerant soybean cultivars to soybean cyst nematode. *Agronomy Journal* **83**: 571-576.

Mittler R. 2017. ROS Are Good. *Trends in Plant Science* **22**(1): 11-19.

Motte H, Beeckman T. 2018. The evolution of root branching: increasing the level of plasticity. *Journal of Experimental Botany* **70**(3): 785-793.

Muller J-P, Rehbock K, Wyss U. 1981. Growth of *Heterodera schachtii* with remarks on amounts of food consumed. *Rev. Nématol* **4**.

Nicol JM, Turner SJ, Coyne DL, Nijs Ld, Hockland S, Maafi ZT 2011. Current Nematode Threats to World Agriculture. In: Jones J, Gheysen G, Fenoll C eds. *Genomics and Molecular Genetics of Plant-Nematode Interactions*. Dordrecht: Springer Netherlands, 21-43.

Okushima Y, Fukaki H, Onoda M, Theologis A, Tasaka M. 2007. ARF7 and ARF19 regulate lateral root formation via direct activation of LBD/ASL genes in Arabidopsis. *The Plant Cell* **19**(1): 118-130.

Olmo R, Cabrera J, Diaz-Manzano FE, Ruiz-Ferrer V, Barcala M, Ishida T, Garcia A, Andres MF, Ruiz-Lara S, Verdugo I, et al. 2020. Root-knot nematodes induce gall formation by recruiting developmental pathways of post-embryonic organogenesis and regeneration to promote transient pluripotency. *New Phytol* **227**(1): 200-215.

Olmo R, Cabrera J, Moreno-Risueno MA, Fukaki H, Fenoll C, Escobar C. 2017. Molecular transducers from roots are triggered in Arabidopsis leaves by root-knot nematodes for successful feeding site formation: a conserved post-embryogenic *de novo* organogenesis program? *Front Plant Sci* **8**: 875.

Olszak M, Truman W, Stefanowicz K, Sliwinska E, Ito M, Walerowski P, Rolfe S, Malinowski R. 2019. Transcriptional profiling identifies critical steps of cell cycle reprogramming necessary for *Plasmodiophora brassicae*-driven gall formation in Arabidopsis. *Plant J* **97**(4): 715-729.

Oosterbeek M, Lozano-Torres JL, Bakker J, Goverse A. 2021. Sedentary Plant-Parasitic Nematodes

Alter Auxin Homeostasis via Multiple Strategies. *Front Plant Sci* **12**: 668548.

Paige KN. 2018. Overcompensation, environmental stress, and the role of endoreduplication. *American Journal of Botany* **105**(7): 1105-1108.

Peer WA, Blakeslee JJ, Yang H, Murphy AS. 2011. Seven Things We Think We Know about Auxin Transport. *Molecular Plant* **4**(3): 487-504.

Perianez-Rodriguez J, Rodriguez M, Marconi M, Bustillo-Avendaño E, Wachsman G, Sanchez-Corrionero A, De Gernier H, Cabrera J, Perez-Garcia P, Gude I, et al. 2021. An auxin-regulable oscillatory circuit drives the root clock in Arabidopsis. *Sci Adv* **7**(1).

Petrasek J, Friml J. 2009. Auxin transport routes in plant development. *Development* **136**(16): 2675-2688.

Pfaffl MW. 2001. A new mathematical model for relative quantification in real-time RT-PCR. *Nucleic Acids Res* **29**(9): e45.

Poncini L, Wyrsch I, Denervaud Tendon V, Vorley T, Boller T, Geldner N, Metraux JP, Lehmann S. 2017. In roots of *Arabidopsis thaliana*, the damage-associated molecular pattern AtPep1 is a stronger elicitor of immune signalling than flg22 or the chitin heptamer. *PLoS One* **12**(10): e0185808.

Raza MM, Bebber DP. 2022. Climate change and plant pathogens. *Curr Opin Microbiol* **70**: 102233.

Ren S-C, Song X-F, Chen W-Q, Lu R, Lucas WJ, Liu C-M. 2019. CLE25 peptide regulates phloem initiation in Arabidopsis through a CLERK-CLV2 receptor complex. *Journal of Integrative Plant Biology* **61**(10): 1043-1061.

Replogle A, Wang J, Bleckmann A, Hussey RS, Baum TJ, Sawa S, Davis EL, Wang X, Simon R, Mitchum MG. 2011. Nematode CLE signaling in Arabidopsis requires CLAVATA2 and CORYNE. *Plant J* **65**(3): 430-440.

Ristaino JB, Anderson PK, Bebber DP, Brauman KA, Cunniffe NJ, Fedoroff NV, Finegold C, Garrett KA, Gilligan CA, Jones CM, et al. 2021. The persistent threat of emerging plant disease pandemics to global food security. *Proceedings of the National Academy of Sciences* **118**(23): e2022239118.

Rodiuc N, Vieira P, Banora MY, de Almeida Engler J. 2014. On the track of transfer cell formation by specialized plant-parasitic nematodes. *Front Plant Sci* **5**: 160.

Ruan Y-L, Xu S-M, White R, Furbank RT. 2004. Genotypic and Developmental Evidence for the Role of Plasmodesmatal Regulation in Cotton Fiber Elongation Mediated by Callose Turnover. *Plant Physiology* **136**(4): 4104-4113.

Schindelin J, Arganda-Carreras I, Frise E, Kaynig V, Longair M, Pietzsch T, Preibisch S, Rueden C, Saalfeld S, Schmid B, et al. 2012. Fiji: an open-source platform for biological-image analysis. *Nat Methods* **9**(7): 676-682.

Schmidt R, Kunkowska AB, Schippers JH. 2016. Role of Reactive Oxygen Species during Cell Expansion in Leaves. *Plant Physiol* **172**(4): 2098-2106.

Schneider HM, Lynch JP. 2020. Should Root Plasticity Be a Crop Breeding Target? *Front Plant Sci* **11**: 546.

Shah SJ, Anjam MS, Mendy B, Anwer MA, Habash SS, Lozano-Torres JL, Grundler FMW, Siddique S. 2017. Damage-associated responses of the host contribute to defence against cyst nematodes but not

root-knot nematodes. *J Exp Bot* **68**(21-22): 5949-5960.

Sheng L, Hu X, Du Y, Zhang G, Huang H, Scheres B, Xu L. 2017. Non-canonical WOX11-mediated root branching contributes to plasticity in Arabidopsis root system architecture. *Development* **144**(17): 3126-3133.

Shimadzu S, Furuya T, Kondo Y. 2022. Molecular Mechanisms Underlying the Establishment and Maintenance of Vascular Stem Cells in *Arabidopsis thaliana*. *Plant and Cell Physiology* **64**(3): 274-283.

Shin SY, Park S-J, Kim H-S, Jeon J-H, Lee H-J. 2022. Wound-induced signals regulate root organogenesis in Arabidopsis explants. *BMC Plant Biology* **22**(1): 133.

Siddique S, Coomer A, Baum T, Williamson VM. 2022a. Recognition and Response in Plant-Nematode Interactions. *Annu Rev Phytopathol* **60**: 143-162.

Siddique S, Matera C, Radakovic ZS, Hasan MS, Gutbrod P, Rozanska E, Sobczak M, Torres MA, Grundler FM. 2014. Parasitic worms stimulate host NADPH oxidases to produce reactive oxygen species that limit plant cell death and promote infection. *Sci Signal* **7**(320): ra33.

Siddique S, Radakovic ZS, De La Torre CM, Chronis D, Novak O, Ramireddy E, Holbein J, Matera C, Hutten M, Gutbrod P, et al. 2015. A parasitic nematode releases cytokinin that controls cell division and orchestrates feeding site formation in host plants. *Proc Natl Acad Sci U S A* **112**(41): 12669-12674.

Siddique S, Radakovic ZS, Hiltl C, Pellegrin C, Baum TJ, Beasley H, Bent AF, Chitambo O, Chopra D, Danchin EGJ, et al. 2022b. The genome and lifestage-specific transcriptomes of a plant-parasitic nematode and its host reveal susceptibility genes involved in trans-kingdom synthesis of vitamin B5. *Nat Commun* **13**(1): 6190.

Siddique S, Sobczak M, Tenhaken R, Grundler FM, Bohlmann H. 2012. Cell wall ingrowths in nematode induced syncytia require UGD2 and UGD3. *PLoS One* **7**(7): e41515.

Sijmons PC, Grundler FMW, von Mende N, Burrows PR, Wyss U. 1991. *Arabidopsis thaliana* as a new model host for plant-parasitic nematodes. *The Plant Journal* **1**(2): 245-254.

Sikder MM, Vestergard M. 2019. Impacts of Root Metabolites on Soil Nematodes. *Front Plant Sci* **10**: 1792.

Smant G, Helder J, Goverse A. 2018. Parallel adaptations and common host cell responses enabling feeding of obligate and facultative plant parasitic nematodes. *Plant J* **93**(4): 686-702.

Sobczak M, Golinowski W, Grundler FMW. 1997. Changes in the structure of *Arabidopsis thaliana* roots induced during development of males of the plant parasitic nematode Heterodera schachtii. *European Journal of Plant Pathology* **103**(2): 113-124.

Stadler R, Wright KM, Lauterbach C, Amon G, Gahrtz M, Feuerstein A, Oparka KJ, Sauer N. 2005. Expression of GFP-fusions in Arabidopsis companion cells reveals non-specific protein trafficking into sieve elements and identifies a novel post-phloem domain in roots. *The Plant Journal* **41**(2): 319-331.

Stitz M, Kuster D, Reinert M, Schepetilnikov M, Berthet B, Reyes-Hernández J, Janocha D, Artins A, Boix M, Henriques R, et al. 2023. TOR acts as a metabolic gatekeeper for auxin-dependent lateral root initiation in *Arabidopsis thaliana*. *The EMBO Journal* **42**(10): e111273.

Tahir MM, Tong L, Fan L, Liu Z, Li S, Zhang X, Li K, Shao Y, Zhang D, Mao J. 2022. Insights into the complicated networks contribute to adventitious rooting in transgenic MdWOX11 apple microshoots under

nitrate treatments. *Plant, Cell & Environment* **45**(10): 3134-3156.

Tateno M, Brabham C, DeBolt S. 2016. Cellulose biosynthesis inhibitors - a multifunctional toolbox. *J Exp Bot* **67**(2): 533-542.

Teklu M, Beniers A, Been TH, Schomaker CH, Molendijk L. 2018. *Methods for the estimation of partial resistance in the glasshouse of potato cultivars/genotypes against Potato Cyst Nematodes & Root-knot Nematodes*.

Trudgill DL. 1991. Resistance to and Tolerance of Plant Parasitic Nematodes in Plants. *Annual Review of Phytopathology* **29**(1): 167-192.

Trudgill DL, Cotes LM. 1983. Tolerance of potato to potato cyst nematodes (*Globodera rostochiensis* and *G. pallida*) in relation to the growth and efficiency of the root system. *Annals of Applied Biology* **102**(2): 385-397.

Trudgill DL, Evans K, Parrott DM. 1975. Effects of Potato Cyst-Nematodes On Potato Plants. *Nematologica* **21**(2): 183-191.

Tytgat T, De Meutter J, Vanholme B, Claeys M, Verreijdt L, Gheysen G, Coomans A. 2002. Development and pharyngeal gland activities of *Heterodera schachtii* infecting *Arabidopsis thaliana* roots. *Nematology* **4**(8): 899-908.

Urwin PE, Lilley CJ, McPherson MJ, Atkinson HJ. 1997. Resistance to both cyst and root-knot nematodes conferred by transgenic Arabidopsis expressing a modified plant cystatin. *Plant J* **12**(2): 455-461.

Van de Peer Y, Ashman T-L, Soltis PS, Soltis DE. 2020. Polyploidy: an evolutionary and ecological force in stressful times. *The Plant Cell* **33**(1): 11-26.

van den Berg T, Korver RA, Testerink C, Ten Tusscher KH. 2016. Modeling halotropism: a key role for root tip architecture and reflux loop remodeling in redistributing auxin. *Development* **143**(18): 3350-3362.

van den Hoogen J, Geisen S, Routh D, Ferris H, Traunspurger W, Wardle DA, de Goede RGM, Adams BJ, Ahmad W, Andriuzzi WS, et al. 2019. Soil nematode abundance and functional group composition at a global scale. *Nature* **572**(7768): 194-198.

van der Graaff E, Laux T, Rensing SA. 2009. The WUS homeobox-containing (WOX) protein family. *Genome Biology* **10**(12): 248.

Vanholme B, W VANT, Vanhouteghem K, J DEM, Cannoot B, Gheysen G. 2007. Molecular characterization and functional importance of pectate lyase secreted by the cyst nematode *Heterodera schachtii*. *Mol Plant Pathol* **8**(3): 267-278.

Verbelen JP, De Cnodder T, Le J, Vissenberg K, Baluska F. 2006. The Root Apex of Arabidopsis thaliana Consists of Four Distinct Zones of Growth Activities: Meristematic Zone, Transition Zone, Fast Elongation Zone and Growth Terminating Zone. *Plant Signal Behav* **1**(6): 296-304.

Verbon EH, Liberman LM. 2016. Beneficial Microbes Affect Endogenous Mechanisms Controlling Root Development. *Trends Plant Sci* **21**(3): 218-229.

Vilches Barro A, Stöckle D, Thellmann M, Ruiz-Duarte P, Bald L, Louveaux M, von Born P, Denninger P, Goh T, Fukaki H, et al. 2019. Cytoskeleton Dynamics Are Necessary for Early Events of Lateral Root Initiation in Arabidopsis. *Current Biology* **29**(15): 2443-2454.e2445.

Villordon A, Clark C. 2018. Variation in Root Architecture Attributes at the Onset of Storage Root For-

mation among Resistant and Susceptible Sweetpotato Cultivars Infected with Meloidogyne incognita. *HortScience* **53**(12): 1924-1929.

Walerowski P, Gundel A, Yahaya N, Truman W, Sobczak M, Olszak M, Rolfe S, Borisjuk L, Malinowski R. 2018. Clubroot Disease Stimulates Early Steps of Phloem Differentiation and Recruits SWEET Sucrose Transporters within Developing Galls. *Plant Cell* **30**(12): 3058-3073.

Wan Q, Zhai N, Xie D, Liu W, Xu L. 2023. WOX11: the founder of plant organ regeneration. *Cell Regen* **12**(1): 1.

Wang C, Liu Y, Li S-S, Han G-Z. 2015. Insights into the Origin and Evolution of the Plant Hormone Signaling Machinery. *Plant Physiology* **167**(3): 872-886.

Wang J, Dhroso A, Liu X, Baum TJ, Hussey RS, Davis EL, Wang X, Korkin D, Mitchum MG. 2021. Phytonematode peptide effectors exploit a host post-translational trafficking mechanism to the ER using a novel translocation signal. *New Phytologist* **229**(1): 563-574.

Wang L-Q, Li Z, Wen S-S, Wang J-N, Zhao S-T, Lu M-Z. 2020. WUSCHEL-related homeobox gene PagWOX11/12a responds to drought stress by enhancing root elongation and biomass growth in poplar. *Journal of Experimental Botany* **71**(4): 1503-1513.

Wang LQ, Wen SS, Wang R, Wang C, Gao B, Lu MZ. 2021. PagWOX11/12a activates PagCYP736A12 gene that facilitates salt tolerance in poplar. *Plant Biotechnol J* **19**(11): 2249-2260.

Warmerdam S, Sterken MG, van Schaik C, Oortwijn MEP, Sukarta OCA, Lozano-Torres JL, Dicke M, Helder J, Kammenga JE, Goverse A, et al. 2018. Genome-wide association mapping of the architecture of susceptibility to the root-knot nematode *Meloidogyne incognita* in *Arabidopsis thaliana*. *New Phytol* **218**(2): 724-737.

Wieczorek K, Golecki B, Gerdes L, Heinen P, Szakasits D, Durachko DM, Cosgrove DJ, Kreil DP, Puzio PS, Bohlmann H, et al. 2006. Expansins are involved in the formation of nematode-induced syncytia in roots of *Arabidopsis thaliana*. *Plant J* **48**(1): 98-112.

Wildermuth MC. 2010. Modulation of host nuclear ploidy: a common plant biotroph mechanism. *Current Opinion in Plant Biology* **13**(4): 449-458.

Williamson VM, Kumar A. 2006. Nematode resistance in plants: the battle underground. *Trends in Genetics* **22**(7): 396-403.

Willig JJ, Guarneri N, Loon Tv, Wahyuni S, Astudillo-Estévez IE, Xu L, Willemsen V, Goverse A, Sterken MG, Lozano-Torres JL, et al. 2023a. WOX11-mediated adventitious lateral root formation modulates tolerance of Arabidopsis to cyst nematode infections. *bioRxiv*: 2023.2008.2011.553027.

Willig JJ, Guarneri N, van Steenbrugge JJM, de Jong W, Chen J, Goverse A, Lozano Torres JL, Sterken MG, Bakker J, Smant G. 2022. The Arabidopsis transcription factor TCP9 modulates root architectural plasticity, reactive oxygen species-mediated processes, and tolerance to cyst nematode infections. *Plant J* **112**(4): 1070-1083.

Willig JJ, Sonneveld D, van Steenbrugge JJM, Deurhof L, van Schaik CC, Teklu MG, Goverse A, Lozano-Torres JL, Smant G, Sterken MG. 2023b. From root to shoot; Quantifying nematode tolerance in Arabidopsis thaliana by high-throughput phenotyping of plant development. *J Exp Bot*.

www.climate.nasa.gov

www.epa.gov/climate-indicators

Wyss U, Zunke U. 1986. Observations on the behavior of second-stage juveniles of *Heterodera schachtii* inside host root. *Revue de Nematologie* **9**.

Xiao C, Zhang T, Zheng Y, Cosgrove DJ, Anderson CT. 2015. Xyloglucan Deficiency Disrupts Microtubule Stability and Cellulose Biosynthesis in Arabidopsis, Altering Cell Growth and Morphogenesis *Plant Physiology* **170**(1): 234-249.

Xiong D, Wang R, Wang Y, Li Y, Sun G, Yao S. 2023. SLG2 specifically regulates grain width through WOX11-mediated cell expansion control in rice. *Plant Biotechnology Journal* **21**(9): 1904-1918.

Xu L, Liu F, Lechner E, Genschik P, Crosby WL, Ma H, Peng W, Huang D, Xie D. 2002. The SCF(-COI1) ubiquitin-ligase complexes are required for jasmonate response in Arabidopsis. *Plant Cell* **14**(8): 1919-1935.

Xu Q, Wang Y, Chen Z, Yue Y, Huang H, Wu B, Liu Y, Zhou D-X, Zhao Y. 2023. ROS-stimulated protein lysine acetylation is required for crown root development in rice. *Journal of Advanced Research* **48**: 33-46.

Ye BB, Shang GD, Pan Y, Xu ZG, Zhou CM, Mao YB, Bao N, Sun L, Xu T, Wang JW. 2020. AP2/ERF Transcription Factors Integrate Age and Wound Signals for Root Regeneration. *Plant Cell* **32**(1): 226-241.

Yu MH, Steele AE. 1981. Host-Parasite Interaction of Resistant Sugarbeet and *Heterodera schachtii*. *J Nematol* **13**(2): 206-212.

Zandalinas SI, Fritschi FB, Mittler R. 2021. Global Warming, Climate Change, and Environmental Pollution: Recipe for a Multifactorial Stress Combination Disaster. *Trends in Plant Science* **26**(6): 588-599.

Zhang G, Zhao F, Chen L, Pan Y, Sun L, Bao N, Zhang T, Cui CX, Qiu Z, Zhang Y, et al. 2019. Jasmonate-mediated wound signalling promotes plant regeneration. *Nat Plants* **5**(5): 491-497.

Zhang L, Lilley CJ, Imren M, Knox JP, Urwin PE. 2017a. The Complex Cell Wall Composition of Syncytia Induced by Plant Parasitic Cyst Nematodes Reflects Both Function and Host Plant. *Front Plant Sci* **8**: 1087.

Zhang L, Zhang F, Melotto M, Yao J, He SY. 2017b. Jasmonate signaling and manipulation by pathogens and insects. *J Exp Bot* **68**(6): 1371-1385.

Zhang S, Li C, Si J, Han Z, Chen D. 2022. Action Mechanisms of Effectors in Plant-Pathogen Interaction. *Int J Mol Sci* **23**(12).

Zhao D, You Y, Fan H, Zhu X, Wang Y, Duan Y, Xuan Y, Chen L. 2018. The Role of Sugar Transporter Genes during Early Infection by Root-Knot Nematodes. *Int J Mol Sci* **19**(1).

Zhao P, Zhang J, Chen S, Zhang Z, Wan G, Mao J, Wang Z, Tan S, Xiang C. 2023. ERF1 inhibits lateral root emergence by promoting local auxin accumulation and repressing ARF7 expression. *Cell Reports* **42**(6): 112565.

Zhou W, Lozano-Torres JL, Blilou I, Zhang X, Zhai Q, Smant G, Li C, Scheres B. 2019. A jasmonate signaling network activates root stem cells and promotes regeneration. *Cell* **177**(4): 942-956 e914.

English summary

Plants are resilient organisms, as they adapt their growth in response to environmental conditions. Historically, crop breeding has largely focused on traits like yield, commercial viability, uniformity, and disease resistance. However, the potential to enhance the ability of plants to withstand both biotic and abiotic stresses has remained mostly unexplored. Such potential is gaining paramount importance due to the increasing impact of climate change, which is introducing new combinations of stress factors that challenge the sustainability of agriculture.

Biotic stress by soil-borne plant-parasitic nematodes causes at least 12.3% of global yield losses yearly, mostly due to endoparasitic cyst and root-knot nematodes. Endoparasitic nematodes disrupt plant growth by inflicting mechanical damage to root tissues, impeding water and nutrient uptake, and establishing feeding structures within plant roots. In Chapter 1 of this thesis, I explore how infections by endoparasitic nematodes alter plant root system architecture. I propose that this plasticity in root development is an adaptive response to mitigate the adverse effects of biotic stress by endoparasitic nematodes on plant growth.

Chapter 2 delves into the mechanisms by which plants perceive and respond to cyst nematode damage in their roots. In response to increasing nematode densities, we observe that plants develop clusters of secondary roots at infection sites. This response is dependent on specific damage-signaling pathways, particularly involving the plant hormone jasmonate and the jasmonate-responsive ERF109 transcription factor. Our findings suggest that the transient induction of jasmonate-dependent signaling via ERF109 induces the local production of the plant hormone auxin at nematode infection sites, which triggers the formation of secondary roots.

In Chapter 3, we further investigate the molecular signaling downstream of auxin that initiates secondary root formation at cyst nematode infection sites. Secondary roots can be induced through either a canonical lateral rooting pathway mediated by ARF7 and ARF19 auxin response factors or a non-canonical adventitious lateral rooting pathway dependent on the transcription factor WOX11. We find that nematode infection induces adventitious lateral rooting via WOX11, which is typically associated with abiotic stress conditions and has been observed to mitigate the impact of drought and high salinity on overall plant growth. Our experiments using Arabidopsis mutants reveal that WOX11-mediated root architecture plasticity helps alleviate the effects of cyst nematode infection on overall plant growth, potentially by restoring the flow of water and minerals through the plant. Therefore, we conclude that WOX11 is pivotal in enhancing plant tolerance to biotic stress caused by endo-

parasitic cyst nematodes.

Tolerance maintains plant growth and functioning despite nematode infection and, therefore, may benefit nematode parasitism by providing a steady level of nutrients. In Chapter 4, we explore the hypothesis that WOX11-mediated adventitious lateral rooting may promote nematode parasitism by increasing the flow of minerals and assimilates toward nematode feeding structures. Through measurements of nematode feeding site expansion, female growth, and offspring size, our data suggests that WOX11 restricts cell expansion within nematode feeding structures, thus attenuating nematode feeding and reducing female fecundity. We also found that WOX11 achieves this by modulating cell-wall extensibility, particularly by regulating reactive oxygen species. Importantly, this role of WOX11 in cell size control is distinct from its role in adventitious lateral rooting.

While Chapters 2 and 3 approach root plasticity from a plant-centered perspective, Chapter 4 shifts to a primarily pathogen-centered perspective. Thus, in Chapter 5, we illustrate how switching between these two perspectives can change our understanding of plant interactions with endoparasitic nematodes and help develop novel research questions. To demonstrate this, we provide different examples of plant cellular reprogramming that occur during plant-nematode interactions, and that can be interpreted as benefiting the nematode, the plant, or both. Furthermore, we apply this two-point perspective to plant interactions with another biotrophic pathogen, the protist *Plasmodiophora brassicae,* which causes clubroot disease. We identify parallels in plant cellular reprogramming induced by these two unrelated pathogens and propose hypotheses on the evolution of biotrophic parasitism.

In Chapter 6, I consolidate the findings from all the experimental chapters into a comprehensive model. This model outlines how plant perception of mechanical damage from nematode host invasion triggers a cascade of events that independently stimulate root growth and attenuate the expansion of nematode feeding structures. This, in turn, enhances plant tolerance to nematode parasitism and reduces nematode offspring size. We conclude by discussing how this knowledge can contribute to the development of plants that are resilient to multiple biotic and abiotic stresses, offering a promising solution to mitigate the impact of climate change on agriculture.

Acknowledgments

This thesis is the result of a long journey, along which I received help and support from many people.

First, I would like to thank my supervisory team. My promotor, Geert, for being such a caring, supportive, and inspiring mentor. Your questions and feedback were always a great motivation for me to dig deeper. My co-promotors, Aska and José. Aska, I really enjoyed our brainstorming sessions and valued your original and creative ideas. José, you became my co-promotor when I was halfway through my first year and had to completely change the topic of my research. You helped me come up with a new project and introduced me to your network. Mark, you were the co-promotor of my initial research project and you taught me the wonders of big data analysis on R. Besides that, we had many nice conversations about careers and life in general, with useful tips I took along during my journey.

Then, I'd like to thank my paranymphs. Jaap-Jan, having you as my research companion made these five years not only a fruitful but also a joyful experience. Much of what is in this book is a blend of our ideas and the result of countless discussions and experiments performed together. We made a great, resilient team from the beginning to the end, supporting and complementing each other in the highs and the (few) lows. Joliese, to me you are not only a very generous colleague but also a friend, a good listener, and a warm presence. I remember when you came to the lab to help me out transferring many pots of silver sand to paper bags. I was so happy to have you there and chat together during that very repetitive work.

Furthermore, I am very grateful to the whole Nematology family, for all the fun times, coffee breaks, lab outings, Christmas lunches, barbecues, bouldering, and many other social events. It is special to have so many colleagues willing to create a welcoming and collaborative atmosphere. Manouk and Lisette, I appreciate your help with the administration and paperwork. And also thanks to all lab technicians, for ensuring a structured, efficient, and safe lab. Casper, thank you for all your creative ideas to solve technical issues, for banishing radio channels, and for making the spit lab a cool and fun place to work.

Among the postdocs and researchers, I would especially like to thank Pieter, Lisa, Arne, and André. Pieter, you were an immense resource of knowledge and ideas and you made me discover how complex and fascinating plant cell walls are. Lisa, you inspired me a lot with your way of teaching and supervising students, and also with the beautiful drawings you made for your thesis book. Arne, you contacted me after one of my presentations to the chair group, suggesting to test my mutant lines

with the protist *Plasmodiophora brassicae.* Unfortunately, *P. brassicae* did not infect our plants *in vitro*, but it did make it to an opinion paper and chapter of this thesis. Thank you for initiating this collaboration! André, with you I could not only talk about nematodes but also about making music and writing songs. We still have to play Bossanova together sometime!

Now, a bit shout-out to my fellow PhD candidates at Nematology. You all contributed to a cohesive and supportive group, which was indispensable for my well-being and mental health. Here are a few specific words about people and moments I remember or hold dear, but please note that this is not an exhaustive list. Joris, we started and finished our PhDs almost at the same time. Thank you for always being open for a talk (sometimes in Dutch) and for your curiosity and gentleness. Sara, thank you for the laughters, the dinners together and all your advices about where to go on holidays. Thanks to you I discovered the beauty of the coral reef in Egypt and had some amazing hikes in Norway. Anna and Yuhao, thank you for all the work discussions and the chats in the office. Robbert, for organizing many social events at Nema. Alex and Alex, and Vera, for your tips about diving. Jorge, for your positive energy, humor, and memes. Geartsje, for joining me and Joliese on a late-summer swim, on a chilly grey day during the last lab outing. Mijke, for sharing your tips on breathing and relaxation. Arno, for your humor and for making me feel I was not the only one taking many holiday days. Marijke, for being an inspiring example of a healthy work/life balance. Myrna, for your structure when chairing the PhD meetings during the Covid pandemic. Iqbal, for the practice presentation for our talks at Lunteren. Dennie, for sharing your tips on taking notes with the Zettelkasten method.

I also would like to thank my students, Youri, Marie-Emma, Yunsong, Hang, Willemijn, Garam, Wouter, and Rob, for their hard work. Rob, it was really fun to work in the greenhouse together and learn about the 'behind the scenes' at Lidl. And I also have to acknowledge you for suggesting me the Lofi music for focussing when writing.

Moreover, thanks to all collaborators that contributed to the chapters of this thesis. Especially Viola, from whom I learned a lot about plant developmental and cellular biology. I really value all your feedback and inputs, it helped me see my work from a different perspective. Misghina, you always said "Hey, Nina!" with a big smile every time we would cross paths in Radix. Thank you for your positive energy and also for teaching me how to grind cysts and count nematode eggs.

Then, I would like to extend my gratitude to the fellow co-founders of the Young Nematologists Network (YNN): Unnati, Olivera, Boris, Jaap-Jan, Nasamu, Xorla, and Adam. We grew up as a very good team that supported each other and that managed to organize many online events including a conference with more than 200

participants!

Besides, I would like to spend a few words to acknowledge the support I received outside of the academic environment but that was essential for me to perform at work as I did.

Thanks to my dearest friends: Sanne, Milos, Ainhoa, Jana, Paola, Eleonora, Arianna, Itziar, Piero. Despite the physical distance at times, you were always there for me. Also thanks to all my current and past housemates, Louise, Gabriela, Emma, Jana, Minou, Ishani, Silvia, Miguel, Michele, Adi, Maïmouna, for being my friends and confidents, and for making me feel at home.

Thanks to the GoalTrainers calisthenics group, it was a bless to be able to train with such a diverse and fun group, outdoors, no matter the weather, and completely recharge after a full day at work.

Alex, thank you for all your love. For coming *aaall* the way from Utrecht almost every weekend to be together and also for all the beautiful trips and adventures. And I can finally acknowledge all your help with my presentations, job applications, emails, illustrations... are you the one who actually wrote my thesis? Unfortunately not, that would have spared me a lot of time, but you gave me a lot of useful feedback that definitely had an impact on the final outcome.

Last but not least, mamma e papá. Beh, inizialmente grazie per avermi fatta e cresciuta con tanto amore. Mi avete sempre aiutato e supportato nelle mie scelte, anche se questo avrebbe voluto dire che mi sarei allontanata da casa per studiare e poi fare ricerca. Ogni volta che torno a casa mi accogliete con braccia aperte, tanto cibo buono, un giardino pieno di piante rigogliose, dei piccoli amici animali di cui vi prendente cura e una casa che contiene tutte le vostre opere d'arte e di ingegno. Non siete forse scienziati, ma in fondo ho imparato da voi un certo approccio di ricerca, sia interiore che della natura.

List of publications

Lapin D, Kovacova V, Sun X, Dongus JA, Bhandari D, von Born P, Bautor J, **Guarneri N**, Rzemieniewski J, Stuttmann J, Beyer A, Parker JE. 2019. A coevolved EDS1-SAG101-NRG1 module mediates cell death signaling by TIR-domain immune receptors. *The Plant Cell* 31(10): 2430–2455.

Willig JJ, **Guarneri N,** van Steenbrugge JJM, de Jong W, Chen J, Goverse A, Lozano Torres JL, Sterken MG, Bakker J, Smant G. 2022. The Arabidopsis transcription factor TCP9 modulates root architectural plasticity, reactive oxygen species-mediated processes, and tolerance to cyst nematode infections. *Plant J* **112**(4): 1070-1083.

Guarneri N*, Willig JJ*, Sterken MG, Zhou W, Hasan MS, Sharon L, Grundler FMW, Willemsen V, Goverse A, Smant G, Lozano-Torres JL. 2023. Root architecture plasticity in response to endoparasitic cyst nematodes is mediated by damage signaling. *New Phytol* 237(3): 807-822.

Willig JJ*, **Guarneri N***, Loon Tv, Wahyuni S, Astudillo-Estévez IE, Xu L, Willemsen V, Goverse A, Sterken MG, Lozano-Torres JL, Smant G. 2023. WOX11-mediated adventitious lateral root formation modulates tolerance of Arabidopsis to cyst nematode infections. *bioRxiv*: 2023.2008.2011.553027.

Guarneri N, Willig JJ, Willemsen V, Goverse A, Sterken MG, Nibbering P, Lozano-Torres JL, Smant G. 2023. WOX11-mediated cell size control in Arabidopsis attenuates fecundity of endoparasitic cyst nematodes**.** *bioRxiv*: 2023.10.27.564344

*These authors contributed equally

About the author

Nina Guarneri was born in Cremona, Italy, in 1994. Her academic journey reflects a keen interest in unraveling the intricacy of biological processes, particularly focusing on plants and their interactions with the environment.

Nina earned a BSc in Biology at the University of Turin, after completing a thesis on plant recognition of wounding. Seeking to deepen her expertise, Nina pursued an MSc at Wageningen University, graduating *cum laude* with a specialization in Plant Pathology and Entomology, and a minor in Genetics of Plant Development. Her MSc major thesis delved into the role of an unknown protein in plant susceptibility to endoparasitic root-knot nematodes. Subsequently, Nina obtained an Erasmus scholarship to conduct an MSc minor thesis at the Max Planck Institute for Plant Breeding Research in Cologne. Here, she refined her skills in molecular plant biology and bioinformatics, investigating the co-evolution of a protein complex and signaling module in plant immunity.

To train as an independent scientist, Nina embarked on a PhD at Wageningen University & Research, focusing on root adaptive responses to infections by cyst nematodes. Her collaborative efforts during the PhD journey resulted in three publications in high-impact journals, with three additional manuscripts currently under review.

Next to her research, Nina is a co-founder of the Young Nematologists Network, actively contributing to the organization of online seminars, workshops, and conferences. Her commitment extends beyond the laboratory, fostering the professional development of early-career Nematologists worldwide.

Education Statement

Education Statement of the Graduate School Experimental Plant Sciences

Issued to: Nina Guarneri
Date: 20 March 2024
Group: Nematology
University: Wageningen University & Research

1) Start-Up Phase	date	cp
► **First presentation of your project**		
The role of strigolactones in plant-nematode interaction	4 Apr 2019	1,5
► **Writing or rewriting a project proposal**		
► **MSc courses**		
Subtotal Start-Up Phase		1,5

2) Scientific Exposure	date	cp
► **EPS PhD days**		
EPS PhD days 'Get2Gether', Soest (NL)	11-12 Feb 2019	0,6
EPS PhD days 'Get2Gether', Soest (NL)	10-11 Feb 2020	0,6
EPS PhD days 'Get2Gether', online	1-2 Feb 2021	0,4
► **EPS theme symposia**		
EPS theme 1 symposium 'Developmental Biology of Plants', Leiden (NL)	31 Jan 2019	0,3
EPS theme 1 symposium 'Developmental Biology of Plants', Wageningen (NL)	5 Feb 2020	0,3
EPS theme 1 symposium 'Developmental Biology of Plants', Wageningen (NL)	14 Jun 2022	0,3
EPS theme 2 symposium & Willie Commelin Scholten Day 'Interactions between Plants and Biotic Agents', Wageningen (NL)	1 Feb 2019	0,3
EPS theme 2 symposium & Willie Commelin Scholten Day 'Interactions between Plants and Biotic Agents', Utrecht (NL)	4 Feb 2020	0,3
EPS theme 2 symposium & Willie Commelin Scholten Day 'Interactions between Plants and Biotic Agents', online	9 Feb 2021	0,2
EPS theme 2 symposium & Willie Commelin Scholten Day 'Interactions between Plants and Biotic Agents', online	8 Feb 2022	0,2
► **National platform meetings**		
Annual Meeting 'Experimental Plant Sciences', Lunteren (NL)	8-9 Apr 2019	0,6
Annual Meeting 'Experimental Plant Sciences', online	12-13 Apr 2021	0,5
Annual Meeting 'Experimental Plant Sciences', Lunteren (NL)	11-12 Apr 2022	0,6
NWOLife congress 2019 'Communication in life", Bunnik (NL)	28-29 May 2019	0,6
NWOLife congress 2022 'Resilience', Egmond aan Zee (NL)	24-25 May 2022	0,6
► **Seminars (series), workshops and symposia**		
Seminar: Tina Kyndt	16 May 2019	0,1
Seminar: Enrico Scarpella "Control of vein patterning by auxin", Ari-Pekka Mähönen "Stem cell dynamics in the vascular cambium of Arabidopsis root"	19 Jun 2019	0,2
Seminar: Erik Andersen, "Parasite anthelmintic resistance mechanisms from C. elegans natural diversity"	14 Nov 2019	0,1
Seminar: Sebastian Eves van den Akker, "Plant Immunity and development-altering 'toolbox' of parasitic nematodes"	13 Feb 2020	0,1
Seminar: Jan Lohmann, "From transcription to shoot morphogenesis"	16 Jan 2020	0,1
Seminar: Leendert Molendijk, "Applied Nematology in the Polder"	30 Jan 2020	0,1
Seminar: Plantae Presents - Niko Geldner and Sarah Blizard, online	29 Apr 2020	0,2
Seminar: Stefan Geisen, "Challenges as a PhD and postdoc in Science and tips to overcome those"	20 Jan 2021	0,1

CONTINUED ON NEXT PAGE

Seminar: Corné M.J. Pieterse, “The plant microbiome and plant health”; Paola Bonfante, “Arbuscular mycorrhizal fungi: living in between plants and endobacteria”; Gabriel Castrillo, “Coordination between the microbiota and the root endodermis is required for plant mineral nutrient homeostasis”	15 Apr 2021	0,2
Seminar: Joe Kieber, "Another brick in the wall: Regulating cell wall synthesis in plants"	30 May 2022	0,1
Seminar: Robert Koller, "Monitoring spatial and temporal growth and carbon dynamics in roots by co-registration of Magnetic Resonance Imaging and Positron Emission Tomography"	28 Sep 2022	0,1
Seminar: Lieven De Veylder, "Evolutionary conservation of the wound regeneration pathway"	8 Jun 2023	0,1
Symposium: Live Online Event Root Zone Breeding, online	19 May 2020	0,2
Symposium: NIOO Terrestrial Ecology - WUR Nematology Symposium, Wageningen (NL)	5 Jul 2023	0,2
► **Seminar plus**		
► **International symposia and congresses**		
International Society for Molecular Plant-Microbe Interactions (IS-MPMI)	14-18 Jul 2019	1,5
Virtual Nematology Conference (VNC) 2021, online	26-28 May 2021	0,6
(FR)	1-6 May 2022	1,5
► **Presentations**		
Poster: "Understanding the role of strigolactones in cyst nematode-plant interaction", Glasgow (UK), IS-MPMI congress	17 Jul 2019	1,0
Talk: "The cyst nematode *Heterodera schachtii* triggers *de novo* root organogenesis in Arabidopsis", online, VNC 2021	27 May 2021	1,0
Talk: "The cyst nematode *Heterodera schachtii* triggers ERF109- and WOX11-dependent *de novo* root organogenesis in Arabidopsis", online, Annual EPS	13 Apr 2021	1,0
Talk: "Root architecture plasticity in response to endoparasitic cyst nematodes is mediated by damage signaling", online, EPS Theme 2 symposium	8 Feb 2022	1,0
Poster: "Root architecture plasticity in response to endoparasitic cyst nematodes is mediated by damage signaling", Antibes Juans-les-Pins (FR), ICN 2022	2 May 2022	1,0
Poster:"Damage-induced root plasticity in response to parasitic nematodes", Egmond aan Zee (NL), NWOLife 2022	24 May 2022	1,0
Talk: "The dual role of ERF109, WOX11 and LBD16 in root plasticity responses and plant susceptibility to parasitic cyst nematodes", Utrecht (NL), EPS PhD	30 Aug 2022	1,0
Poster: "The dual role of ERF109, WOX11 and LBD16 in root plasticity responses and plant susceptibility to parasitic cyst nematodes", Utrecht (NL),	30 Aug 2022	1,0
► **Interviews**		
► **Excursions**		
EPS company visit to BASF Nunhems	25 Oct 2019	0,2
Subtotal Scientific Exposure		20,1

3) In-Depth Studies	*date*	*cp*
► **Advanced scientific courses & workshops**		
PhD course, Pathobiomes and Plant Immunity, online	7-18 Jun 2021	2,0
EPS PhD Summer School “Environmental Signaling in Plants”, Utrecht (NL)	29-31 Aug 2022	0,9
► **Journal club**		
Paper Club at Nematology	2019-2020	1,5
► **Individual research training**		
Subtotal In-Depth Studies		4,4

4) Personal Development	*date*	*cp*
► **General skill training courses**		
EPS Introduction Course, Wageningen (NL)	11 Jun 2019	0,3
WGS PhD Competence Assesment, Wageningen (NL)	Sep 2019	0,3
WGS course Supervising BSc & MSc thesis students, Wageningen (NL)	13-14 Feb 2020	0,6
WGS course Project and Time Management, online	2021	1,5

A

	WGS course Career Orientation, Wageningen (NL)	2022	1,5
►	**Organisation of scientific meetings, PhD courses or outreach activities**		
	conference	2021	0,5
	Organisation of Young Nematologist Network activities: 1 social event, 3 seminars, 3 workshops, 1 online conference	2022-2023	2,5
►	**Membership of EPS PhD Council**		
	Subtotal Personal Development		7,2

5) Teaching & Supervision Duties		*date*	*cp*
►	**Courses**		3,0
	NEM-20306 Research Methodology in Plant Sciences	May-Jun 2019	
	PHP-30806 Molecular Aspects of Bio Interactions	Nov-Dec 2019	
	NEM-30306 Host-Parasite Interactions	Apr 2020	
►	**Supervision of BSc/MSc projects**		3,0
	BSc project 'An analysis of differentially expressed genes related to JA, auxin and WOX11 during infection of Arabidopsis by *Heterodera schachtii*'	2020	
	BSc project 'Does *de novo* root organogenesis in response to beet cyst nematode infection affect root and shoot growth of Arabidopsis?'	2021-2022	
	MSc project 'The beet cyst nematode *Heterodera schachtii* induces *de novo* root organogenesis via WOX11 in *Arabidopsis thaliana*'	2020-2021	
	MSc project 'The role of *de novo* root organogenesis in Arabidopsis susceptibility to the beet cyst nematode *Heterodera schachtii*'	2020-2021	
	MSc project 'The beet cyst nematode *Heterodera schachtii* induces *de novo* root organogenesis via ERF109'	2020-2021	
	MSc project 'The role of COI1 and ERF109 in *Heterodera schachtii*-induced secondary root formation'	2020-2021	
	MSc project 'Investigating the effect of *de novo* root organogenesis on beet cyst nematode development in Arabidopsis'	2021-2022	
	MSc project 'The role of ERF109, WOX11 and LBD16 in radial hypertrophy of syncytia'	2022	
	Subtotal Teaching & Supervision Duties		6,0

TOTAL NUMBER OF CREDIT POINTS*	**39,2**
Herewith the Graduate School declares that the PhD candidate has complied with the educational requirements set by the Educational Committee of EPS with a minimum total of 30 ECTS credits.	
** A credit represents a normative study load of 28 hours of study.*	

A

The research described in this thesis was financially supported by the TKI project grant TU18152 of the Dutch Top Sector Horticulture & Starting Materials.

Financial support from Wageningen University for printing this thesis is gratefully acknowledged.

Cover design and thesis layout by Nina Guarneri

Printed by Gildeprint on FSC-certified paper